TECHNISCHE UNIVERSITÄT WIEN

DIPLOMA THESIS

Azaindolo[3,2,1-*jk*]carbazole based Donor-Acceptor Materials as Potential TADF Emitters

conducted at the

Institute of Applied Synthetic Chemistry

at the **TU Wien**

under the supervision of

Univ.Prof. Dipl.-Ing. Dr.techn. Johannes **Fröhlich**

advised by

Dipl.-Ing. Thomas **Kader**

and

Dipl.-Ing. Dr.techn. Paul **Kautny**

by

Nikolaus **Poremba**, BSc.

Matr.-Nr.: 01127607

Vivenotgasse 20/13, 1120 Wien

Vienna, April 22, 2019

“Just because something doesn't do what you planned it to do,

doesn't mean it's useless.”

— Thomas A. Edison

Danksagung

In erster Linie möchte ich mich bei Univ.Prof. Dr. **Johannes Fröhlich** bedanken, der mir die Chance ermöglicht hat, diese Diplomarbeit in seiner Forschungsgruppe durchführen und verfassen zu können.+

Ich bedanke mich zudem herzlichst bei meinen Betreuern, Dipl.-Ing. **Thomas Kader** und Dipl.-Ing. Dr. **Paul Kautny**, für ihre exzellente fachliche und menschliche Unterstützung während meiner gesamten Arbeitsdurchführung.

Zusätzlich möchte ich mich an dieser Stelle bei meinen Laborkollegen Dipl.-Ing. Dr. **Brigitte Holzer**, Dipl.-Ing. **Dorian Bader**, **Birgit Meindl** und **Paul Getreuer** für die überaus angenehme, lustige und lehrreiche Zeit während der Arbeit bedanken, sowie für viele ausgezeichnete, selbstgemachte Mehlspeisen und Eissorten.

Ohne die Unterstützung meiner Familie wäre ich nicht an diesem Punkt in meinem Leben angelangt. Meine Großmutter **Hedwig Poremba** und meine Mutter **Monika Poremba** haben mich zu dem Menschen erzogen, der ich heute bin, und dafür danke ich ihnen von Herzen. Bei meinem Vater bedanke ich mich für jeden Ausflug, jede musikalische Auszeit und jeden Ratschlag während der letzten Jahre.

Großer Dank gilt auch meiner Freundin **Emma Ruzowitzky**, die mir immer zugehört hat, geholfen hat, meine Gedanken zu ordnen und mich bei meinen Entscheidungen unterstützt hat. Für ihre liebevolle Beihilfe, besonders in den letzten Wochen, bin ich sehr dankbar.

Auch auf meine engsten Freunde, **Thomas Schwartz**, **Nino Kneidinger**, **Ferdinand Köstler** und **Gerhard Uhrovcsik**, konnte ich immer in allen Lebenslagen meiner Studienzeit zählen und möchte ihnen deshalb diese Zeilen widmen.

Zuletzt möchte ich noch meinem ehemaligen Chemieprofessor, Ostr. Prof. **Alfred Moser**, der einst mein Interesse in diesem Fachgebiet durch seinen einzigartigen schulischen Unterricht geweckt und gefördert hat, meinen großen Dank aussprechen.

Abstract

Throughout the last decades, the field of organic optoelectronics gained constantly more importance in our everyday world and thereby research and development in this sector exhibits a need to improve these materials. Organic Light Emitting Diodes (OLEDs) are already in use for many electronical applications, including commercial TV screens and smartphones of everyday usage.

Their biggest advantage lies in the fact, that organic semiconductors are soft materials. This results in flexible, thin and lightweight devices, which show good luminous efficacies, small contrast rates, as well as low production costs and no toxic containments. These properties arise also big interest in the use as lighting sources. Towards this development, different strategies of OLED designs can be achieved, including many factors, that need improvement.

Latest research in our group introduced novel bipolar host materials for Phosphorescent Organic Light Emitting Diodes (PhOLEDs), based on oxadiazole electron acceptors and planarized triarylamines as donors. It was observed, that an increase of triarylamine planarization, leads to a decrease of the donor strength in the molecule as a consequence. Furthermore, fully planarized indolo[3,2,1-*jk*]carbazole (ICz) even showed weak acceptor character.

The introduction of electron withdrawing nitrogen atoms in the ICz scaffold induced an increase of acceptor strength. In addition to the lowered HOMO and LUMO levels, high triplet energies were preserved. The aim of this work is the synthesis of novel donor-acceptor systems as potential Thermally Activated Delayed Fluorescence (TADF) emitters. Theoretical calculations for several bipolar systems using N-incorporated ICz acceptors with different nitrogen amounts and varying its position showed promising electro-luminescent properties, such as small singlet-triplet-energy gaps ($\Delta \mathbf{E}_{ST} < 0.2$ eV), as well as a broad spectral range to cover. Hence, not only the amount, but also the position of the additional nitrogen in the structure has influence on the HOMO/LUMO levels, a comparison of acceptors with alternating strength in the final materials is also possible.

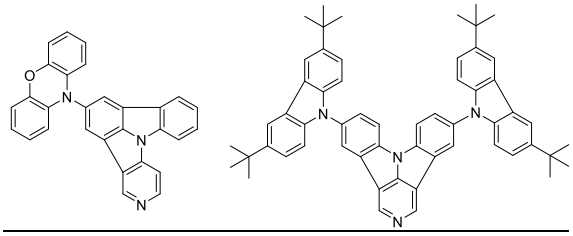

Potential bipolar TADF-emitters

In the course of this thesis a comprehensive synthetic approach towards the bipolar materials, including the required building blocks, was established. Furthermore, electrochemical and photophysical properties of the target materials were studied in detail.

Kurzfassung

In den letzten Jahrzehnten gewann das Gebiet der organischen Optoelektronik immer mehr an Geltung, weshalb stetiges Interesse an der weiteren Verbesserung der Materialien besteht. Organische Licht emittierende Dioden (OLEDs) finden heutzutage bereits in vielen elektronischen Geräten Anwendung im Alltag. Dazu zählen insbesondere Fernsehgeräte und Smartphones.

Durch die Verwendung von organischen Materialien in OLEDs können dünne, flexible und leichte Geräte gebaut werden, die eine gute Lichtausbeute, hohen Kontrast, sowie geringe Produktionskosten aufweisen und dabei keine toxischer Inhaltsstoffen verwenden. Diese Eigenschaften erregen dadurch auch großes Interesse in der Verwendung als Lichtquellen. Durch die ständige Entwicklung gibt es verschiedene Strategien und Funktionsprinzipien, die in OLEDs Anwendung finden, dabei aber noch verbessert werden müssen.

In unserer Forschungsgruppe wurden bipolare Host-Materialien für phosphoreszente OLEDs, basierend auf Oxadiazol Elektronen Akzeptoren und planarisierten Triarylaminen als Donoren, entwickelt. Es konnte beobachtet werden, dass eine Erhöhung der Planarisierung der Triarylamine, eine Senkung der Donorstärke zur Folge hatte. Des Weiteren konnte gezeigt werden, dass komplett planarisiertes Indolo[3,2,1-*jk*]carbazol (ICz) sogar leichten Akzeptorcharakter aufweist. Zusätzliches Einbringen von Stickstoff in das ICz Gerüst führt zu einer Erhöhung der Akzeptorstärke. Neben der Senkung der HOMO/LUMO Levels konnten die hohen Triplettenergien dabei erhalten bleiben. Ziel dieser Arbeit, war die Synthese neuer Donor-Akzeptor Systeme, die potenzielle Anwendung als *Thermally Activated Delayed Fluorescence* (TADF) Emitter finden. Berechnungen für verschiedene bipolare Systeme, unter der Verwendung von stickstoffmodifizierten ICz Akzeptoren mit unterschiedlichem Stickstoffgehalt und -position, zeigten vielversprechende elektrolumineszente Eigenschaften, wie optimale Singulett-Triplett-Energie Abstände ($\Delta \mathbf{E}_{ST} < 0.2$ eV), sowie ein breiter spektraler Bereich. Da nicht nur Anzahl, sondern auch Position des eingebauten Stickstoffs Einfluss auf HOMO und LUMO Level haben, ist ein Vergleich verschieden starker Akzeptoren in den Endmaterialen möglich.

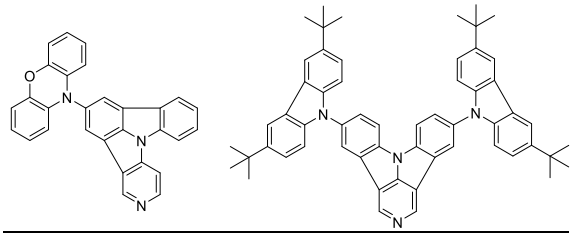

Potenzielle bipolare TADF-emitter

Im Rahmen dieser Arbeit wurde eine ausführliche Synthesestrategie zur Herstellung der bipolaren Systeme, sowie der dafür notwendigen Bausteine entwickelt. Zusätzlich beinhaltet die Arbeit eine ausführliche Diskussion der elektrochemischen und photophysikalischen Eigenschaften dieser Materialien.

Abbreviations

Besides common abbreviations in the English language and chemical element symbols short forms listed below are used.

abs.	absolute	eq.	equivalents
acac	acetylacetonate	GC	gas chromatography
ACN	acetonitrile	HR-MS	high resolution mass spectrometry
aq.	aqueous	ICz	indolo[3,2,1-*jk*]carbazole
BHA	Buchwald Hartwig amination	ISC	inter system crossing
CHA	CH-activation	NBS	*N*-bromosuccinimide
CBP	4,4′-bis(9-carbazolyl)-1,1′-biphenyl	NCS	*N*-chlorosuccinimide
Cz	carbazole	NHC-ligand	1,3-bis(2,6-diisopropylphenyl)-1*H*-imidazol-3-ium chloride
dba	dibenzylideneacetone	NMR	nuclear magnetic resonance
DCM	dichloromethane	PE	petroleum ether
DMA	*N,N*-dimethylacetamide	pic	picolinato
DMAcr	9,9-dimethyl-9,10-dihydroacridine	PXZ	10*H*-phenoxazine
DMF	*N*,*N*-dimethylformamide	ppy	phenylpyridinato
DMSO	dimethylsulfoxide	rt	room temperature
dppf	1,1’-bis(diphenylphosphino) ferrocene	TADF	thermally activated delayed fluorescence
DMTBCz	3,6-di-tert-butyl-9H-carbazole	TLC	thin layer chromatography
EA	ethylacetate	THF	tetrahydrofuran

General Remarks

Labeling of substances

Identification of substances was achieved by strict sequential numbering. Substances previously reported in literature receive Arabic numbers, whereas substances unknown to literature are labeled with Roman numbers.

References to literature citations

References to literature are given within the text by superscript Arabic numbers in square brackets.

Nomenclature

The nomenclature of chemical compounds not described in literature was based on the rules of Chemical Abstracts. Other compounds, reagents and solvents may be described by simplified terms, trivial or trade names.

Table of Contents

A. FORMULA SCHEME 1

A.1 DONOR SYNTHESIS 2
A.2 ACCEPTOR SYNTHESIS 2
A.2.1 Synthesis of carbolines 2
A.2.2 Pre-functionalized approaches 3
A.2.3 Post-functionalized approaches 5
A.3 DONOR-ACCEPTOR COUPLING 7
A.4 SYNTHESIS OF THE PD-NHC CATALYST 8

B. GENERAL PART 9

B.1 ORGANIC ELECTRONICS 10
B.2 ORGANIC LIGHT EMITTING DIODES (OLEDS) 10
B.2.1 History 10
B.2.2 Working principle 11
B.2.3 Host Materials and Phosphorescent OLEDs (PhOLEDs) 14
B.2.4 Thermally activated delayed fluorescence (TADF)[18] 16
B.3 ARYLAMINE BASED MATERIALS 17
B.4 GOAL OF THE THESIS 19

C. SPECIFIC PART 20

C.1 INTRODUCTION 21
C.2 DONOR SYNTHESIS 28
C.2.1 9,9-Dimethyl-9,10-dihydroacridine 28
C.3 TOWARDS ACCEPTOR STARTING MATERIALS 29
C.3.1 Synthesis of carbolines 29
C.3.2 Synthesis of β-carboline 29
C.3.3 Synthesis of γ-carboline 29
Metal assisted route 29
Microwave assisted route 30
C.4 SYNTHESIS OF PYRROLODIPYRIDINE (PDP) 31
C.5 SYNTHESIS OF PRE-FUNCTIONALIZED CARBOLINES 31
C.6 SYNTHESIS OF ACCEPTORS 33
C.6.1 Synthesis of 2-bromopyrido[3',4':4,5]pyrrolo[3,2,1-jk]carbazole/Br-5NICz 33
C.6.2 Synthesis of 2-bromopyrido[4',3':4,5]pyrrolo[3,2,1-jk]carbazole/Br-6NICz 34
C.6.3 Synthesis of 2-bromopyrido[3,4-b]pyrido[4',3':4,5]pyrrolo[3,2,1-hi]indole/Br-6,10NICz 36
C.6.4 Synthesis of 5-bromodibenzo[b,e]pyrido[3,4,5-gh]pyrrolizine/Br-2NICz 37
C.6.5 Synthesis of 5,11-dibromodibenzo[b,e]pyrido[3,4,5-gh]pyrrolizine/Br_2-2NICz 41
C.6.6 Synthesis of 11-bromobenzo[b]dipyrido[4,3-e:3',4',5'-gh]pyrrolizine/Br-5,11NICz 42
C.7 DONOR-ACCEPTOR SYSTEMS 44
C.8 SYNTHESIS OF PD-NHC-CATALYST 46
C.9 CHARACTERIZATION 47
C.9.1 Absorption and fluorescence 47
C.9.2 Phosphorescence 49
C.9.3 Cyclic voltammetry (CV) 49
C.9.4 Summary 50
C.10 RESULTS AND DISCUSSION 51

D. EXPERIMENTAL PART 52

D.1 GENERAL REMARKS 53
D.2 CHROMATOGRAPHIC METHODS 53
D.2.1 Thin layer chromatography 53
D.2.2 Column Chromatography 53
D.3 SUBLIMATION 53
D.4 MICROWAVE ASSISTED REACTIONS 54
D.5 ANALYTICAL METHODS 54
D.5.1 NMR-Spectroscopy 54
D.5.2 GC-MS measurements 55
D.5.3 Absorption spectroscopy 55
D.5.4 Fluorescence and phosphorescence spectroscopy 55
D.5.5 Cyclic voltammetry (CV) 55
D.6 SYNTHESIS AND CHARACTERIZATION OF THE COMPOUNDS 56
D.6.1 Donor synthesis 56
Methyl 2-(phenylamino)benzoate 56
2-(2-(Phenylamino)phenyl)propan-2-ol 57
9,9-Dimethyl-9,10-dihydroacridine 58
D.6.2 Acceptor synthesis 58
D.6.3 Synthesis of carbolines 58
2,3,4,9-Tetrahydro-1*H*-pyrido[3,4-*b*]indole-3-carboxylic acid 58
9*H*-Pyrido[3,4-*b*]indole / **β**-carboline 59
N-(2-Bromophenyl)pyridin-4-amine 60
5*H*-Pyrido[4,3-*b*]indole / **γ**-carboline 60
N-Acetyl-3-bromo-4-piperidone, hydrobromide 61
5*H*-Pyrido[4,3-*b*]indole / γ-carboline 62
3-Chloro-*N*-(pyridin-4-yl)pyridin-4-amine 62
5*H*-Pyrrolo[3,2-*c*:4,5-*c'*]dipyridine 63
D.6.4 Synthesis of pre-functionalization carboline derivatives 64
6-Bromo-9*H*-pyrido[3,4-*b*]indole 64
8-Bromo-5*H*-pyrido[4,3-*b*]indole 64
D.6.5 Synthesis of functionalized carboline derivatives 65
9-(3-Chloropyridin-4-yl)-9*H*-carbazole 65
6-Bromo-9-(2-nitrophenyl)-9*H*-pyrido[3,4-*b*]indole 66
2-(6-Bromo-9*H*-pyrido[3,4-*b*]indol-9-yl)aniline 66
6-Bromo-9-(2-bromophenyl)-9*H*-pyrido[3,4-*b*]indole 67
9-(4-Chloropyridin-3-yl)-9*H*-pyrido[3,4-*b*]indole 68
5-(2-Bromophenyl)-5*H*-pyrido[4,3-*b*]indole 68
3,5-Dichloro-*N*,*N*-diphenylpyridin-4-amine 69
4-Nitro-*N*-phenylaniline 70
3,5-Dichloro-*N*-(4-nitrophenyl)-*N*-phenylpyridin-4-amine 70
5-(2-Bromo-4-nitrophenyl)-5*H*-pyrido[4,3-*b*]indole 71
8-Bromo-5-(2-nitrophenyl)-5*H*-pyrido[4,3-*b*]indole 72
2-(8-Bromo-5*H*-pyrido[4,3-*b*]indol-5-yl)aniline 72
5-(2-Bromophenyl)-5*H*-pyrrolo[3,2-*c*:4,5-*c'*]dipyridine 73
5-(2-Bromo-4-nitrophenyl)-5*H*-pyrrolo[3,2-*c*:4,5-*c'*]dipyridine 74
D.6.6 Ring closure towards acceptors 74
General procedure 1 (GP1): CHA 74
Pyrido[3',4':4,5]pyrrolo[3,2,1-*jk*]carbazole 75
Pyrido[3,4-*b*]pyrido[4',3':4,5]pyrrolo[3,2,1-*hi*]indole 75
Dibenzo[*b,e*]pyrido[3,4,5-*gh*]pyrrolizine 76
Dibenzo[*b,e*]pyrido[3,4,5-*gh*]pyrrolizine 76
5-Nitrodibenzo[*b,e*]pyrido[3,4,5-*gh*]pyrrolizine 77
5-Nitrodibenzo[*b,e*]pyrido[3,4,5-*gh*]pyrrolizine 78
Benzo[*b*]dipyrido[4,3-*e*:3',4',5'-*gh*]pyrrolizine 78
5-Nitrobenzo[*b*]dipyrido[3,2-e:3',4',5'-*gh*]pyrrolizine 79
Diazotization 80

2-Bromopyrido[4',3':4,5]pyrrolo[3,2,1-*jk*]carbazole 80
D.6.7 Synthesis of post-functionalization carboline derivatives 81
2-Bromopyrido[3',4':4,5]pyrrolo[3,2,1-*jk*]carbazole 81
2-Bromopyrido[3,4-*b*]pyrido[4',3':4,5]pyrrolo[3,2,1-*hi*]indole 82
5,11-Dibromodibenzo[*b,e*]pyrido[3,4,5-*gh*]pyrrolizine 82
5-Bromodibenzo[*b,e*]pyrido[3,4,5-*gh*]pyrrolizine 83
Dibenzo[*b,e*]pyrido[3,4,5-*gh*]pyrrolizin-5-amine 84
5-Bromodibenzo[*b,e*]pyrido[3,4,5-*gh*]pyrrolizine 84
D.6.8 Synthesis of donor-acceptor systems 85
General procedure 2 (GP2): Buchwald-Hartwig Amination 85
10-(Pyrido[3',4':4,5]pyrrolo[3,2,1-*jk*]carbazol-2-yl)-4a,5a,9a,10a-tetrahydro-10*H*-phenoxazine 85
10-(Pyrido[4',3':4,5]pyrrolo[3,2,1-*jk*]carbazol-2-yl)-4a,5a,9a,10a-tetrahydro-10*H*-phenoxazine 86
10-(Pyrido[3,4-*b*]pyrido[4',3':4,5]pyrrolo[3,2,1-*hi*]indol-2-yl)-10*H*-phenoxazine 87
5,11-Bis(9,9-dimethylacridin-10(9*H*)-yl)dibenzo[*b,e*]pyrido[3,4,5-*gh*]pyrrolizine 88
5,11-Di(10*H*-phenoxazin-10-yl)dibenzo[*b,e*]pyrido[3,4,5-*gh*]pyrrolizine 88
Solid Phase Reaction 89
5,11-Bis(3,6-di-tert-butyl-9*H*-carbazol-9-yl)dibenzo[*b,e*]pyrido[3,4,5-*gh*]pyrrolizine 89
D.6.9 Synthesis of the Pd-NHC catalyst 90
[1,3-Bis[2,6-bis(1-methylethyl)phenyl]-1,3-dihydro-2H-imidazol-2-yliden]chloro(η3-2propen-1-yl)palladium 90

E. BIBLIOGRAPHY 91

A. Formula Scheme

A.1 Donor synthesis

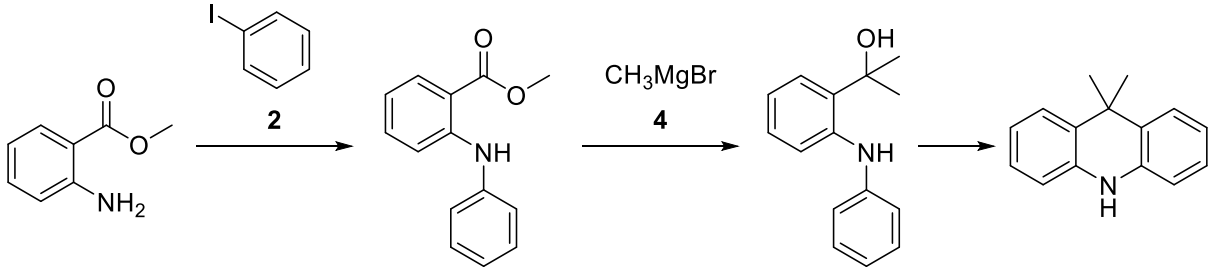

1 3 5 6

A.2 Acceptor synthesis

A.2.1 Synthesis of carbolines

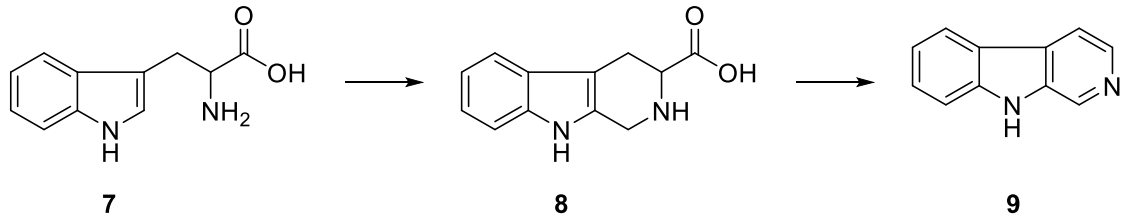

7 8 9

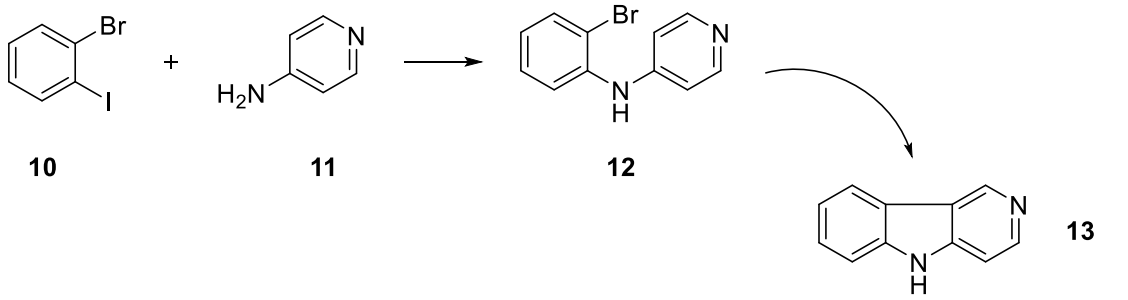

10 11 12 13

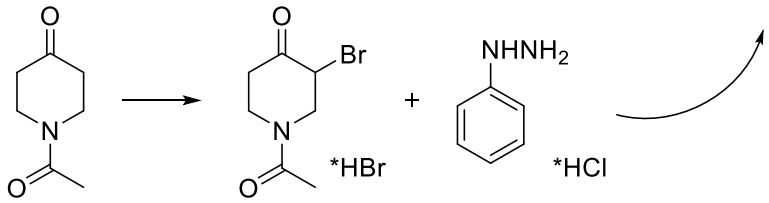

14 15 16

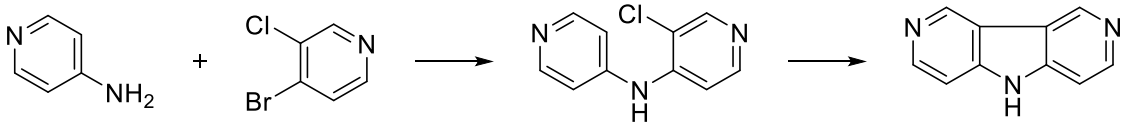

11 17 18 19

A.2.2 Pre-functionalized approaches

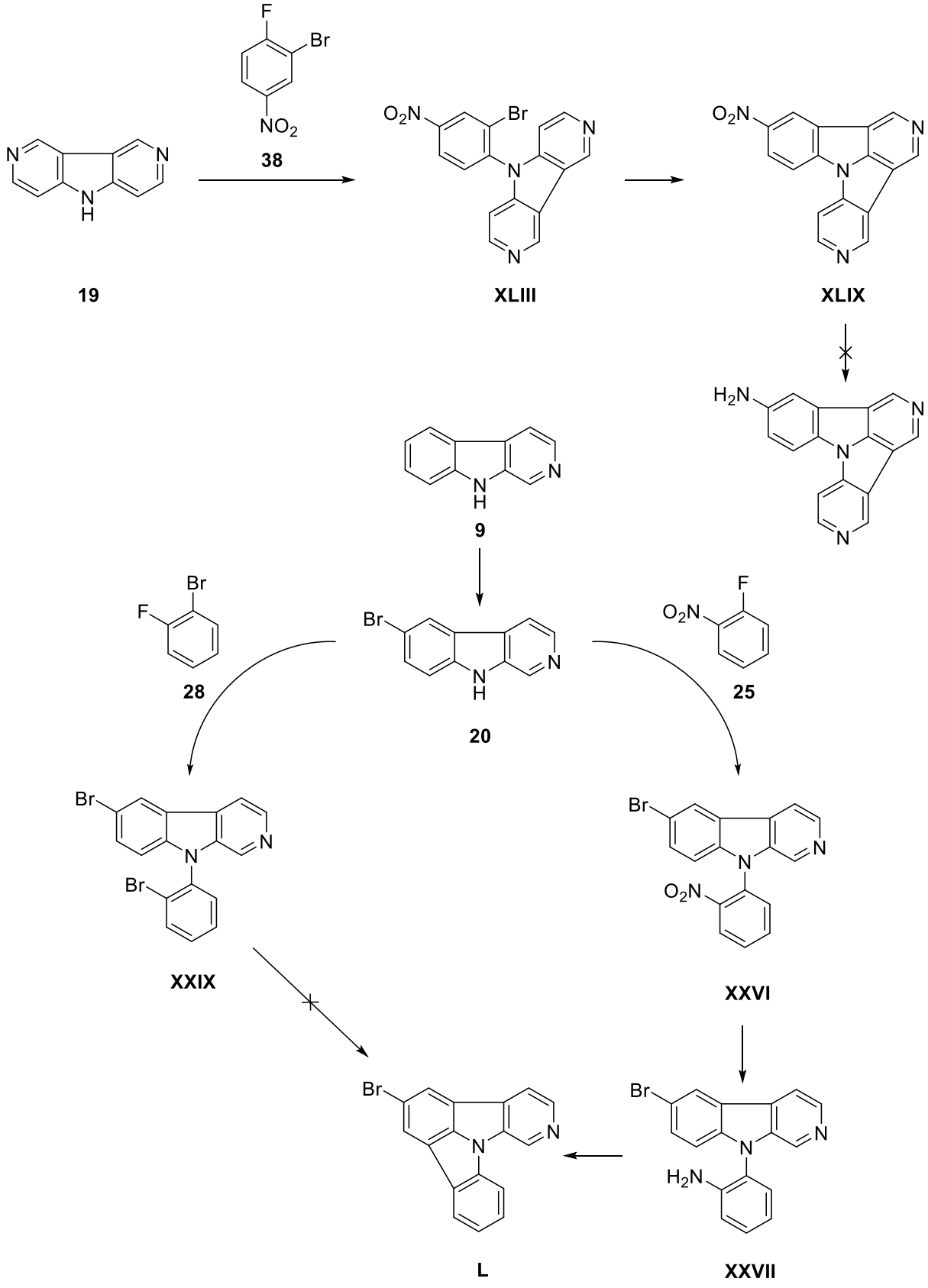

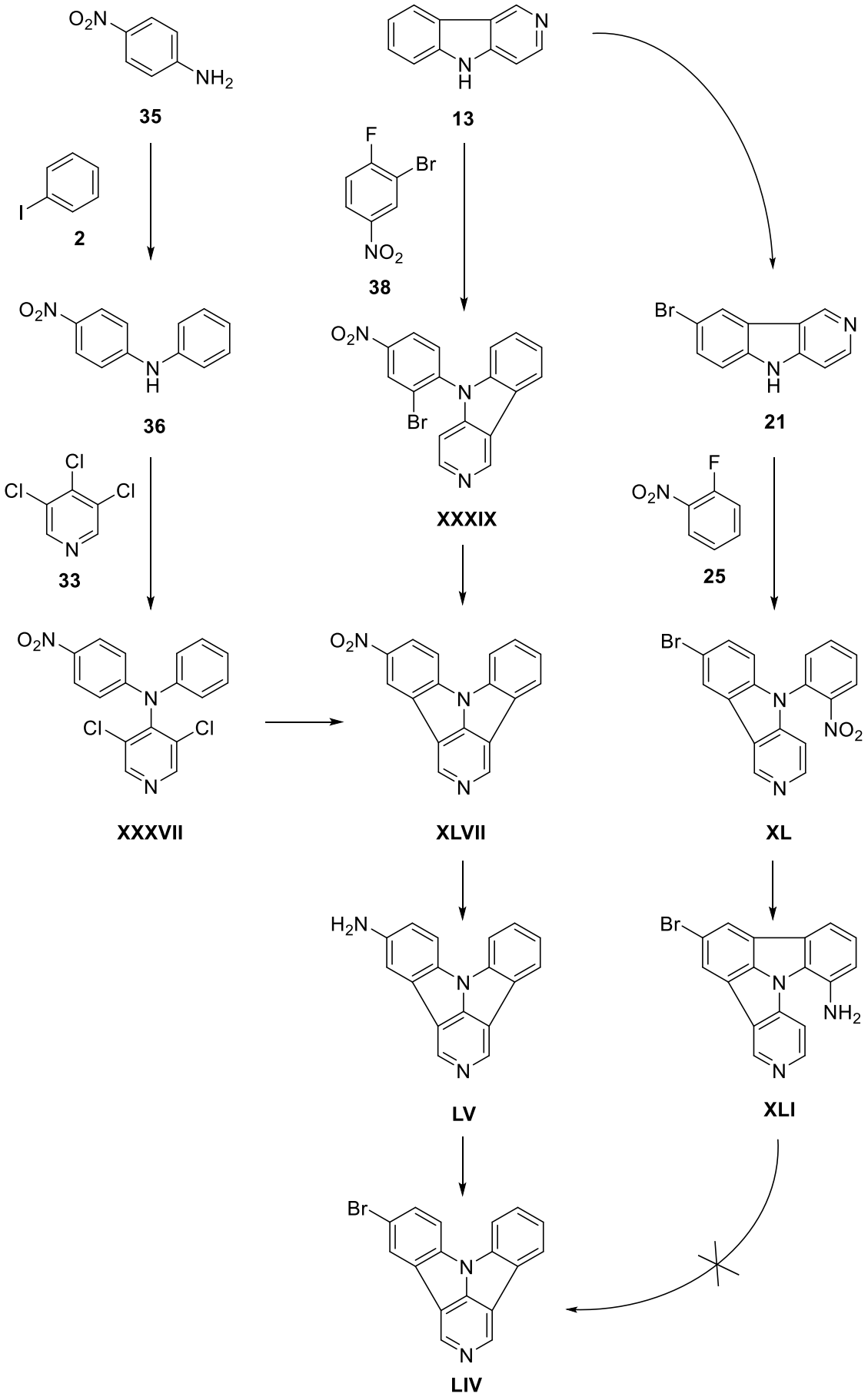
O2N
NH2
35
I
2
O2N
N
H
36
Cl
Cl
Cl
N
33
O2N
N
Cl
Cl
N
XXXVII
N
N
H
13
F
Br
NO2
38
O2N
N
Br
N
XXXIX
O2N
N
N
XLVII
H2N
N
N
LV
Br
N
N
LIV
Br
N
N
H
21
F
O2N
25
Br
N
NO2
N
XL
Br
N
NH2
N
XLI

A.2.3 Post-functionalized approaches

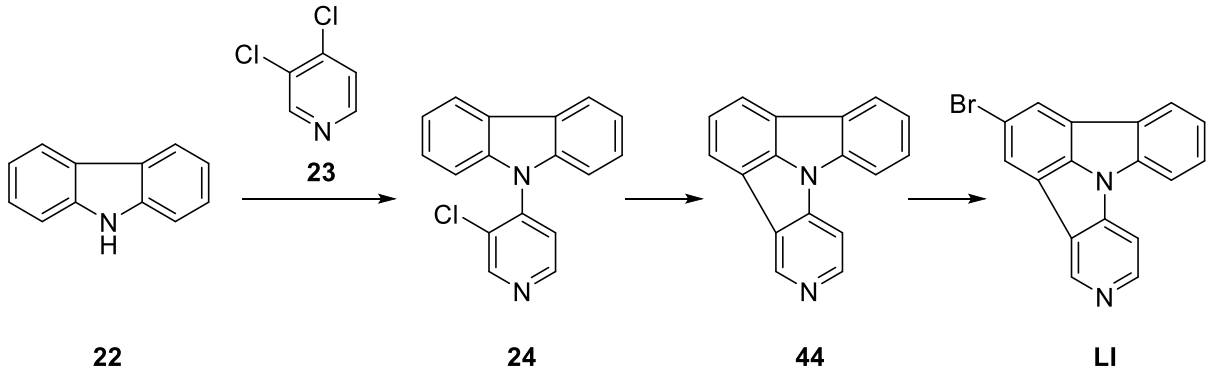

22 **24** **44** **LI**

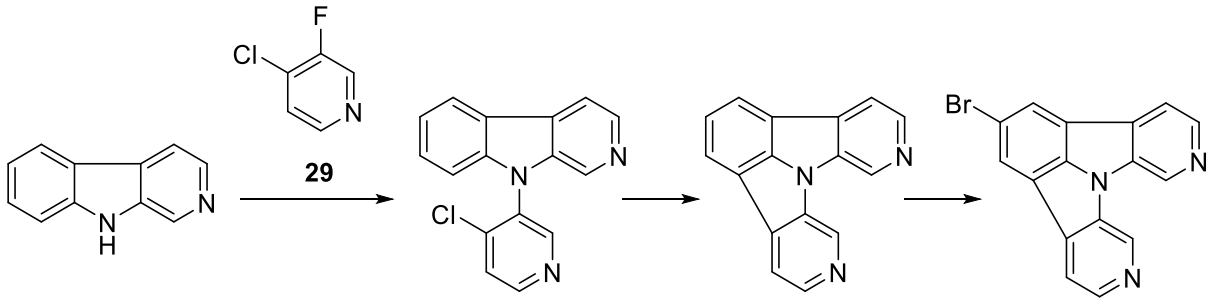

9 **30** **XLV** **LII**

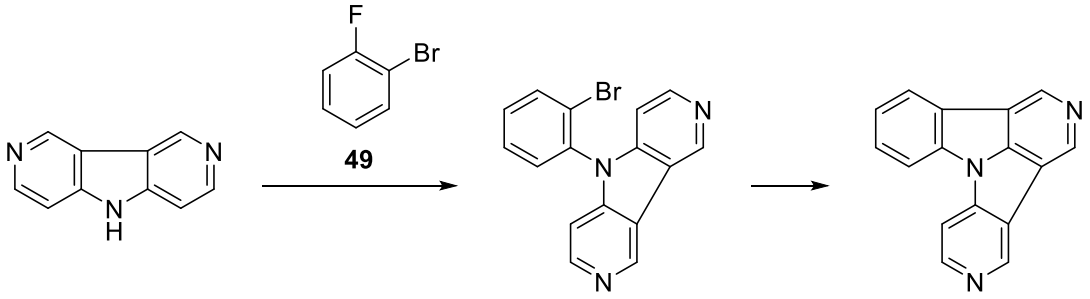

19 **XLII** **48**

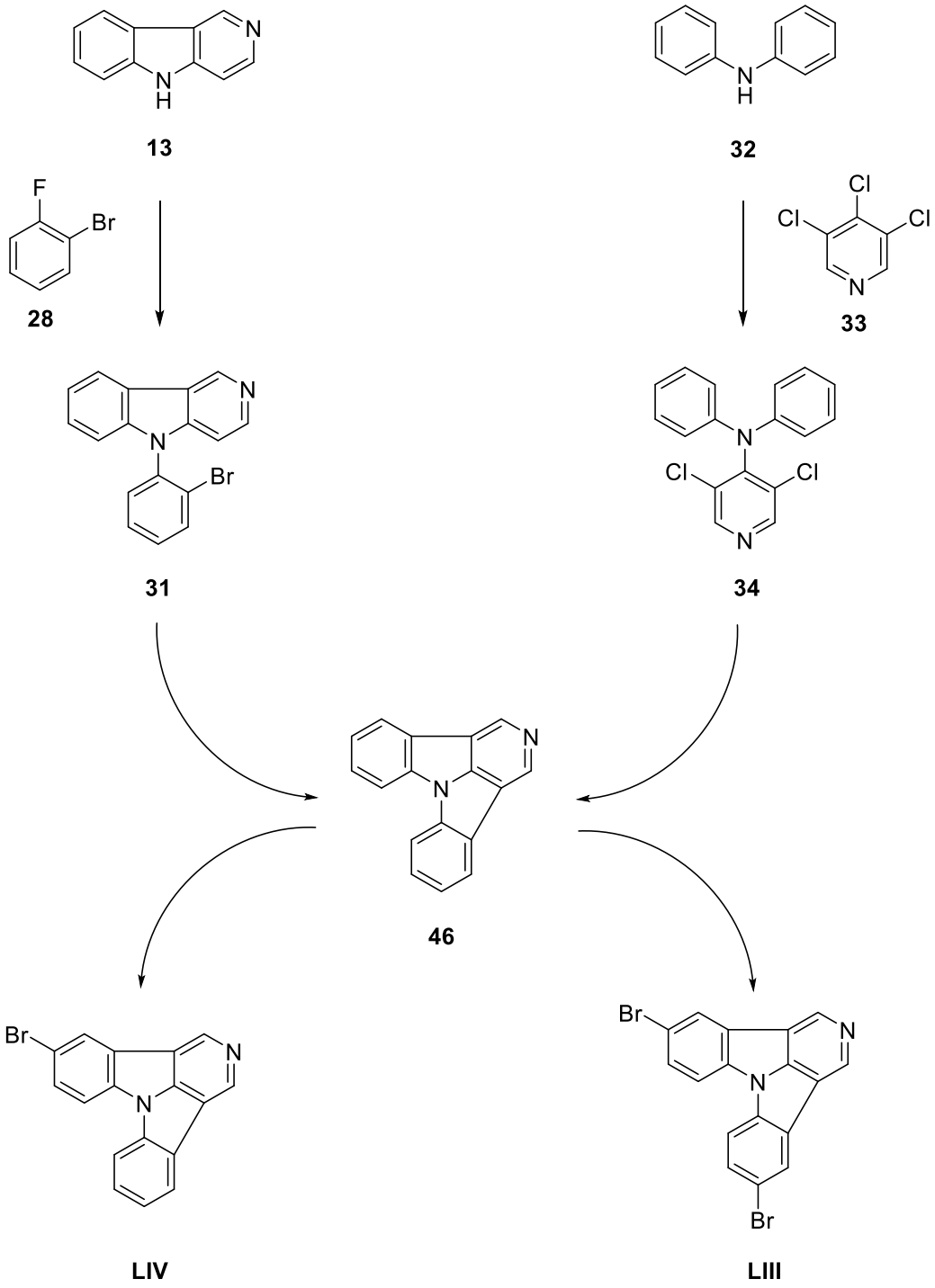
13
32
28
33
31
34
46
LIV
LIII

A.3 Donor-Acceptor coupling

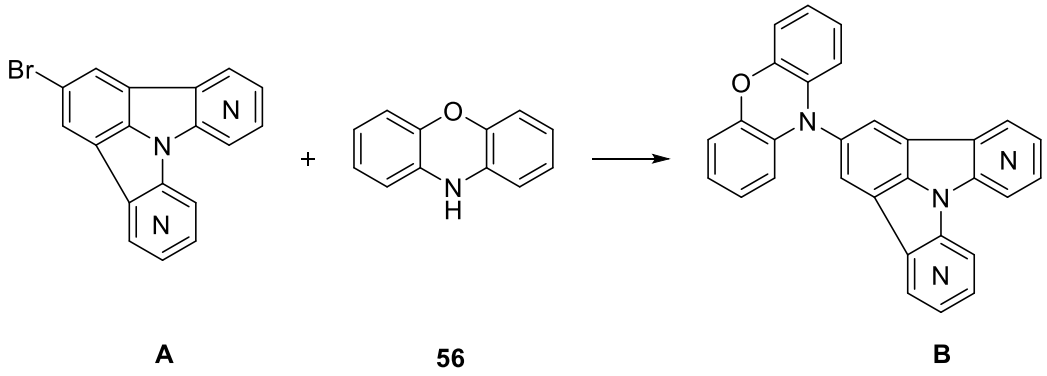

A **56** **B**

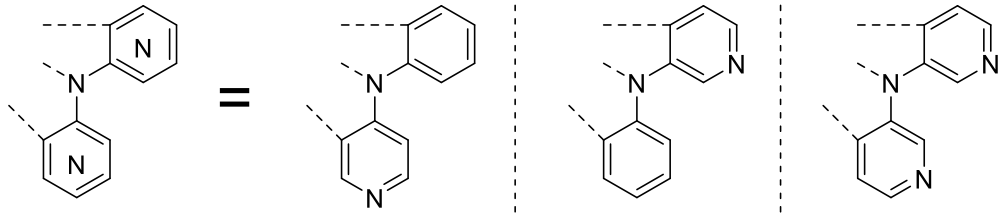

A/B **A: LI** **B: LVII** **A: L** **B: LVIII** **A: LII** **B: LIX**

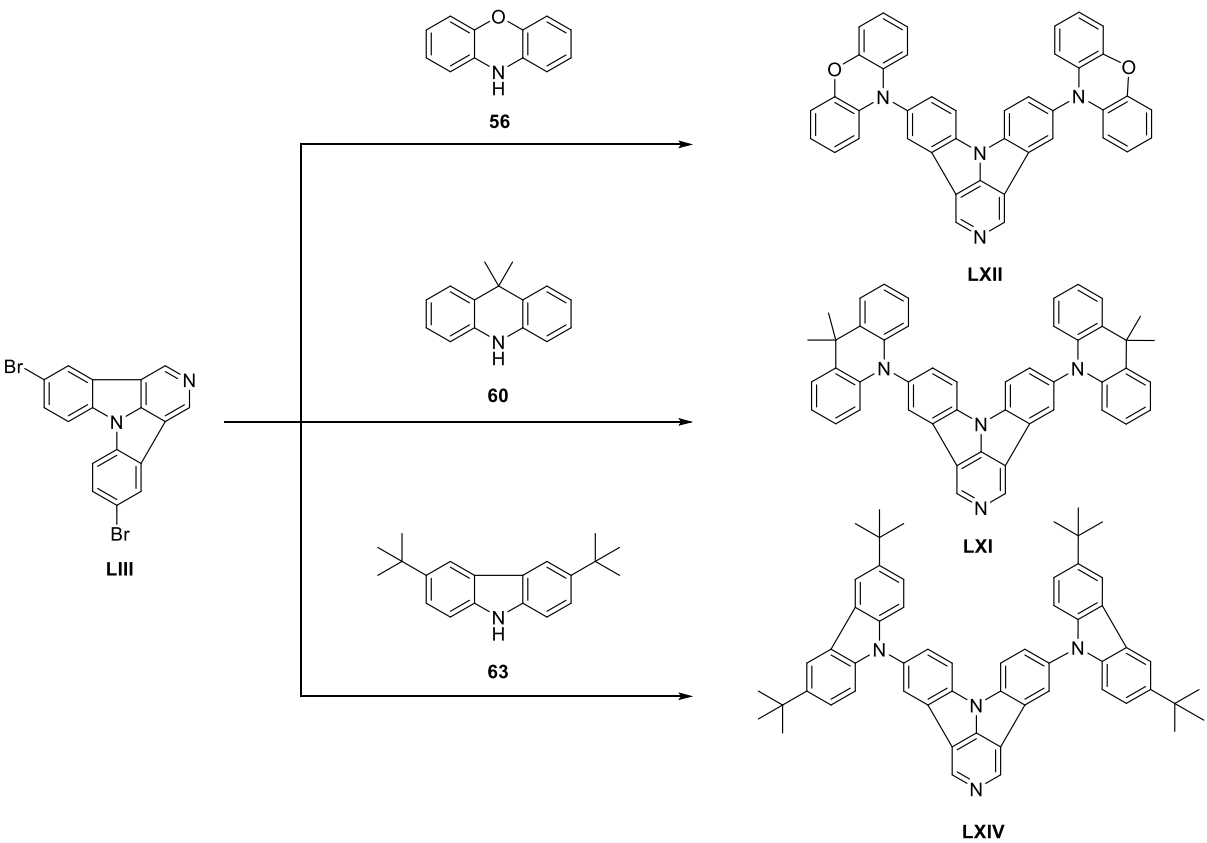

A.4 Synthesis of the Pd-NHC catalyst

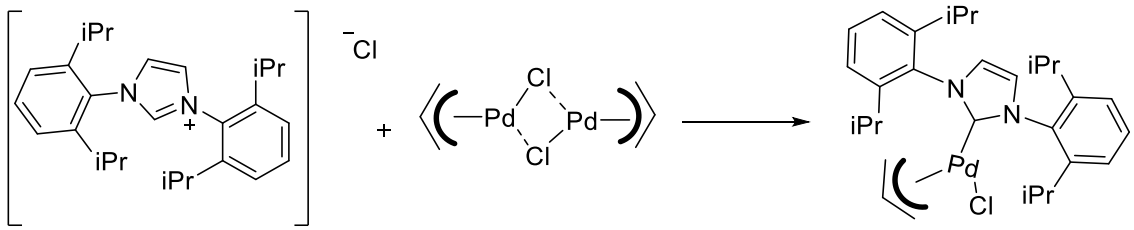

65 **66** **67**

B. General Part

B.1 Organic electronics

The technological highly important field of organic electronics deals with engineering of organic molecules and their use in electronic devices. Especially, their extensive applications in organic semiconductors, such as organic field effect transistors (OFETs), organic photovoltaic cells (OPVs) and organic light emitting diodes makes research and development of this technology very important and promising in today's electronic generation. The ability to create energy efficient, lightweight and flexible devices gives an attractive inducement to further improve materials while keeping extremely low costs. Research in this topic is constantly evolving and thereby new simple processing technologies even manage the use of compounds in specific inks to establish printable conductive dyes. These can be coated on low price substrates over a large area, but still keep the used volume very small.[1],[2] In general, application for organic electronics are limitless in many different technological fields.

B.2 Organic light emitting diodes (OLEDs)

B.2.1 History

In the early 1950s, the French scientist A. Bernanose[3] and his colleagues showed first connections between electroluminescence and molecular excitation due the acceleration of charge carriers in a high electric field. Almost 10 years later Pope *et al.*[4] conducted similar experiments and observed especially electroluminescence in single crystals of anthracene and anthracene crystals, with 10^{-1} mol% tetracene impurity. Though only the containment of traces, luminescence of the impure crystals showed already tetracene fluorescence.

After many years of research and improving, in 1987, Tang and Van Slyke[5] constructed a novel electroluminescent device by using organic materials as emitting elements, which represented the first reasonable OLED device.

Over the years OLED technology improved much more and today they are the most advanced technology within organic electronics. Even if today's OLEDs show less system efficacy at the luminaire level as the classic LEDs do, they have a lot of features, why they should be favored, compared to their inorganic counterparts. The emissive layer of OLEDs contains electroluminescent organic molecules and by the fact that this organic matter shows a soft behavior, the technology finds especial application in all kind of displays. Other than the brittle, rigid LEDs, the resulting flexibility of OLEDs makes fabrication of very thin and bendable devices possible. In addition, there is no need for any backlight emitting compared to LCDs, because photoemission is only generated through applied voltage to the molecules and the device can be kept very thin.[6],[7]

The generation of white light is achieved through a certain tandem structure of a blue, green and red emitter layer or a single layer structure that emits all three of them.[8] Overall, they are not only convenient for small smartphone displays, but also for television screens or large flat panel displays in any shape. The big advantage, compared to LEDs, is, that there is no need for connections of larger screen panels, for example *via* a light guiding panel, as the layer exhibits local homogenous properties. Furthermore, these optoelectronics provide a wide spectral range of colors, but can on the other hand also provide pure white light at good efficiency, as well as keeping a good contrast ratio stable and therefore OLEDs show also a high potential for the use of future light sources. The fact, that they don't contain any toxic substances, like for example mercury, compared to compact fluorescent lamps, is another advantage, not only in production cost, but also in recycling and environmental impact. Of course, costs in general are held very low, as the need of amount for organic substances, to achieve an emissive nanolayer, is not high. [7],[9],[10],[11]

Following table shows the luminous efficacies of common lighting sources. It is to mention, though white OLEDs are yet to achieve 92 lm/W, theoretically calculations predict up to 210 lm/W.[12]

Table B.1: Luminous efficiencies of different lighting devices[13]

Lighting sources	***Luminous efficacy [lm/W]***
Incandescent bulbs	10-22
Fluorescent bulbs	25-115
High-intensity discharge lamps	25-140
Low-pressure sodium lamps	60-150
(O)LED	27-92

B.2.2 Working principle

OLEDs are current-driven devices that utilize emissions from electronical excited states of molecules. The mechanism of organic semiconductors proceeds through a different mechanism than the energy band model of inorganic LEDs. As in organic materials, only weak forces, like Van-der-Waals interactions, are present, no valence and conducting bands are formed. In the easiest case, also referring to first OLEDs, the device consists of a single layer structure, where the emissive layer is placed between a cathode and an anode. If voltage is applied, electrons are injected at the cathode, while electron holes form at the anode. In

molecular disordered systems, the charge transfer takes place in hopping process, referred to a certain sequential redox process over molecules. Electrons are transferred through the lowest unoccupied molecular orbital (LUMO) from the anion radical of a molecule to another nearby neutral molecule for transport. On the other hand, electron-hole transport is established by the sequential transfer from electrons of a neutral molecule to a cation radical using the highest occupied molecular orbital (HOMO).

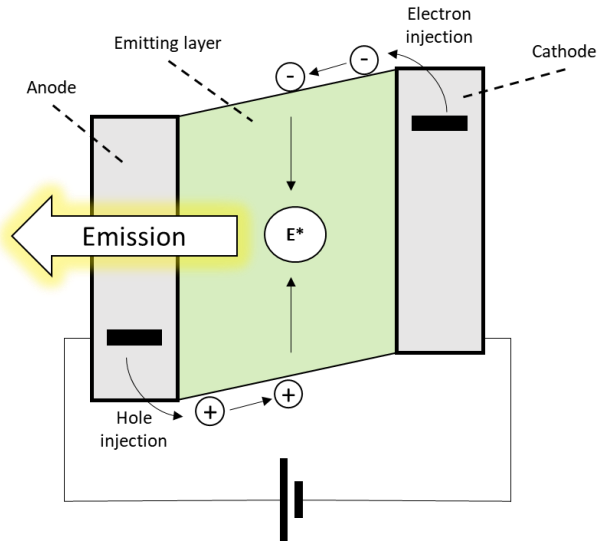

Figure B.1: Operation principle of an OLED.

As the electrons and the corresponding holes migrate through the layer, they recombine, as they meet, and form an electronical excited state of the molecule, called exciton. If an exciton relaxes back into the ground state, energy is translated into photoemission. Hence, the emitted wavelength, and thereby the emitted color, depends on the type and structure of the photoluminescent organic molecules, as it corresponds to the HOMO-LUMO gap of the material. Due to spin-statistics singlet and triplet states are formed in a ratio of 1:3 in OLEDs. Therefore, early OLED technology could only use ¼ of the energy of excitation, corresponding to the excited singlet state (S_1) and thereby causing fluorescence when relaxing back to the ground state (S_0). Unfortunately, the major part of the electric excitation, which refers to ¾, was converted into non-radiative decay, because of relaxing from the triplet state (T_1) to the ground state.[6] As an upcoming result, research investigated several approaches to improve this internal quantum energy, which will be discussed below.

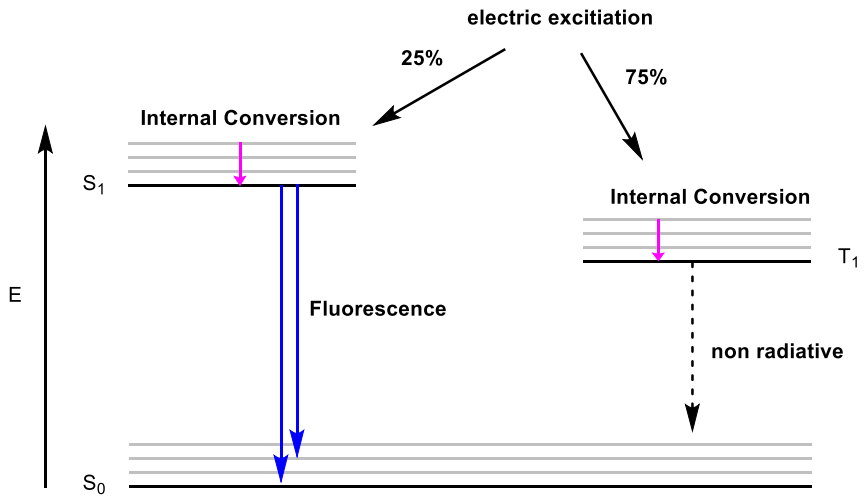

Scheme B.1: Jablonski Scheme of an early OLED emitter.

As already mentioned, structurally early OLEDs consisted of a three-layer system: two electrodes and the emissive layer. These layers are usually applied *via* spin or slot die coating[14], as well as vapor deposition.[15]

In classical physical vapor deposition (PVD), the material of need is vaporized, using a specific heat source and transported through a vacuum to the substrate. *Via* a temperature gradient the vapor condenses onto the surface, creating a thin layered deposit.[15] Conventional spin coating relates to a simple technique of fabrication, by the addition of a thin, planar film to a surface. In order to deposit the desired layer, the component has to be diluted first. Subsequently, the solution is dispensed on the spinning substrate, leading to a layer thickness, determined by spinning speed, surface tension and viscosity of the solution. The final coating is usually obtained by removing the solvent due evaporation.[16] On the other hand, the slot die coating process uses a liquid, which is delivered through an immobile slot gap onto a moving substrate, filling the space in between. As the liquid forms a coating bead and a layer is carried away by moving the substrate, in relation to the gap, a thin film is obtained. To dry the coating, usually solidification or evaporation is used.[14] All announced methods show their advantages and disadvantages, nevertheless they can also be used to generate multilayered structures.

To gain high internal quantum efficiency for electroluminescence, both electrodes must inject either holes or electrons optimally in the organic layer. This can be achieved by low driving voltage, good charge balance, and confinement of the injected charge carriers. As a result, the probability of emissive recombination increases. This can be realized by introducing hole-transport and electron transport layers located between the electrodes the emissive layer. The energy barriers for injection of charge carriers are reduced and the recombination rate rises.

These positive effects are realized by adding further layers, for electron or hole transport, as well as blocking layers, in a sandwich structure (see Figure B.2.). The whole device, in particular, can achieve a thickness of 100 – 500 nm. Though systems differ, the following components are always used:[6],[17]

Substrate: helps to support the OLED and gives stability to the device. The substrate is usually glass, a thin foil, or a plastic polymer, which can optionally also be transparent. Usually, the substrate builds the base, where the other components are placed on top, often applied *via* spin or slot coating, as well as vapor deposition.

Anode: usually transparent indium tin oxide (ITO), which promotes the electron-hole injection in the HOMO as an adequate conductor. Polystyrene based polymers are sometimes used as an alternative.

Cathode: silver or aluminum are most common for this component. OLEDs using metals like barium, calcium and even transparent cathodes are also established, depending on the type and application of the device.

Emissive layer: organic molecules which emit a certain wavelength of fluorescence or phosphorescence, caused by electrical excitation. The applied current is proportional to the brightness of the OLED.[17]

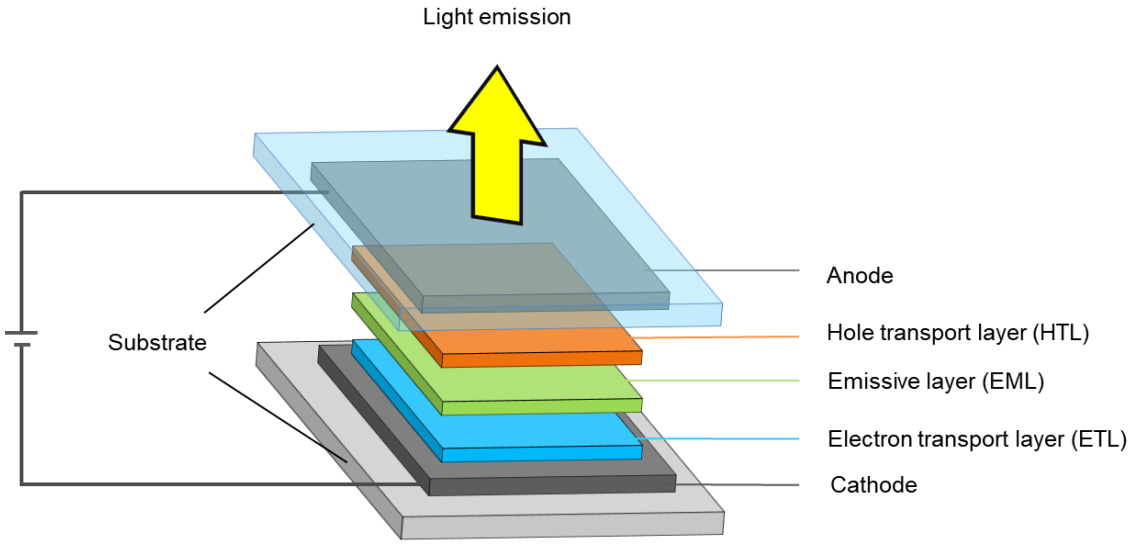

Figure B.2: Multilayer structure of an OLED device.

B.2.3 Host Materials and Phosphorescent OLEDs (PhOLEDs)

Host materials are often used in OLEDs, as the exhibit kind of a matrix to lower the concentration, especially of phosphorescent and TADF emitters. Thereby, the concentration of excited states is lowered, which reduces processes competitive to photoemission.

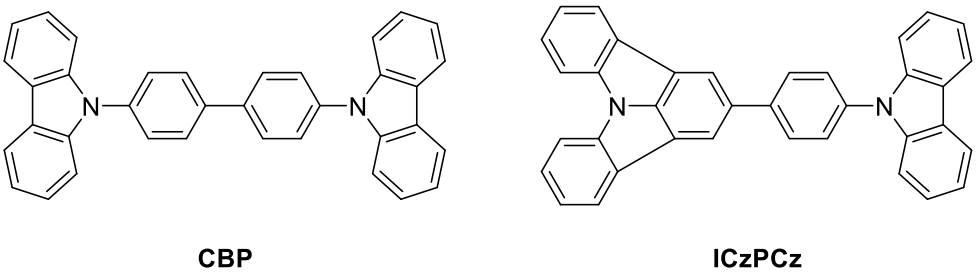

CBP **ICzPCz**

Scheme B.2: Examples for host materials used for OLEDs.[18],[19]

As research improved, it was obvious to develop a method for using all the excitation energy for conversion into visible radiation. A possibility to achieve this, is transforming the excited singlet states (S_1) into triplet states (T_1) and thereby change fluorescence into phosphorescence, which leads to a total internal quantum efficiency of up to 100 %.[6] This can be realized using the process of intersystem crossing (ISC), achieved through spin-orbit coupling[6], caused by heavy atoms. The ISC leads to the mentioned excited state conversion from $S_1 \rightarrow T_1$ and makes utilization of maximum internal quantum yield possible. Cyclometalated Ir or Pt complexes exhibit such high spin coupling behavior and show strongly potential as phosphorescent emitters, because of high efficiency rates even at room temperature.[20] These complexes facilitate the lowest excited triplet state (T_1) to the ground state (S_0) transition ($T_1 \rightarrow S_0$) for electroluminescence by phosphorescence.[21]

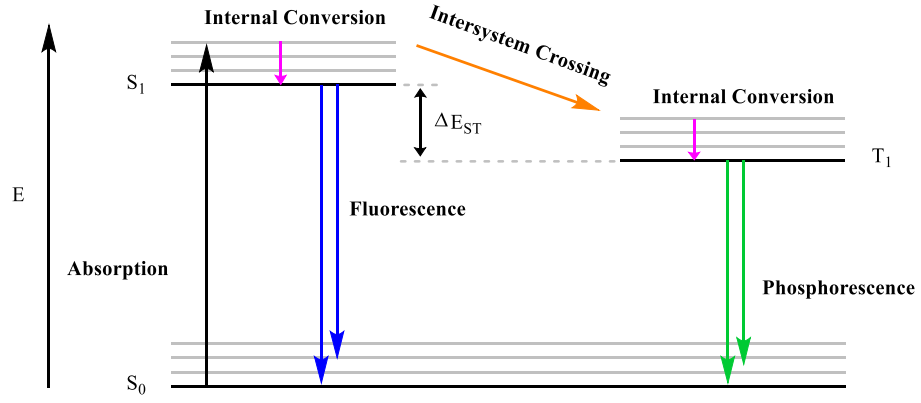

Scheme B.3: Jablonski scheme of a PhOLED emitter.

As a matter of fact, the phosphorescent heavy metal complexes have a relatively long lifetime of the excited triplet state (milliseconds) and cause a resulting dominant triplet-triplet annihilation at high currents.[22] This could also support undesired long-range exciton diffusion, which may lead to quenching in the neighbored layers. Hence, host materials are here a very important solution to reduce these concentration related quenching effects.[18]

Another disadvantage may be the high cost of those heavy metal complexes, though only concentrations of about 10% are used in the emissive layer. Typically iridium complexes used for phosphorescence in OLEDs are shown in Scheme B.4. [18],[23]

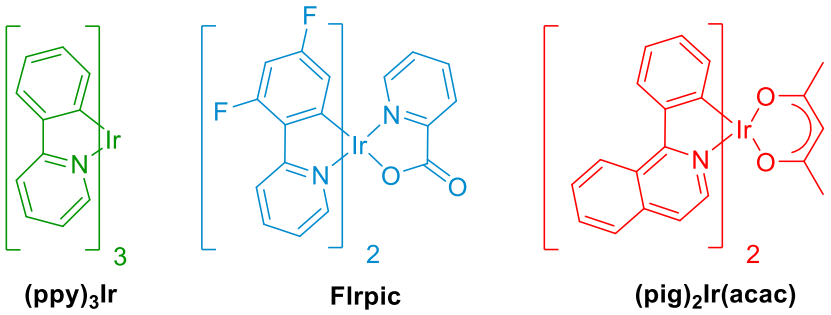

$(ppy)_3Ir$ **FIrpic** **$(pig)_2Ir(acac)$**

Scheme B.4: Common Ir complexes used as triplet emitters in PHOLEDs.

B.2.4 Thermally activated delayed fluorescence (TADF)[18]

A possible method to avoid the discussed disadvantages of heavy metals in emissive layers, is the use of an unimolecular mechanism called thermally activated delayed fluorescence. It consists of prompt fluorescence (PF) and delayed fluorescence (DF). The PF occurs immediately (scale of nanoseconds), caused by fast decay from the excited singlet state (S_1) to the ground state (S_0). On the other hand, DF can be explained through the process of reversed intersystem crossing (RISC), as triplet excitons (T_1) are converted into singlet excitons (S_1) to undergo again PF. Overall the emitted fluorescence is thereby increased to several microseconds, which makes TADF materials very promising for OLED emitting layers. There are four important processes to mention:

- The recombination of electrons and holes lead to a singlet-to-triplet ration of 1:3.
- Vibrational relaxation transfers the high exciton states to lower ones.
- Thermal activation supports the transfer of the generated triplet excitons (T_1) *via* RISC to the singlet exciton (S_1).
- Singlet excitons states (S_1) relax back to the ground state (S_0) under emission of photons as fluorescence.

To increase RISC, which represents the key-step of TADF emission, the energy (ΔE_{ST}) between T_1 and S_1 must be very small. Controversially, as a matter of fact, the fluorescent radiative decay rate (k_r) must be high enough to avoid the transition to non-radiative decays, such as thermal energy. The strategy to obtain these special TADF molecules, which exhibit a spatially separated HOMO and LUMO, is the introduction of steric hindrance in structure, or

the use of certain electron donor-acceptor bipolar systems, that show a small overlap of the HOMO-LUMO. This increases the probability of the charge transfer state.

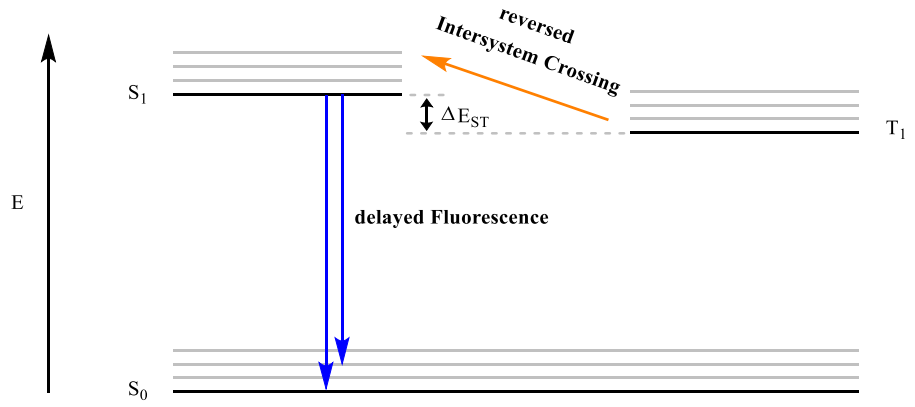

Scheme B.5: Jablonski scheme of a TADF emitter.

Studies showed, delayed fluorescence could already be observed at values of ΔE_{ST} = 0.43 eV for PPZ-4TPT, a molecule that consists of a 5-phenyl-5,10-dihydrophenazine (PPZ) donor unit and a triphenyl-1,2,4-triazole (TPT) acceptor unit. Nevertheless, the ideal energy difference between the excited singlet-triplet state refers to a common gap of ΔE_{ST} = 0.24 eV.[24] As mentioned earlier white OLEDs consist in multilayer form of several layers emitting different wavelengths. The main task, is the development of long-life blue emitters, which exhibit high triplet energies and high photoluminescent quantum yield.[25]

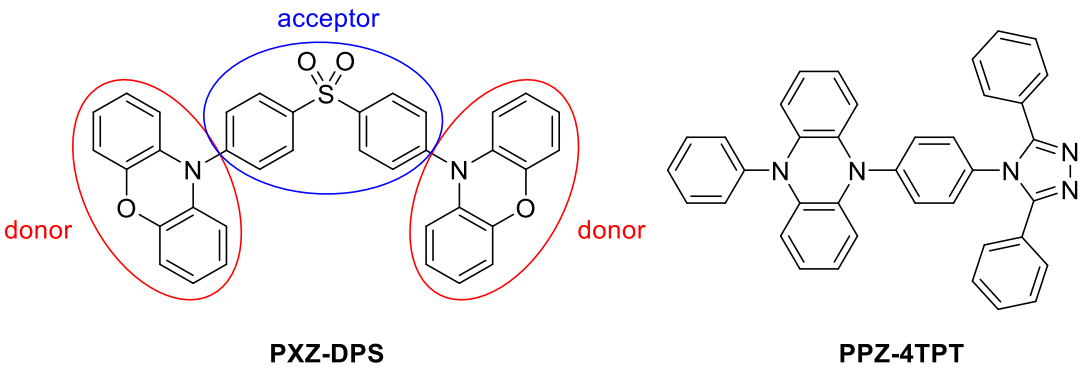

Figure B.3: Examples showing the different parts of a bipolar TADF emitters.[24]

B.3 Arylamine based materials

Materials based on arylamines, like triphenylamine (TPA) or carbazole (Cz), are widely applied as donor structures in the field of OLEDs. In the last years, our research group introduced several novel bipolar systems, utilizing the planarization as tool to control donor strength, as it

decreases with increasing planarization. This can be explained by the contribution of the nitrogen lone pair to the aromaticity of the pyrrole ring generated by planarization.[26] The electrons are less prone to a delocalization in a donor-acceptor system, due the lone pair is more bound to the core of the arylamine. The novel structures exhibit in addition high triplet energies and show good thermal stability, what makes them very attractive in the field of OLED technology.[27],[28] Research in our group showed, as the donor strength lowers, the acceptor properties of indolocarbazole (ICz) simultaneously increase, according to further planarization. Further research on these observations can thereby lead to many novel applications in OLED systems.

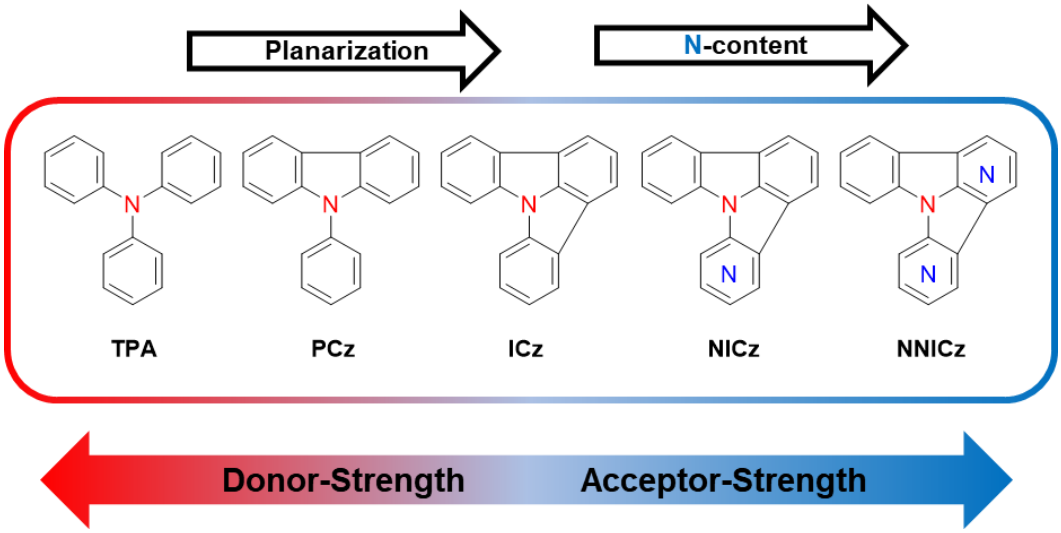

Figure B.4: Influence of planarization and nitrogen content on the electron acceptor/donor properties.[28]

The increase of acceptor properties of ICz derivatives in bipolar systems, utilizing substitution of the framework with cyano groups, led to further improvement of pure blue TADF emitters.[29] Recent studies on the incorporation of electron-withdrawing pyridine-like nitrogen atoms in the ICz scaffold revealed a further increase of the acceptor strength of the molecules. Therefore, the research and development of novel nitrogen-substituted ICz (NICz) based donor-acceptor molecules appears to be a very promising approach to achieve new TADF emitting materials.[28]

B.4 Goal of the thesis

The goal of this thesis is the development of new donor-acceptor systems, which can be potentially applied as TADF emitters in OLEDs.

Earlier research according to Kader *et al.*[28] already showed the influence on the HOMO and LUMO by adding further nitrogen atoms to the ICz scaffold (Scheme B.6). The incorporation has an impact on lowering the HOMO as well as the LUMO. Furthermore, it was observed, that not only the nitrogen amount, but also the exact position of the introduced heteroatom within the scaffold, has large impact on the alteration of the energy levels, which can be explained *via* spatial distributions of the orbitals.

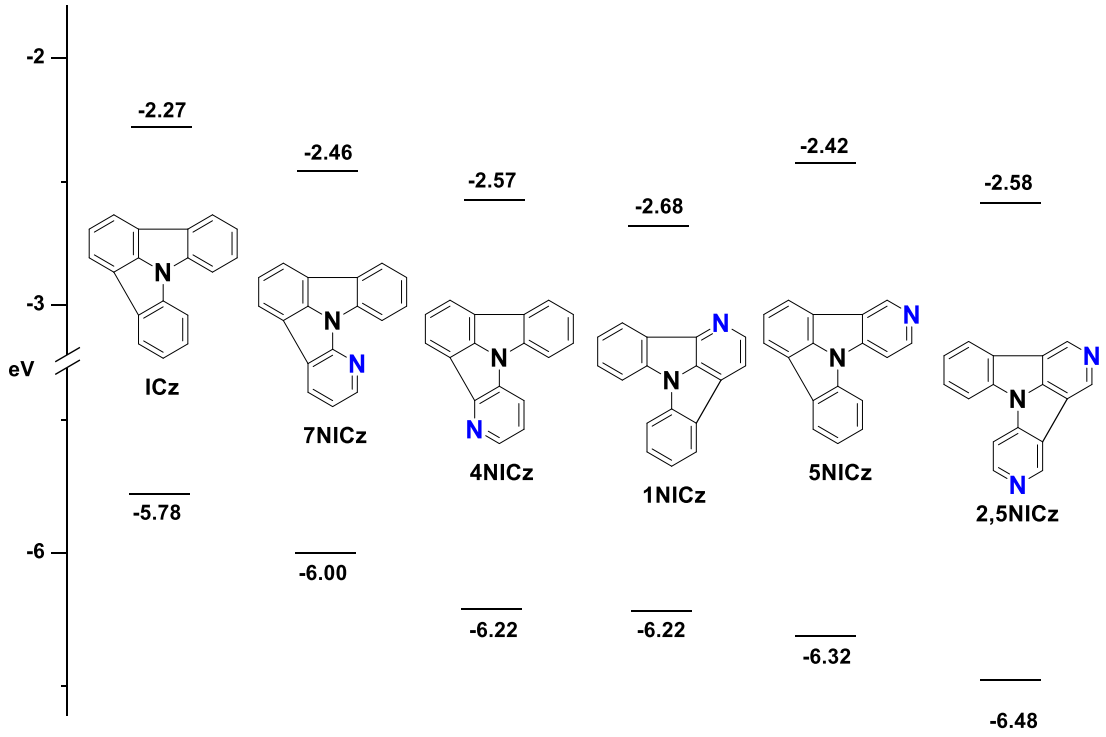

Scheme B.6: Schematic representation of the energy levels of HOMOs and LUMOs in potential scaffolds.[28]

The potential of NICz based emitters, caused by the possibility to fine-tune the molecular properties on the one side, as well as high triplet energies and good thermal stability which were observed for suchlike planarized systems, on the other, makes them interesting for blue and white OLED applications. Therefore, synthesis, properties and characterization exhibit a new contribution concerning OLED technology.

C. Specific Part

C.1 Introduction

Initially, in order to test a selection of several promising donor-acceptor systems on their TADF potential, theoretical calculations based on the density functional theory were conducted. As the focus was on the variation of novel acceptor molecules, common donor units were used to build these desired systems. Out of many possible bipolar molecules, only a few seemed to show optimal properties as TADF emitters, as they had auspicious results on singlet-triplet transition energy (ΔE_{ST} < 0.2 eV). Potential systems, that showed a wide range of different wavelengths over a large scale, were selected. A comparison of ΔE_{ST} and the emission wavelength of the selected systems is shown in Figure C.1.

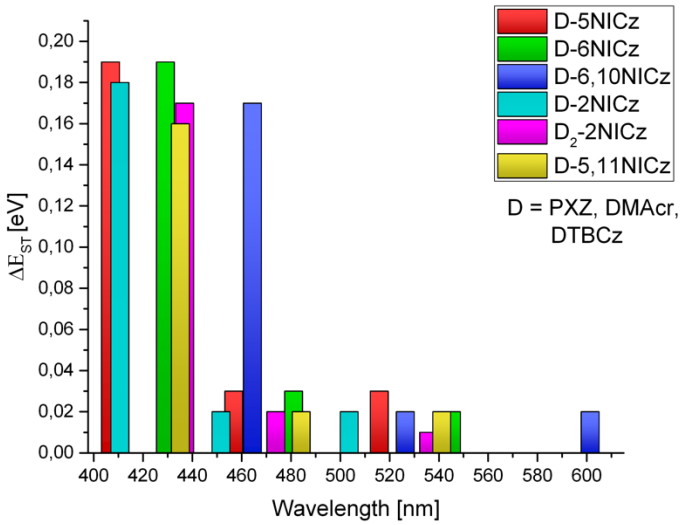

Figure C.1: Calculated emission wavelengths and ΔE_{ST} of potential donor-acceptor systems.

As the synthesis of blue TADF emitters is mainly desired, systems, in the left part of the diagram (Figure C.1), were chosen, by combining three common donors, with different NICz acceptors. Also, systems with proposed photoluminescence around 500 nm should be synthesized. Due the variation of different donors, linked *via* a C-N binding to the NICz acceptors in the system, the suggested first retrosynthetic approach leads to a cut between these two molecules. As the bond refers to a C-N binding, the forward reaction can be conducted using Buchwald-Hartwig amination (BHA).

The catalytic BHA cycle contains an oxidative addition of the halogenated species, followed by transmetallation, using usually a strong base like NaO^{t}Bu or KO^{t}Bu. In a next step the amine is introduced, while releasing an alcohol. At this point β-hydride elimination can occur as an undesired side reaction leading to a dehalogenated arene and an imine product.[30] The regular, desired final step leads to reductive elimination and formation of the C-N bond.

The following Scheme C.1 shows the catalytic cycle of BHA under used conditions within donor-acceptor couplings.

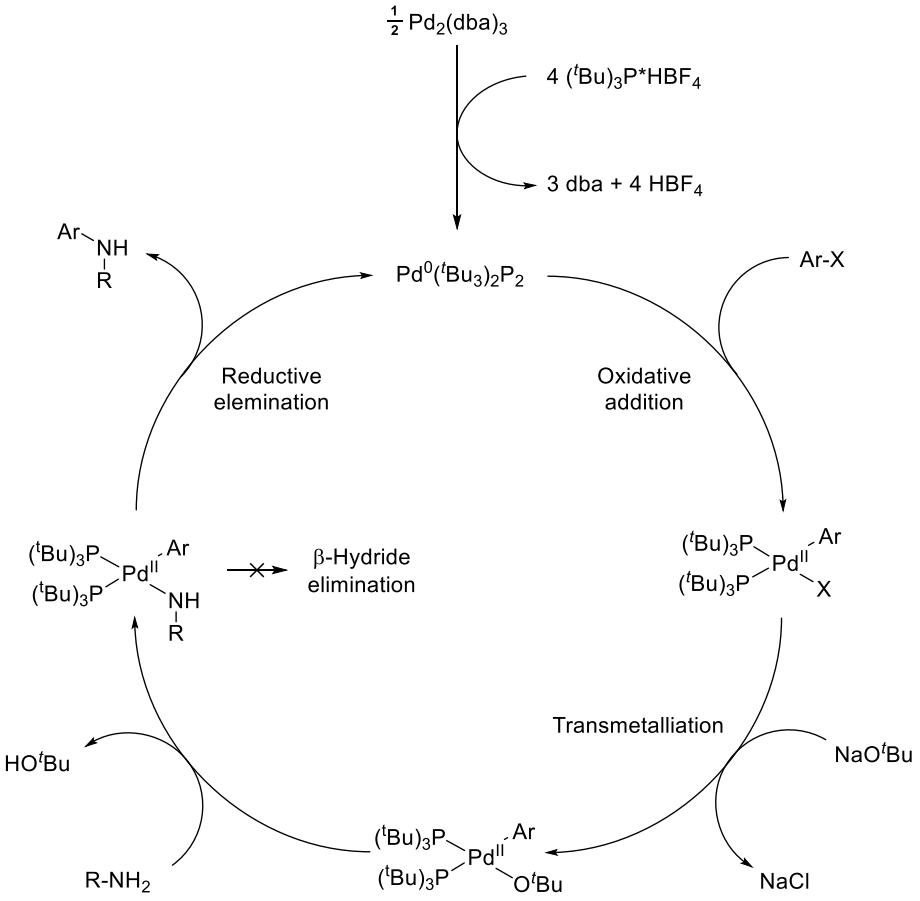

Scheme C.1: Buchwald-Hartwig amination using $Pd_2(dba)_2$, $(^tBu)_3P^*HBF_4$, and NaO^tBu.[31]

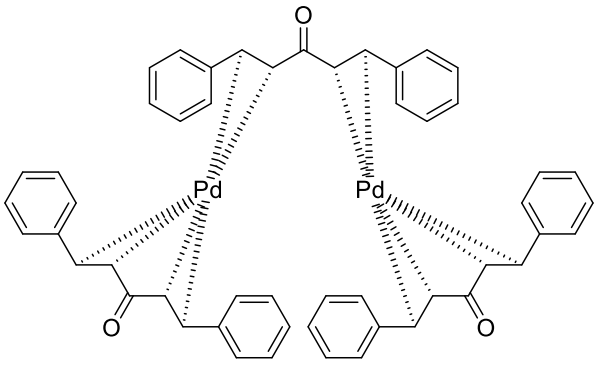

Scheme C.2: Structure of precatalyst $Pd_2(dba)_3$.[32]

As three aromatic rings can be used for positioning the additional nitrogen atoms, several structural types were obtained for the target systems. The different target systems, as well as the retrosynthetic approaches towards them are shown in the following Scheme C.3:

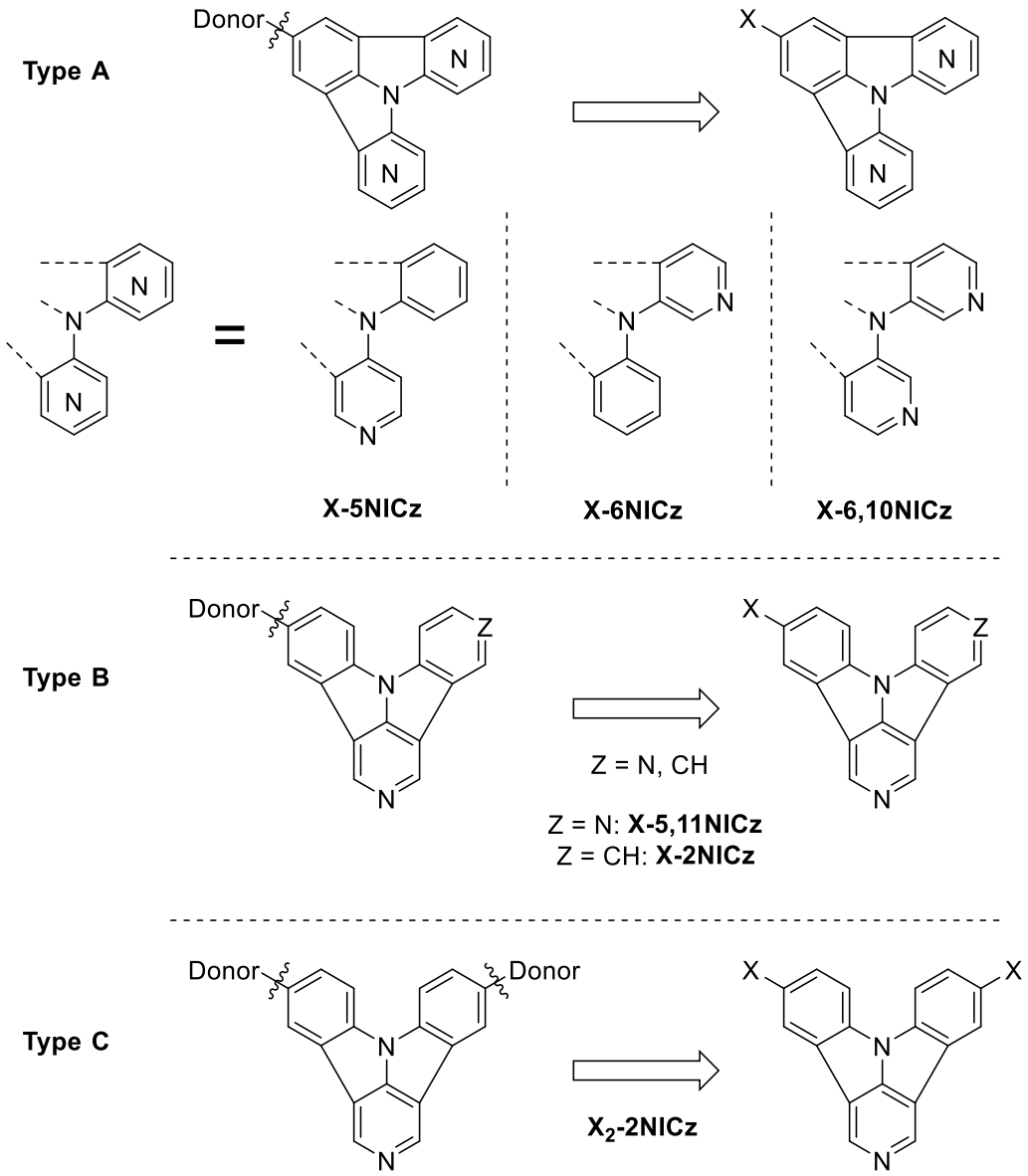

Scheme C.3: Retrosynthetic cleavage of donor-acceptor systems.

Thereby, the functional group X leaves two different approaches to be added to the system: either *via* pre-functionalization at the beginning of the acceptor synthesis, or post-functionalization of the acceptor building block before C-N coupling. Initially, the post-functionalization route was preferred, as the synthesis would be less prone to unwanted side-reactions or dehalogenation during the synthesis.

For the donating species, following building blocks, already applied, not only in blue TADF emitters, were utilized:

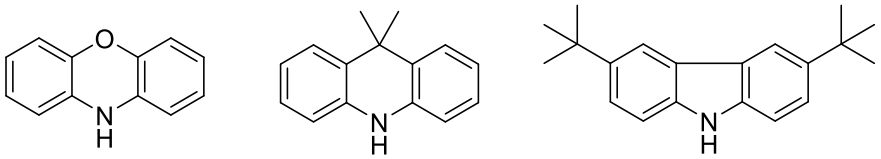

PXZ **DMACR** **DTBCz**

Scheme C.4: Selected donors for bipolar target systems.

These materials are often used as donors, not only because of their donation properties, but also because of their good thermal stability and oxidation reversibility.[33],[34] Phenoxazine (PXZ) and di-*tert*-butyl-carbazole (DTBCz) are commercially inexpensive and easily available. For dimethyldihydroacridin (DMAcr) literature known procedures according to Liu *et al.*[35] and Reddy *et al.*[33] were conducted.

Although the synthesis of NICz isomers is already well established, the synthesis of the functionalized acceptor building blocks is unknown to literature and therefore the main task of the synthetic work in this thesis.

In the case of ICz and similar NICz isomers, the ring closing reaction step towards the planarized systems was already established *via* several synthesis methods: flash vacuum pyrolysis[36],[37], CHA[28] and diazotization[28]. As flash vacuum pyrolysis requires special laboratory equipment, the approach was not conducted and therefore the focus was on CHA and as an alternative, also diazotization. CHA exhibits a very good pathway towards NICz ring closing, because of the high commercial availability of the necessary, low prized, halogenated benzene and pyridine derivatives. Furthermore, according to previous work on triarylamines in the Fröhlich group[27],[28], these pathways were already well researched.

Following retrosynthetic schemes show the disconnection of not functionalized structures, for better overview and understanding. Based on the different target acceptor types, the major described strategies for ring closing (CHA, diazotization) lead to subsequent carboline (Cb) disconnections (see Scheme C.5). These can be divided into two strategies which differ in where the functionality for the ring closing is placed. Approach Cb-a starts from commercially available pyridine derivatives and carbolines that can be synthesized straightforward. In contrast Cb-b needs functionalization on the carboline scaffold which represents a more challenging and time-consuming synthesis and is thereby not considered in this work.

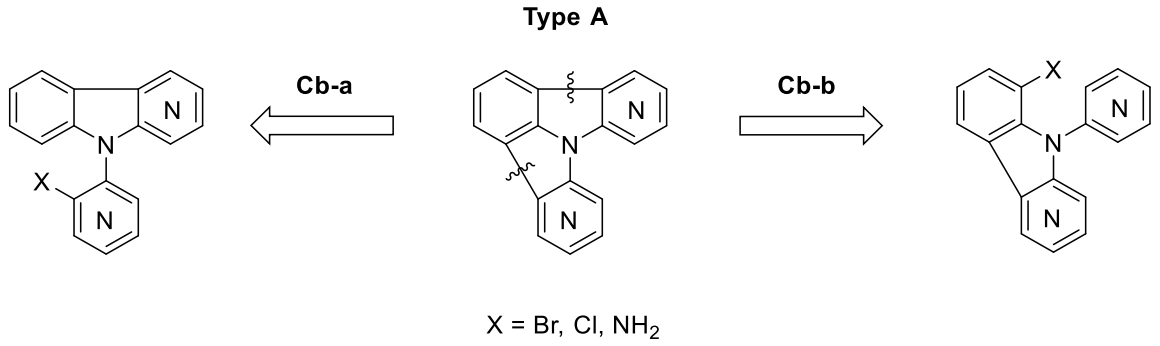

Scheme C.5: Possible disconnection approaches for type A acceptors.

Though simultaneously ring closing *via* double CHA might not lead to the desired product, because of selectivity for type A acceptors, for type B, in the case of Z = CH, it appeared to be also a good opportunity for receiving the final structures. Furthermore, this triarylamine (TAA) synthetic strategy was already established in a modified version by Kautny *et al.*[27]

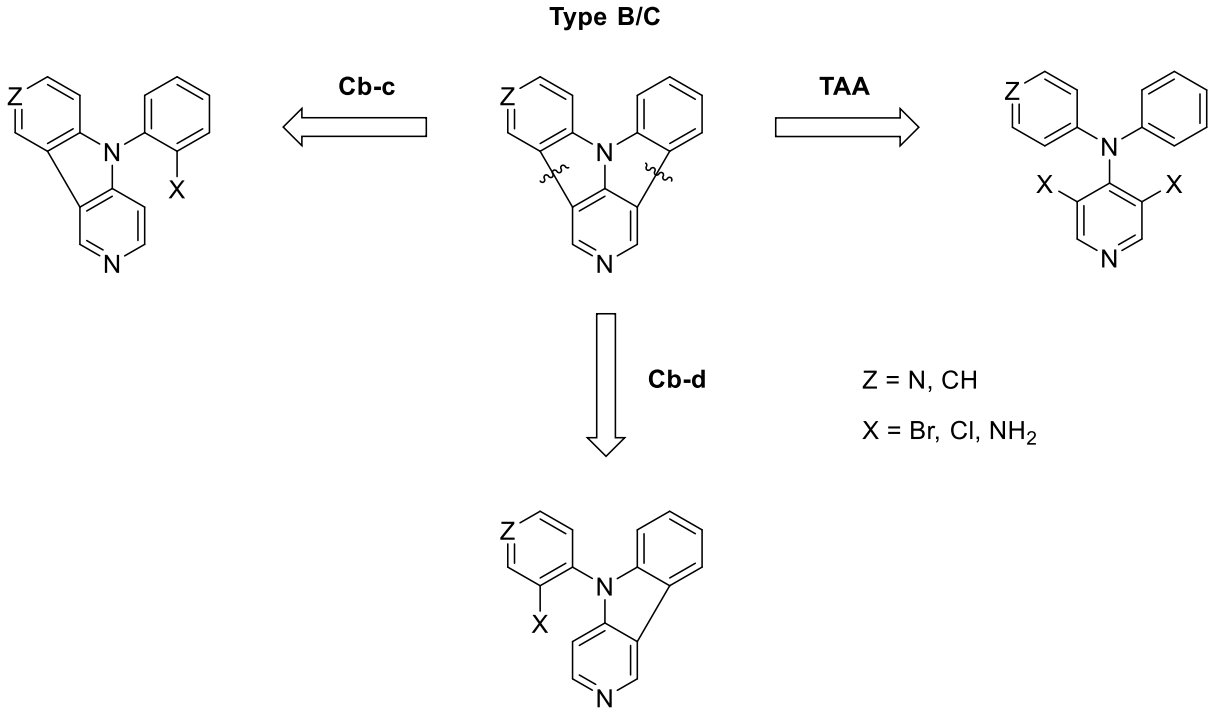

Scheme C.6: Possible disconnection approaches of type B/C acceptors.

As already mentioned for all acceptor types, the closing of the ring should be tried first, using the CHA of the Cb routes. In case the approach and variations appeared to fail, for some structure accomplishments, the diazotization route was chosen according to the procedure of Dunlop and Tucker.[38]

Anyhow, for both CHA and diazotization, an arising challenge in the ring closing step is the possible formation of two different isomers depicted in Scheme C.7.

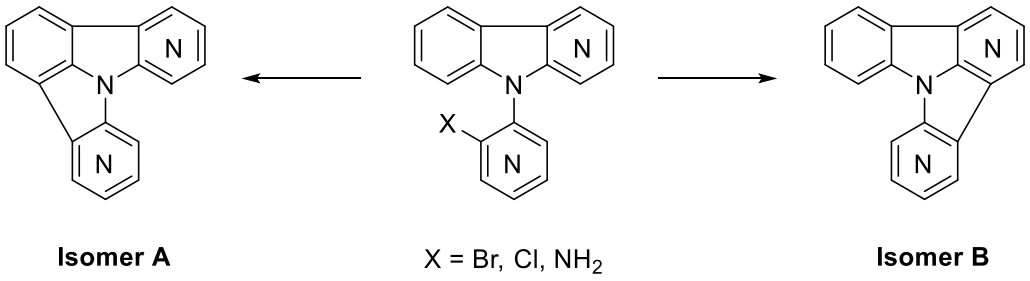

Scheme C.7: Possible ring closing directions, obtaining different NICz isomers in the Cb-a route.

Since CHA is very often used in this thesis, following shows the proposed catalytic cycle for isomer A of type A acceptors:

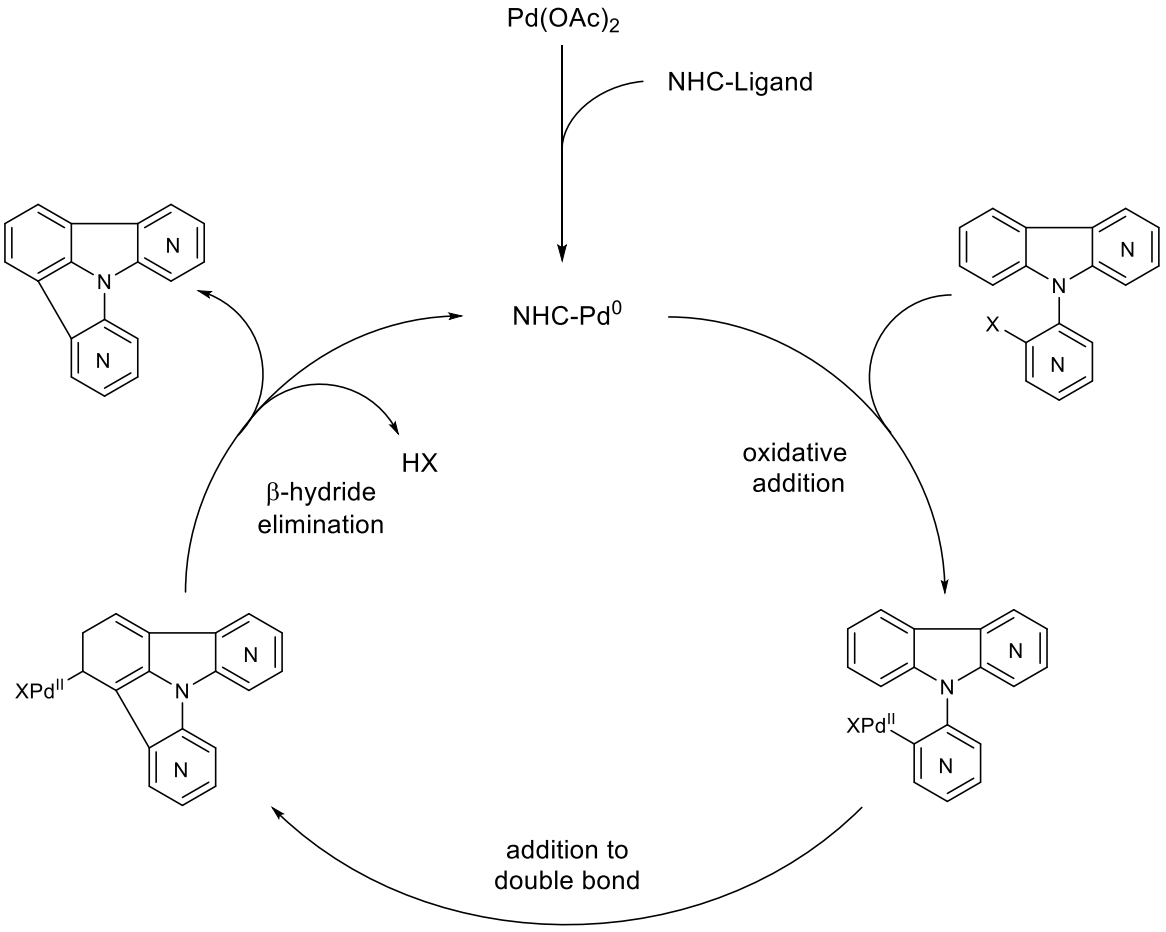

Scheme C.8: Proposed CHA mechanism towards acceptor isomer A.[39]

A final disconnection approach leads to only a few molecules as starting material, including halogenated benzene and pyridine derivatives, carbolines, carbazole (Cz), pyrrolodipyridin (PDP), as well as diphenylamine (DPA) and phenylpyridineamine (PPA) in the case of the TAA route. In the forward synthesis, these C-N bonds can be formed by nucleophilic substitution as primary strategy, respectively BHA or Ullman reaction as alternative.

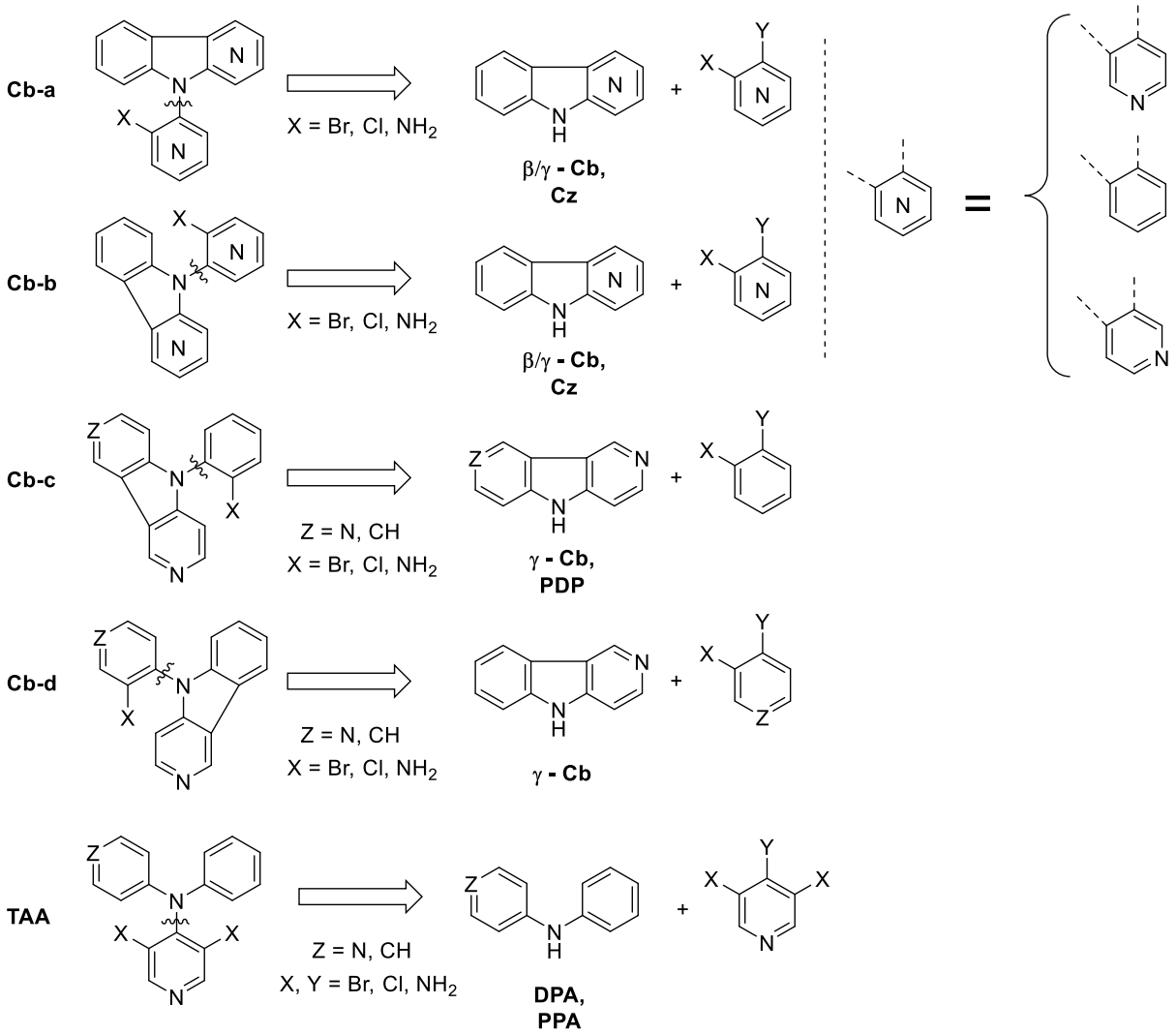

Scheme C.9: Disconnection approach of carboline and triarylamine derivatives to starting materials.

C.2 Donor Synthesis

C.2.1 9,9-Dimethyl-9,10-dihydroacridine

As already mentioned, synthesis of DMAcr was conducted, as the starting materials are inexpensive, easy to handle and lead to good yields over a 3-step reaction.

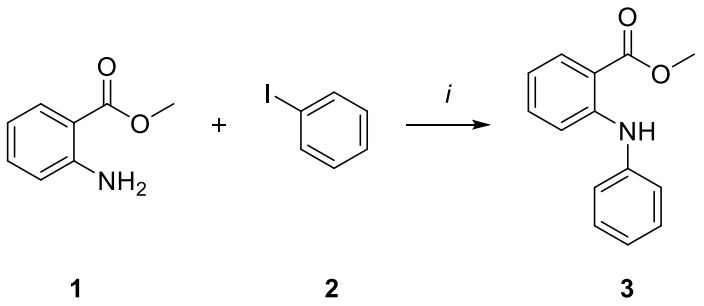

Scheme C.10: Synthesis of **3** *via* Ullmann condensation. i: Cu, K_2CO_3, *o*-DCB, 180 °C.

According to a protocol of Liu *et al.*[35], the reaction was performed using an Ullmann condensation to achieve the desired product. The synthesis gave compound **3** with an overall yield of 80%.

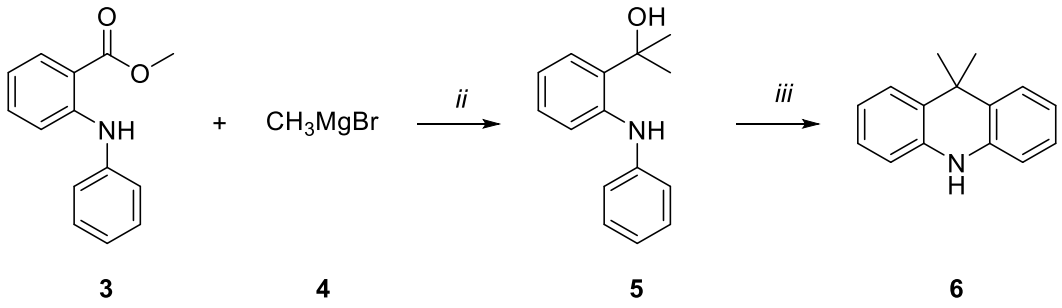

Scheme C.11: Synthesis of **6** using Grignard reaction and ring closing under acidic conditions.
ii: THF, 0 °C → 50 °C → rt. iii: H_3PO_4, rt.

Conversion of the ester to the alcohol was conducted using the commercially available Grignard reagent, yielding almost quantitative amounts of **5** with 99%. The last step used an acid supported ring closing leading to 92% yield of **DMAcr (6)**. Both procedures were performed according to Reddy *et al.*[33]

C.3 Towards acceptor starting materials

C.3.1 Synthesis of carbolines

The used synthesis for the carbolines were all literature known, therefore no specific research had to be performed. The different approaches are shown in the following section.

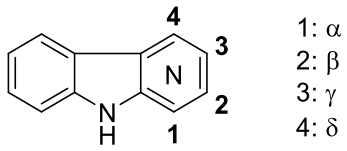

Scheme C.12: Declaration of different carbolines according to their nitrogen position in the scaffold.

C.3.2 Synthesis of β-carboline

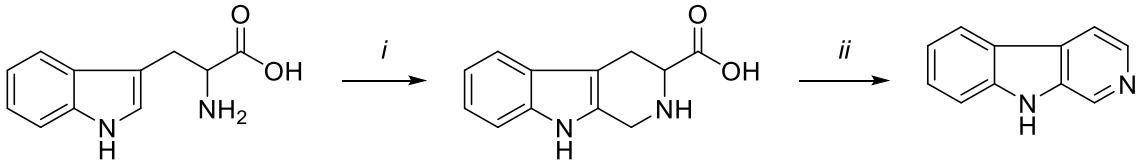

7 **8** **9**

Scheme C.13: Synthesis of β-carboline **9** by Pictet-Spengler cyclization of L-tryptophan, followed by decarboxylation. i: CH_2O, NaOH, H_2O, reflux. ii: NCS, TEA, DMF, rt.

Synthesis of β-carboline **9** was performed in a two-step sequence, starting with the amino acid L-tryptophan. After the ring formation with formaldehyde in aqueous sodium hydroxide *via* Pictet-Spengler cyclization[40],[41], yielding the precursor **8** with 83%, β-carboline **9** was received under decarboxylation[42] with NCS in tetraethylamine and DMF giving 82% yield.

C.3.3 Synthesis of γ-carboline

Metal assisted route

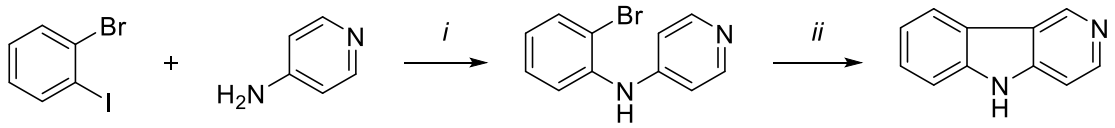

10 **11** **12** **13**

Scheme C.14: Synthesis of γ-carboline **13** using BHA, followed by CHA. i: $Pd_2(dba)_3$, dppf, NaO^tBu, toluene (abs.), reflux. ii: $Pd(OAc)_2$, K_2CO_3, NHC-ligand, DMA, 130 °C.

Synthesis of γ-carboline **13** was conducted in two steps according to Iwaki *et al.*[43]. In a first step, the intermediate **12** was achieved with 56% yield using BHA with $Pd_2(dba)_3$ and dppf as

a catalytic system in toluene and NaO^{t}Bu as a base. Subsequent intramolecular ring closing *via* CHA using $Pd(OAc)_2$ and the NHC-ligand in DMA with K_2CO_3 yielded **13** with 38%. The low yield can be explained by formation of dehalogenated starting material as side product.

Microwave assisted route

Another route to synthesize γ-carboline **13** was using reaction protocols of F. Dennone [44] and Chen *et al.*[45]

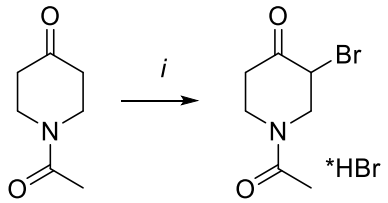

14 **15**

Scheme C.15: Synthesis of **15** *via* bromination. i: Br_2, $CHCl_3$, 0 °C → rt.

Bromination of *N*-acetyl-4-piperidone **14** with bromine in chloroform gave hydrobromide **15** in good yield (86%). The product **15** was further converted to γ-carboline **13** using a modified Fischer indole synthesis *via* microwave assisted reaction[45], adding phenylhydrazine, hydrochloride and acetic acid, giving carboline **13** with moderate yield (33%).

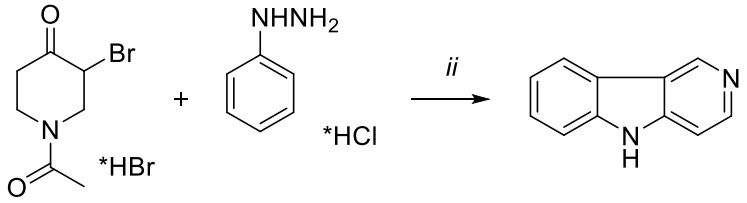

15 **16** **13**

Scheme C.16: Synthesis of γ-carboline **13** by a modified Fischer indole synthesis: i: AcOH, microwave, 200 °C.

C.4 Synthesis of Pyrrolodipyridine (PDP)

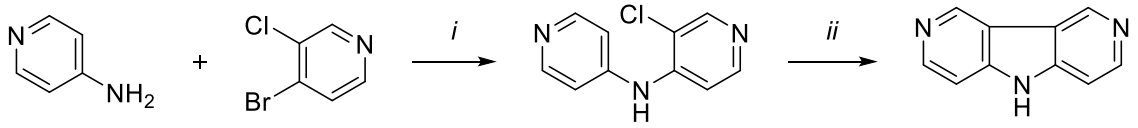

11 **17** **18** **19**

Scheme C.17: Synthesis towards **19** by BHA and CHA. i: $Pd_2(dba)_3$, dppf and NaOtBu in toluene, reflux. ii: $Pd(OAc)_2$, K_2CO_3, NHC-ligand, DMA, 130 °C.

Like the synthesis of γ-carboline, compound **19** was also produced using BHA and CHA according to Iwaki *et al.*[43] The BHA yielded **18** with 85%, followed by selectively, intramolecular ring closing *via* CHA obtaining 57% yield of **19**.

C.5 Synthesis of pre-functionalized carbolines

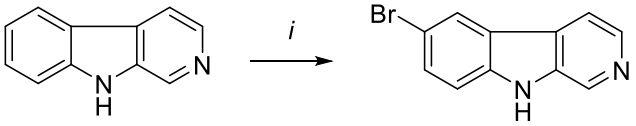

9 **20**

Scheme C.18: Synthesis of eudistomin N by bromination. i: NBS, AcOH, rt.

Bromination of β-carboline was conducted using the procedure of Kamal *et al.*[42] In this case, the bromination using NBS, as a possible weak bromination reagent, already worked out, under activation with acidic acid, with 86% yield of eudistomin N **20**.

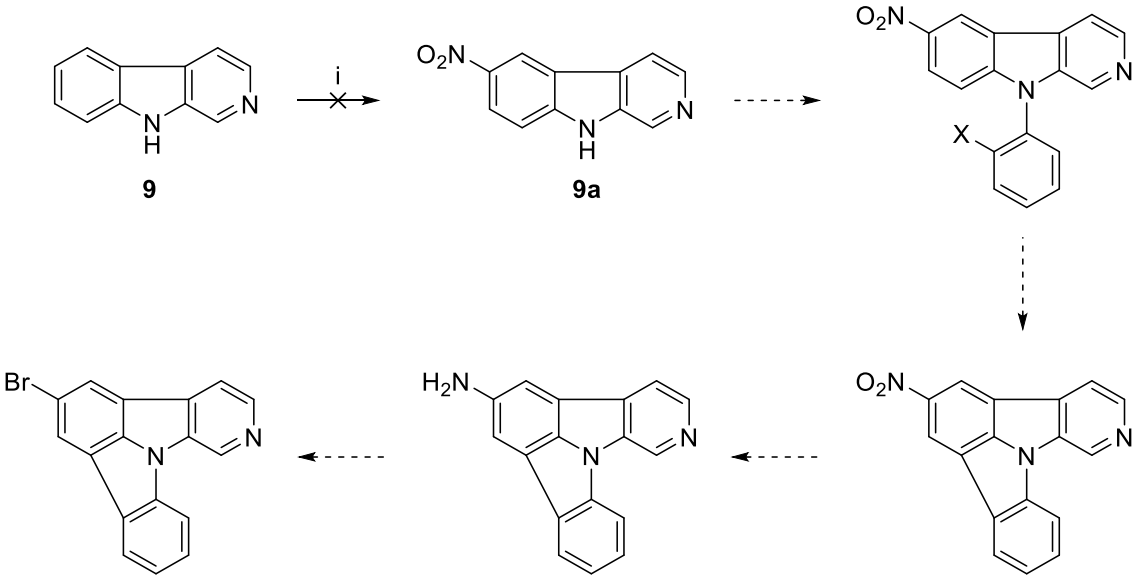

9 **9a**

Scheme C.19: Possible approach towards pre-functionalized, substituted β-carboline derivative. i: see Table C.1.

Another approach for a pre- functionalized β-carboline derivative in order to use it in a further proposed route towards the **Br-6NICz** is shown in Scheme C.19. The idea, in this case, was to introduce the nitro-group before substitution, because CHA ring closing of the substituted compound **20**, with bromine in the *para*-position instead, didn't seem to work as expected.

Unfortunately, the nitration of the β-carboline yielded only traces of the product **9a** and the route was dismissed. A table of different used reaction conditions is shown below.

Table C.1: Conditions of conducted reactions towards nitrated β-carboline

Reagents	***Temperature [°C]***	***Time [h]***	***Literature***
$NaNO_2$, HNO_3, AcOH	50	3.5	Ponce *et al.*[46]
$Cu(NO_3)_2$*$3H_2O$, Ac_2O, MeOH	rt	24	
Ac_2O, HNO_3	-2 → rt	2.5	Kneeteman *et al.*[47]
HNO_3, H_2SO_4	0 → rt	24	-
	80		

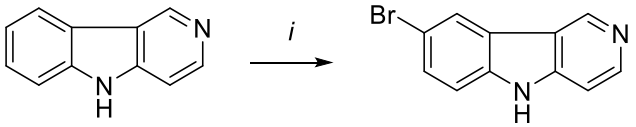

13 **21**

Scheme C.20: Synthesis of compound **21** by bromination. i: NBS, DMF, 0 °C → rt.

The bromination of γ-carboline was performed using *N*-bromosuccinimide in DMF, yielding 53% of the desired product **21.**

Also, in the case of γ-carboline, the idea of introducing a nitro group prior should lead to a more controlled way and better yields, to obtain the bromine in *para*-position, as the achievement of the corresponding acceptor species **Br-2NICz** seemed to be very challenging. The exact proposed route towards the acceptor molecule is shown in Scheme C.21. The first step of the sequence, the nucleophilic substitution was carried out in DMF, using Cs_2CO_3 as a base. Unfortunately, no product formation was observed. As later other approaches were successful (see Scheme C.29 and Scheme C.32) this strategy was not further pursued.

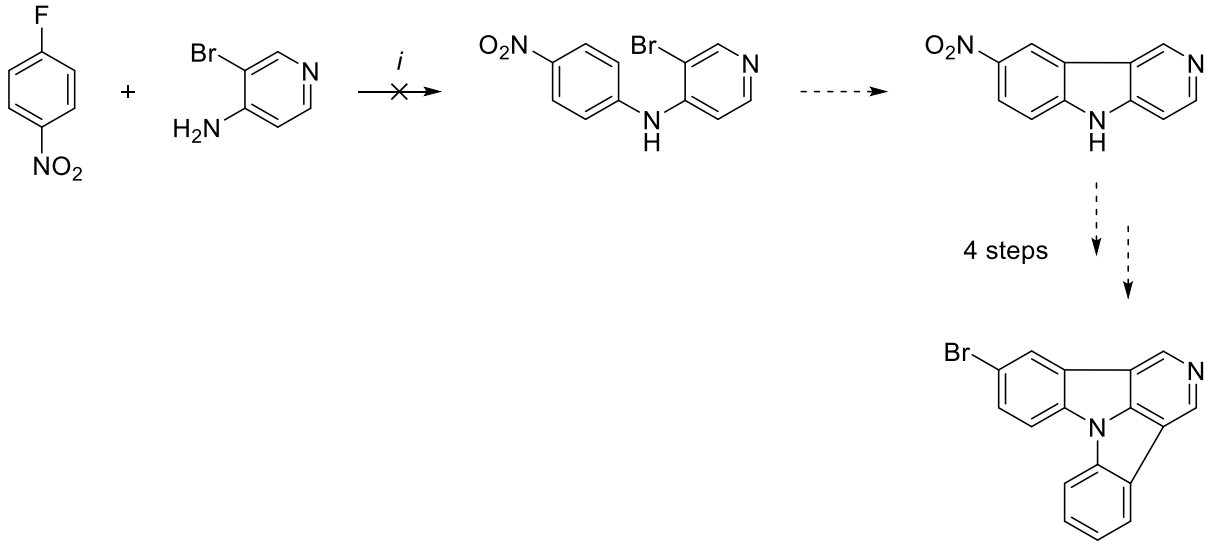

Scheme C.21: Possible approach towards pre-functionalized, substituted γ-carboline derivative. i: Cs_2CO_3, DMF, 130 °C.

C.6 Synthesis of acceptors

As already mentioned, the proposed strategy towards the target acceptor molecules was a substitution of the corresponding carboline moiety, followed by ring closing. Depending on the used strategies and functionalization methods the steps vary between 3 to 4.

C.6.1 Synthesis of 2-bromopyrido[3',4':4,5]pyrrolo[3,2,1-*jk*]carbazole/Br-5NICz

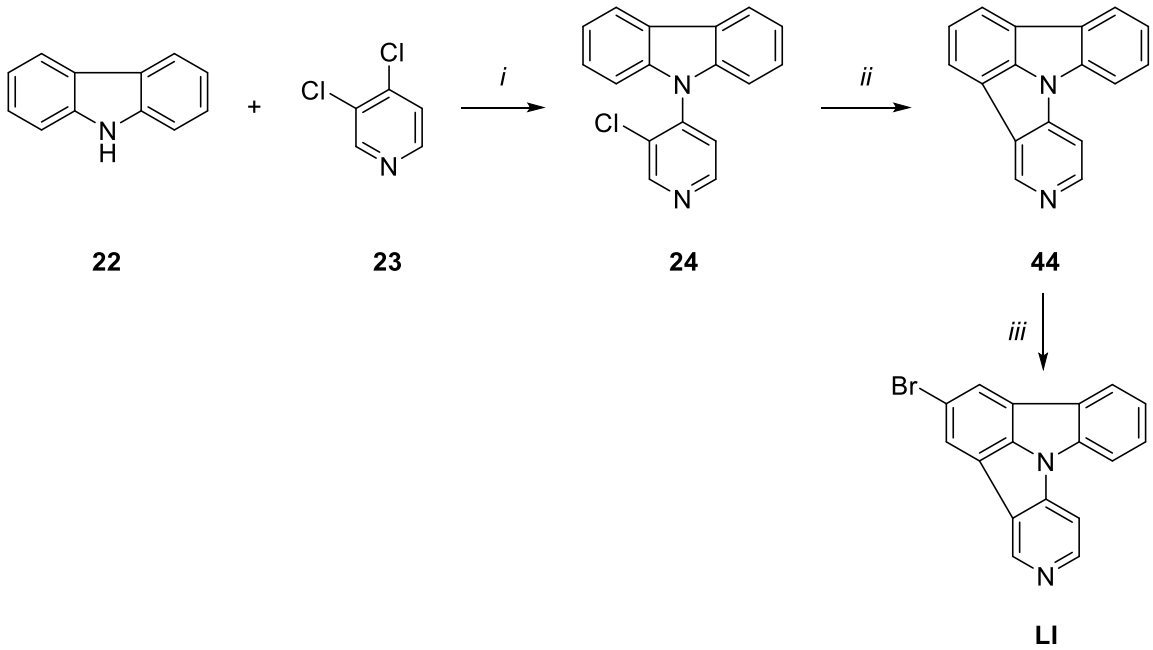

Scheme C.22: Synthesis towards **LI** using substitution, CHA, and bromination. i: Cs_2CO_3, DMF, 130 °C. ii: $Pd(OAc)_2$, K_2CO_3, NHC-ligand, DMA, 130 °C. iii: NBS, MeOH, H_2O, 55 °C.

The synthesis of **LI** required a total of 3 steps, containing substitution, CHA, and bromination of the planarized NICz. In a first step carbazole **22** was substituted with 3,4-dichloropyridin leading to **24** with an overall yield of 83%. Subsequently, the ring was closed *via* CHA and as the selectivity, in this case, doesn't matter, the reaction showed almost a quantitive yield of 98% of **5NICz** (**44**). Both substitution and CHA were performed following the procedure of Kader *et al.*[28] The bromination was conducted using NBS in a mixture of MeOH and water (7:3), for post-functionalization, receiving **Br-5NICz** (**LI**) with 46% yield. The solvent composition for bromination showed, under corresponding conditions, best conversion according to previous work in our group.

C.6.2 Synthesis of 2-bromopyrido[4',3':4,5]pyrrolo[3,2,1-*jk*]carbazole/Br-6NICz

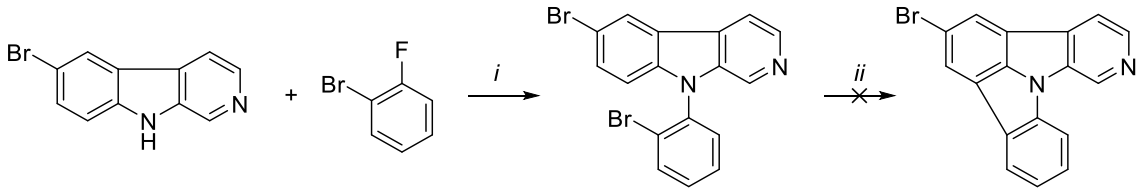

20 **28** **XXIX** **L**

Scheme C.23: Proposed pre-functionalization synthesis towards **L** using substitution and CHA. i: Cs_2CO_3, DMF, 130 °C. ii: Pd-NHC, K_2CO_3, DMA, 130 °C.

To control the position of the functional group of **L** a route of pre-functionalization was chosen, as previous work showed that selective bromination and purification starting from the acceptor building block **6NICz** is very challenging. The substitution of the halogenated benzene derivative was performed according to Kader *et al.*[28] using Cs_2CO_3 as a base and DMF as a solvent and worked with an overall yield of 84% very good. However, the bromine in *para*-position interferes with the intramolecular CHA, as oxidative addition probably occurs first in the sterically less hindered *para*-position. As a result, only the dehalogenated side product together with starting material were isolated *(*Scheme C.23).

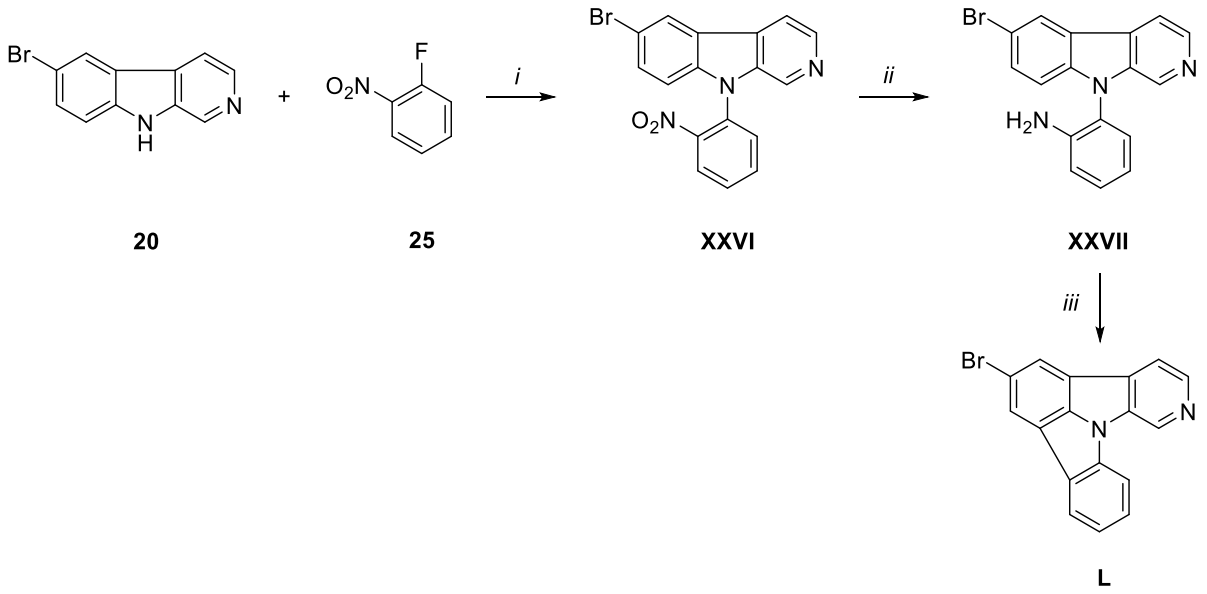

Scheme C.24: Synthesis of **L** by substitution, reduction and diazotization. i: Cs_2CO_3, DMF, 130 °C, ii: $SnCl_2*H_2O$, EtOH, reflux. iii: $NaNO_2$, AcOH, H_2SO_4, H_2O, 0 °C → reflux.

Therefore, an alternative route, leading to the accomplishment of **L** in 3 steps was developed (Scheme C.24). At first, the benzene derivative was added to the carboline moiety *via* nucleophilic substitution using Cs_2CO_3 as a base in DMF, according to a modified procedure of Wharton *et al.*[48] giving 75% yield. In the following step, the nitrogen group was reduced using $SnCl_2*2H_2O$ in EtOH, obtaining 86% yield **XXVI**. The ring was closed *via in situ* generation of the diazonium salt and subsequent decomposition of the salt, using $NaNO_2$ in a mixture of AcOH, H_2SO_4, H_2O. A procedure of Dunlop and Tucker[38] was used for this synthesis. The lower yield of 22% **Br-6NICz (L)** corresponds to troubles during the workup, as well as again the reactivity towards ring closing of the brominated β-carboline derivative. Anyhow the ring closing and thereby the synthesis of the acceptor, could be achieved in the end.

C.6.3 Synthesis of 2-bromopyrido[3,4-*b*]pyrido[4',3':4,5]pyrrolo[3,2,1-*hi*]indole/Br-6,10NICz

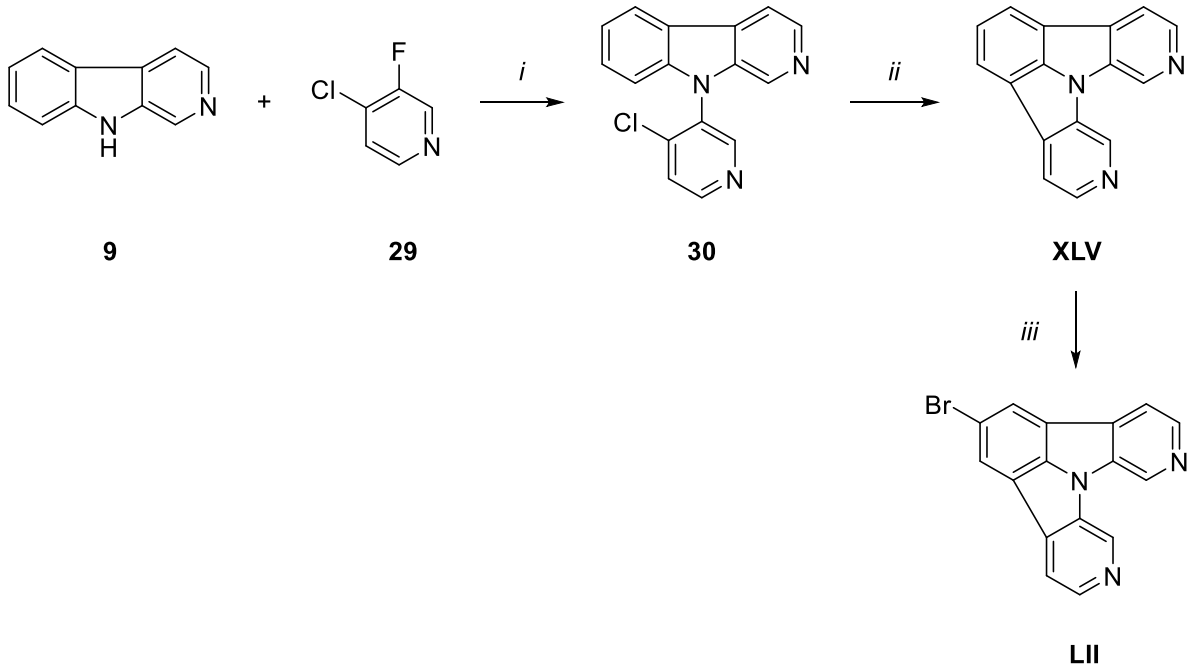

Scheme C.25: Synthesis towards **LII**, *via* substitution, CHA and bromination. i: Cs_2CO_3. DMF 130 °C, ii: $Pd(OAc)_2$, K_2CO_3, NHC-ligand, DMA, 130 °C. iii: Br_2, DMF, rt.

Again, the substitution of the halogenated pyridine was conducted following Kader *et al.*[28] yielding compound **30** with 31%. The low yield can be explained by instability of this certain pyridine, as well as side reaction in position 4 of the pyridine, due to the high reactivity of the para position. Subsequently, the ring was closed *via* metal-catalyzed CHA[28], receiving a yield of 35% of **6,10NICz** (**XLV**), because of dehalogenation of compound **30**. Nevertheless, the bromination, in a third step, achieved by the addition of Br_2 in DMF, yielded in 67% of **Br-6,10NICz (LII)**.

As a variation of the synthesis of **30** another halogenated pyridine species was tried as a reagent. Unfortunately, under none of the following conditions (see Table C.2), the desired product could be established.

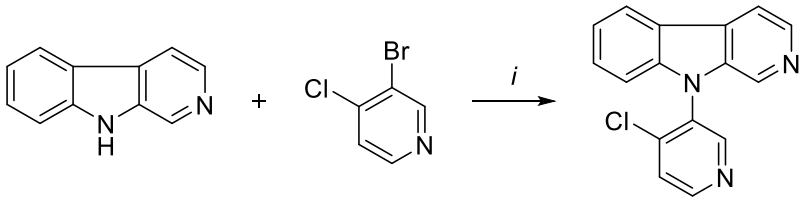

9 **29a** **30**

Scheme C.26: Alternate substitution towards **30.** i: see Table C.2.

Table C.2: Alternate reaction[28] conditions towards **30.**

Reagents	***Temperature [°C]***	***Time [h]***
$Pd_2(dba)_3$, NaO^tBu, $P^t(Bu)_3$*HBF_4, toluene	110	96
$Pd(OAc)_2$, NaO^tBu, BINAP, toluene	110	18
$Pd(OAc)_2$, NaO^tBu, dppf, toluene	110	18
Cu, Na_2CO_3, DMF	130	48
$CuSO_4$*$5H_2O$, K_2CO_3	230	6

C.6.4 Synthesis of 5-bromodibenzo[*b,e*]pyrido[3,4,5-*gh*]pyrrolizine/Br-2NICz

As the preparation of this acceptor building block proofed to be more challenging than expected, different strategies were investigated.

Again, the first route started by substitution and CHA according to Kader *et al.*[28] As mentioned before, the additional nitrogen in the carbazole scaffold in this certain position may decrease the reactivity for nucleophilic substitution reactions. Therefore, compound **31** was isolated only with moderate yield of 55%. Subsequent CHA gave **46** with 67%. Although there are two possible isomers in this reaction step the desired one was formed predominantly. The bromination itself was very tasking, due to the low reactivity of **2NICz** (**46**) towards electrophilic substitution. Mild bromination reagent like NBS showed no conversion towards the desired product at all, on the other hand too rapid addition of concentrated Br_2 to the solution led to formation of the double brominated product. In addition, though in the end yields show 38% product **Br-2NICz** (**LIV**) formation, it was very hard to isolate the product as it is barely soluble. The reaction scheme is shown below.

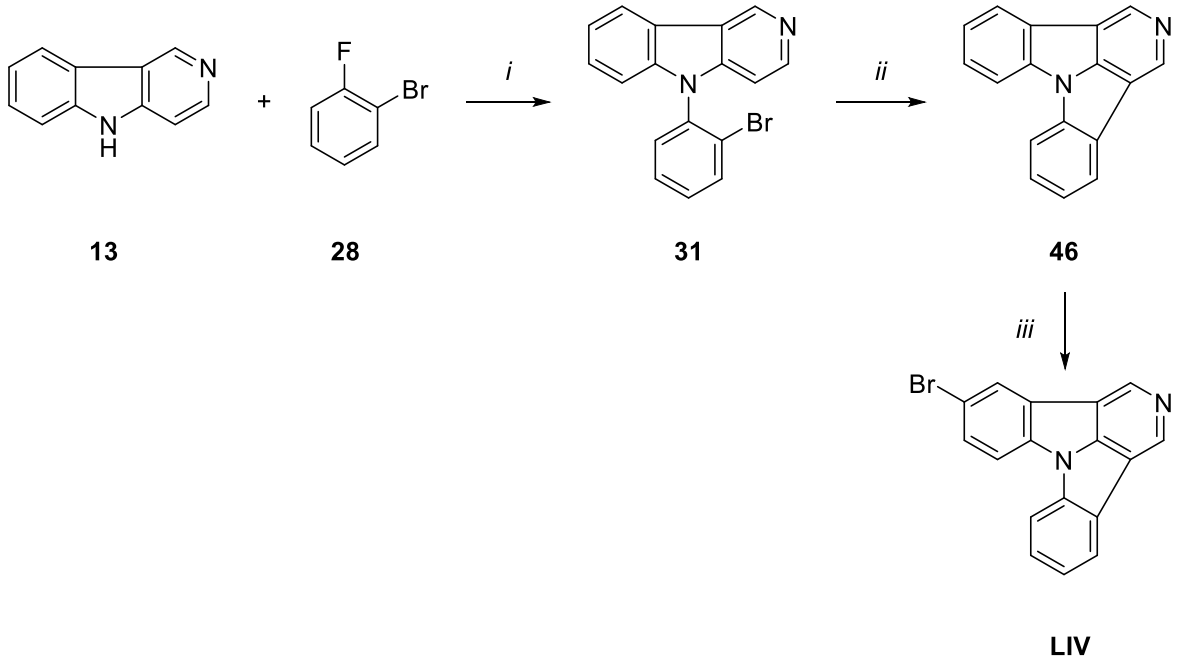

13 **28** **31** **46** **LIV**

Scheme C.27 Synthesis of **LIV** by substitution, CHA and bromination. i: Cs_2CO_3, DMF, 130 °C. ii: $Pd(OAc)_2$, K_2CO_3, NHC-ligand, DMA, 130 °C. iii: Br_2, DMF, 0 °C → 55 °C.

Different reaction conditions, that were also used for the bromination in the last step, achieving almost no yields, are shown in the following table:

Table C.3: Different approaches to achieve bromination as post-functionalization.

Reagents	***Temperature [°C]***	***Time [h]***
NBS, MeOH, H_2O	55	18
NBS, DMF	rt	80
Br_2, $CHCl_3$	reflux	48

Another route to achieve precursor **2NICz** is shown in Scheme C.28. In this case, substitution and double-sided CHA should lead to the product. Both reactions were conducted following a modified protocol of Kautny *et al.*[27] yielding 52%, in case of the substitution to **34**. The low yield corresponds to side products, as during the high temperature, the trichloropyridine rapidly dehalogenated and showed besides decomposition also dimerization. As selectivity doesn't matter, the double-sided CHA works with almost quantitative yields of 99% towards compound **2NICz** (**46**).

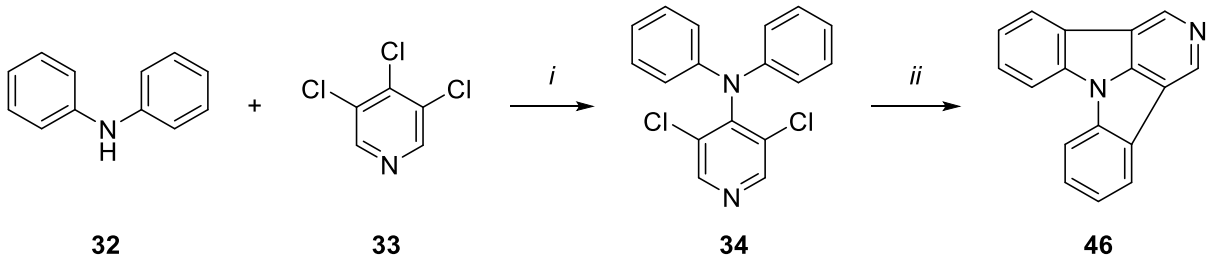

Scheme C.28: Synthesis of **46** *via* substitution and double CHA. i: NaH, DMF, 130 °C. ii: $Pd(OAc)_2$, K_2CO_3, NHC-ligand, DMA, 130 °C.

A different approach was used, introducing a functional group already in the beginning according to the procedure of Wharton *et al.*[48] for substitution. The whole pathway is shown below.

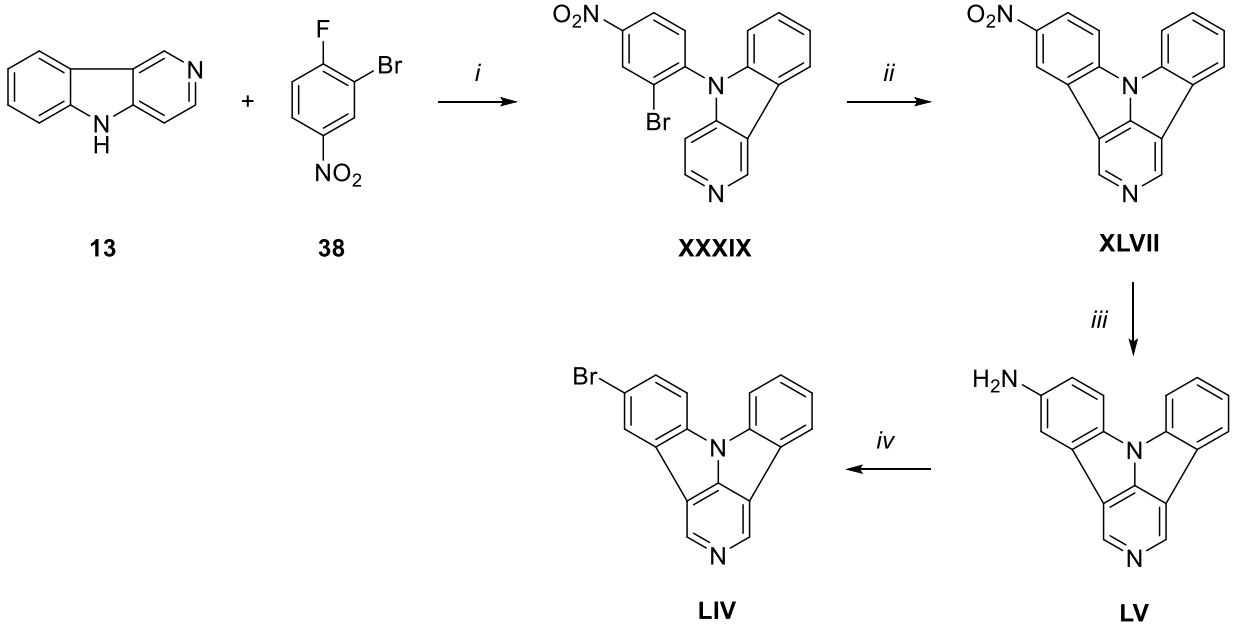

Scheme C.29: Synthesis towards **LV** using a pre-functionalized pathway by substitution, CHA, reduction and Sandmeyer reaction. i: Cs_2CO_3, DMF, 130 °C. ii: Pd-NHC, DMA, 130 °C. iii: $SnCl_2*2H_2O$, EtOH, reflux. iv: $NaNO_2$, CuBr, HBr, H_2O, 0 °C → rt.

The substitution towards **XXXIX** showed yields of 41%, as the reagent easily gets lost of the nitro group at higher temperatures, which was also a matter during the next reactions in Scheme C.29. Though the ring closing *via* CHA[28] could probably lead to both isomers, the expected closing towards the desired isomer could be achieved as favored. Anyhow, the synthesis of **XLVII** only yielded 22%, according to already discussed reasons. Holding the temperature lower, the reduction of the nitro group using $SnCl_2*2H_2O$ and EtOH, following the procedure of Dunlop and Tucker[38], showed, as expected, good yields of 78% of compound **LV**. The final step uses a Sandmeyer reaction to accomplish the final functionalized acceptor.

The reaction was performed using $NaNO_2$ and CuBr in HBr and H_2O according to Fries and Imbert.[49]

A fourth possibility for the synthesis of **LIV** accords to a pre-functionalization and ring closing *via* diazotization instead of CHA, which again may lead to bad yields, because of the bromine.

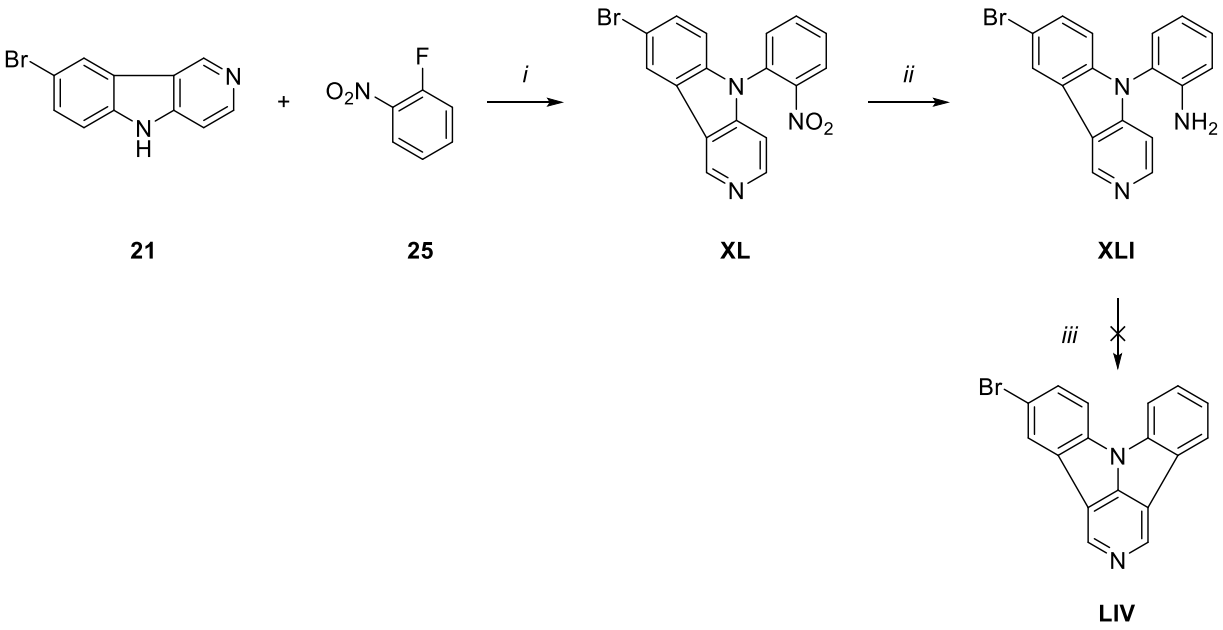

Scheme C.30: Synthetic approach towards **LIV** using substitution, reduction and *in situ* diazotization. i: Cs_2CO_3, DMF, 130 °C. ii: $SnCl_2$*$2H_2O$, EtOH, reflux. iii: $NaNO_2$, AcOH, H_2SO_4, H_2O, 0 °C → reflux.

The substitution was conducted under standard conditions, using Cs_2CO_3 as a base in DMF relating to the work of Wharton *et al.*[48] Product **XL** showed an overall yield of 59%, as again the loss of the nitro group appeared to be a side product according to GC-MS. Subsequently, the nitro group was reduced and in a further reaction desired ring closing performed, both under conditions of Dunlop and Tucker.[38] Though the reduction to the corresponding amine **XLI** worked with an almost quantitative yield of 99%, the *in situ* diazotization towards **LIV** failed and only led to deamination.

In order to try a pre-functionalization route, similar to Scheme C.28, the synthesis of a corresponding precursor is shown below (Scheme C.31).

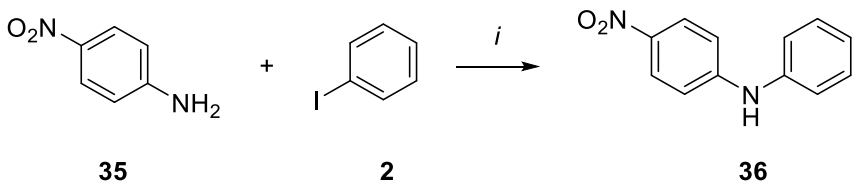

Scheme C.31: Synthesis of compound **36** *via* Ullmann condensation. i: CuI, CsF, DMSO, 130 °C.

The reaction represents an Ullmann condensation, using CuI as a copper source and CsF as a base, following the protocol of Güell and Ribas[50] yielding **36** with 33%, as the iodobenzene decomposes.

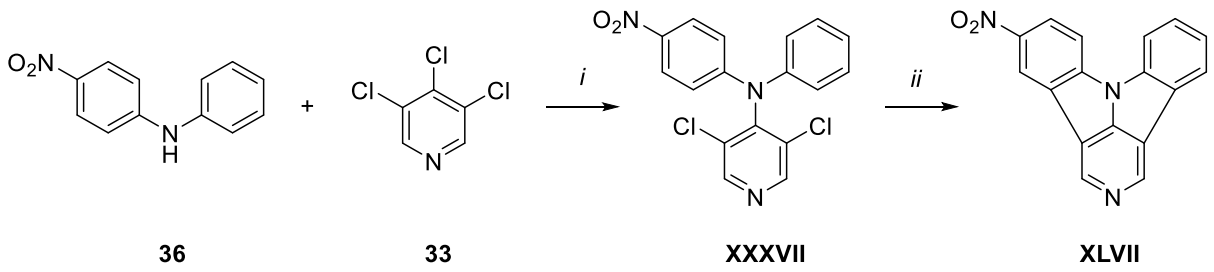

36 **33** **XXXVII** **XLVII**

Scheme C.32: Pre-functionalization synthesis of **XLVII**, by substitution, double CHA. i: NaH, DMF, 130 °C. ii: $Pd(OAc)_2$, K_2CO_3, NHC-ligand, DMA, 130 °C.

The proposed pathway towards **XLVII** therefore shows a combined analog of the routes mentioned in Scheme C.28 and Scheme C.32. The substitution was achieved following a modified procedure according to Kautny *et al.*[27] yielding 29%, as well as the ring closing *via* simultaneously double-sided CHA yielding **XLVII** with 54%. In case of substitution, the same side reactions, as in the unsubstituted form, happened (see above), as well as denitrification for both compounds **XXXVII** and **XLVII**. Due the low overall yield this strategy was not continued, as large scale resynthesis of the compounds would have been necessary, which was beyond the time scope of this thesis.

C.6.5 Synthesis of 5,11-dibromodibenzo[*b,e*]pyrido[3,4,5-*gh*]pyrrolizine/Br_2-2NICz

As the unsubstituted scaffold of **LIII** is the same as **LVI**, synthesis might be possible using almost the same route, because only the amount of bromine varies.

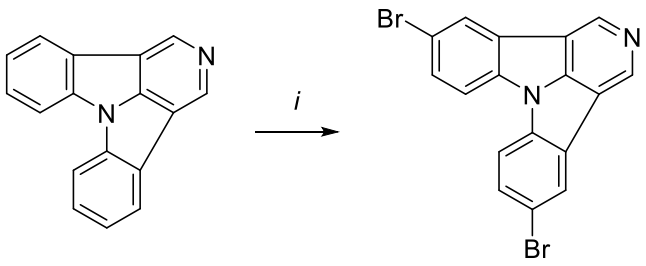

46 **LIII**

Scheme C.33: Synthesis of **LIII** by post-functionalization *via* bromination. i: Br_2, DMF.

As already mentioned in part C.6.4, the bromination of compound **46** was very challenging due to the low reactivity of 46 which therefore demands harsh reaction conditions, which make control of the selectivity very difficult. The best yields were achieved by adding Br_2 in DMF rapidly and concentrated, instead of slow and diluted. Furthermore, it could be observed, that further bromination of mono-substituted product **LVI** to **LIII** only works under conversion of traces, hence, the ring system exhibits less reactivity. Also approaches, using higher and lower temperatures, were outsourced, as well as the addition of $FeCl_3$ as a Lewis acid. In addition, a separation in the work up between the mono- and double-substituted moieties appeared to be time consuming, as also very hard to isolate. Attempts using hot nitrobenzene showed the best results with an overall yield of 49% **Br_2-2NICZ** (**LIII**).

C.6.6 Synthesis of 11-bromobenzo[b]dipyrido[4,3-e:3',4',5'-gh]pyrrolizine/Br-5,11NICz

According to problems, earlier mentioned in this study, synthesis of acceptors, especially having nitrogen atoms in *para*-position in their scaffold, could not be achieved (Scheme C.34). In a post-functionalization approach, the first step was the substitution using Cs_2CO_3 in DMF, yielding **XLII** with 55%. The lower yield relates to a dehalogenated form of the product. For substitution and following ring closing CHA, a protocol according to Kader *et al.*[28] was used. The CHA worked with a good yield of 76% of **48**, as the selectivity also does not matter in this case.

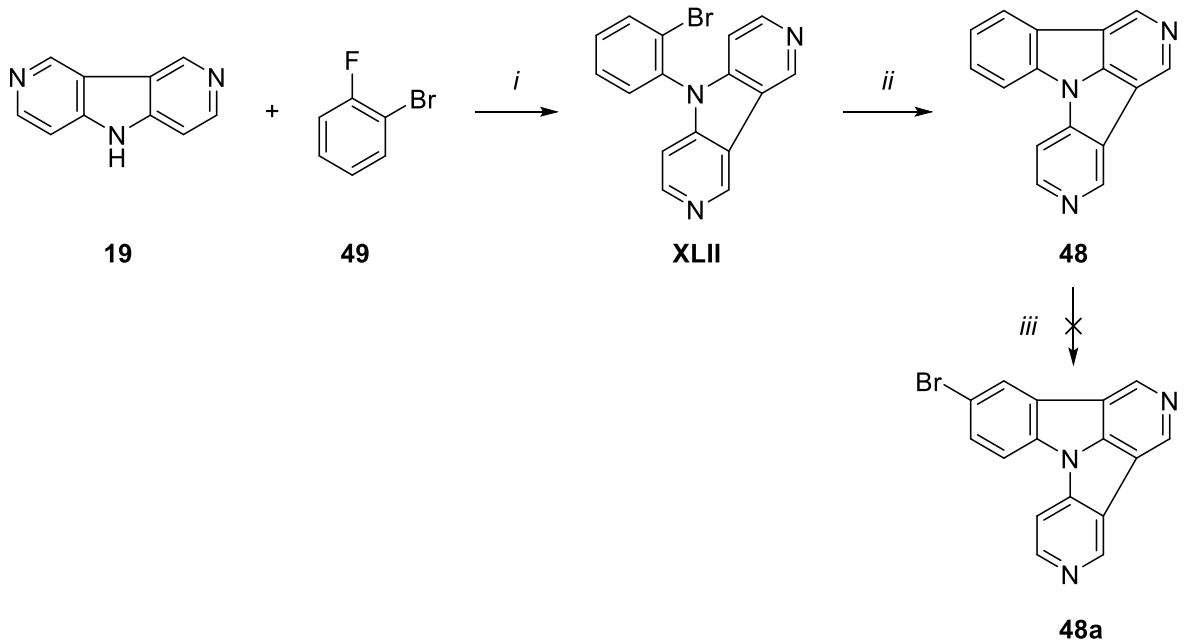

19 **49** **XLII** **48** **48a**

Scheme C.34: Snthesis of **48a** by substitution, CHA and bromination. i: Cs_2CO_3, DMF 130 °C. ii: Pd-NHC, Cs_2CO_3, DMA, 130 °C. iii: see Table C.4.

The bromination towards **Br-5,11NIZC** (**48a**) could finally not be achieved, as the desired bromination in the position showed hardly any conversion. Different tried reaction conditions are shown in Table C.4.

Table C.4: Reaction condition tested for bromination of **48**.

Reagents	***Temperature [°C]***	***Time [h]***
Br_2, $CHCl_3$	reflux	50
Br_2, DMF	rt	71
Br_2, $AlBr_3$/Fe, DMF	60	144

As a result, a different pathway using pre-functionalization was investigated and is shown in Scheme C.35.

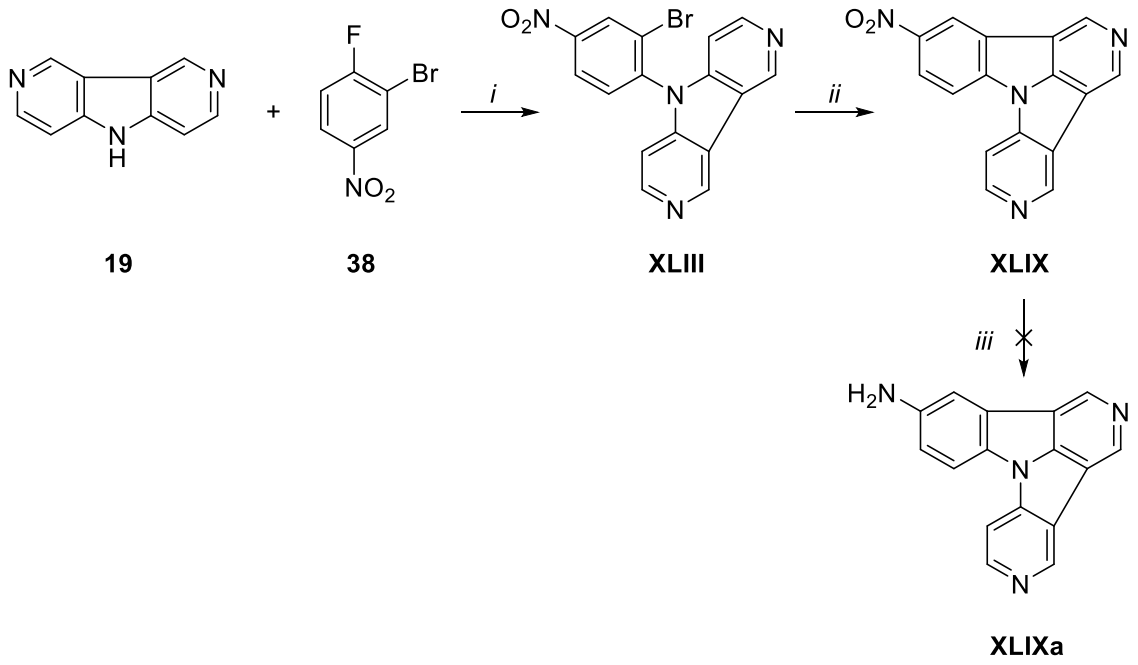

19 **38** **XLIII** **XLIX** **XLIXa**

Scheme C.35: Proposed synthesis towards **XLIXa** by substitution, CHA and reduction. i: NaH, DMF, 50 °C. ii: Pd-NHC, K_2CO_3, DMA, 130 °C. iii: $SnCl_2*2H_2O$, EtOH, reflux.

In a second pathway, the desired acceptor should be achieved *via* substitution of a nitro functionalized halogen derivative, followed by CHA, reduction and Sandmeyer reaction. The substitution was conducted following the procedure of Wharton *et al.*[48] and again, as a side product, the dehalogenated, as well as the denitrated, formed obtaining a yield of 35% of **XLIII**. Also the CHA, according to Kader *et al.*[28], only could achieve 28% of **XLIX**, because of undesired de-functionalized side products. The following reduction could not achieve the next product **XLIXa** in the scheme, as the impact of heating to reflux achieved again cleavage of the nitro group.

C.7 Donor-acceptor systems

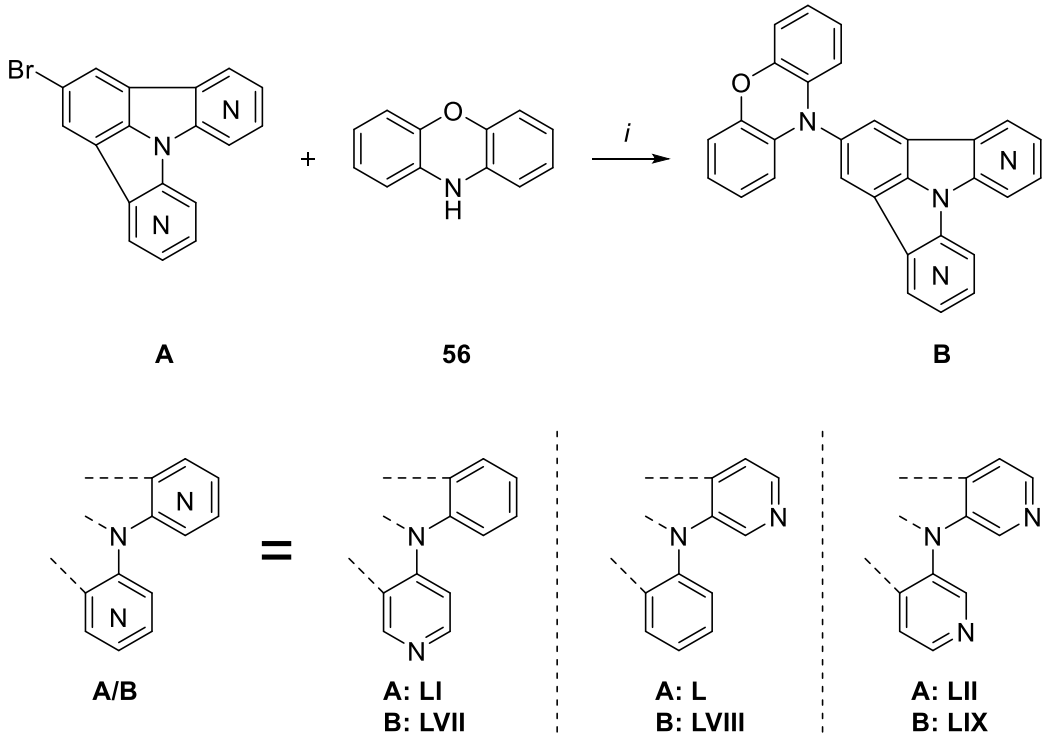

Scheme C.36: General synthesis route towards different mono-donor-acceptor systems using phenoxazine as a donor, *via* BHA. i: $Pd_2(dba)_3$, NaO^tBu, $P(^tBu)_3$*HBF_4, toluene, 110 °C.

Reactions were performed according to a modified procedure according to Iwaki *et al.*[43] In most cases the final products were further purified using high vacuum sublimation. Yields of the corresponding target molecules are shown below.

Table C.5: : Comparison of the yields of the reactions towards target molecules, using phenoxazine as a donor, *via* BHA.

Donor-acceptor system	***Acceptor structure***	***Yield [%]***
PXZ-5NICz (LI)	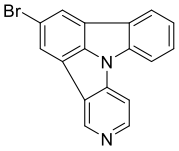	96
PXZ-6NICz (L)	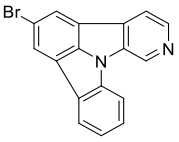	75
PXZ-6,10 (LII)	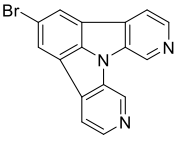	59

Again, the influence of the nitrogen position and amount can be seen *via* the varying yields in Table C.5, as the reaction towards compound **LII** led also to the de-functionalized moiety of the acceptor.

Furthermore, it has to be mentioned, that the solubility of all donor-acceptor systems increased during the coupling, compared to their former acceptor solubility, especially in the case of **LIII**.

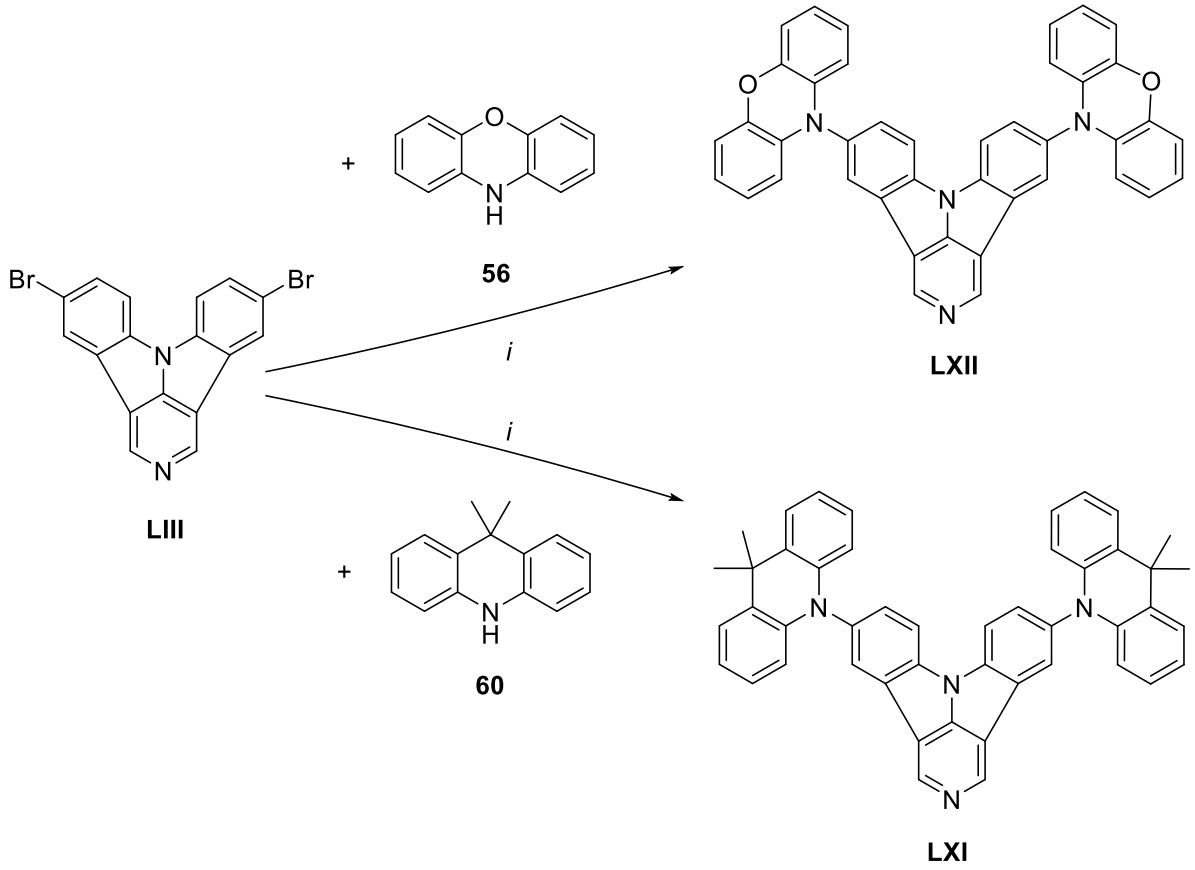

Scheme C.37: Synthesis of **DMAcr$_2$-2NICz (LXI)** and **PXZ$_2$-2NICz (LXII)** by BHA using different donors. i: $Pd_2(dba)_3$, NaO^tBu, $P(^tBu)_3$*HBF_4, toluene, 110 °C.

The preparation of the systems with two donor molecules in their structure was also conducted under the same conditions as for the mono donor-acceptor systems using the procedure of Iwaki *et al.*[43] yielding 63% in the case of **PXZ$_2$-2NICz (LXII)** and 65% of **DMAcr$_2$-2NICz (LXI)**. These kinds of systems could not be sublimated *via* high vacuum sublimation, as their phase transition temperature seems to be very high. On the other hand, this represents the good thermal stability of the compounds.

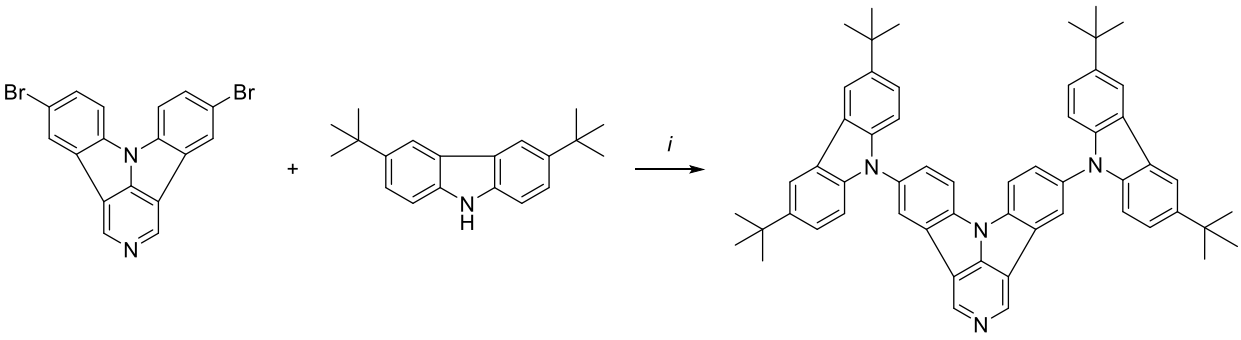

LIII **63** **LXIV**

Scheme C.38: Solid phase synthesis of **DTBCz$_2$-2NICz (LXIV)**. i: K_2CO_3, $CuSO_4$*$5H_2O$, 250 °C.

The synthesis of target molecule **DTBCz$_2$-2NICz (LXIV)**, using a carbazole derivative as a donor, was conducted as a solvent-free Ullman reaction according to Kautny *et al.*[19] obtaining 45% yield.

C.8 Synthesis of Pd-NHC-catalyst

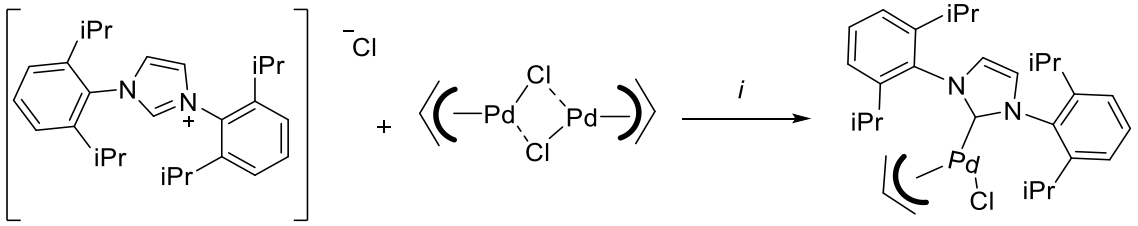

65 **66** **67**

Scheme C.39: Synthesis of the Pd-NHC catalyst **67**. i: *n*-BuLi, THF, rt.

In a lot of CHA reactions, the palladium salt **66** and NHC-ligand **65** were separately used for *in situ* formation of the corresponding catalyst. In small scale reactions the Pd-NHC precatalyst was used in order to achieve better control over catalyst formation. Pd-NHC **67** was synthesized according the procedure of Navarro and Nolan[51].

Big advantages of NHC ligands in general, are their good donor properties and their stability against oxidation and furthermore higher reactivity (sometimes at rt) is achieved and even arylchlorides can be used.[52] A proposed cycle of the generation of the active species is shown below.

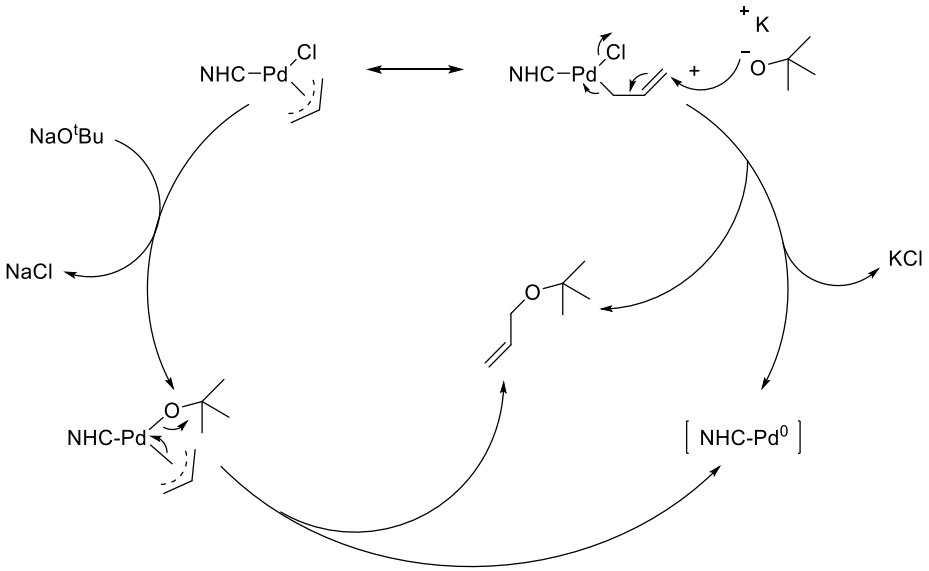

Scheme C.40: Proposed possible activation mechanisms of the Pd-NHC catalyst[53].

C.9 Characterization

In order to determine the photophysical effects and the properties of the synthesized materials, several common optical and electrochemical measurements were conducted. Details are given in the following section.

C.9.1 Absorption and fluorescence

Absorption and fluorescence spectra were recorded in DCM as a 5 µM solution of the target compounds.

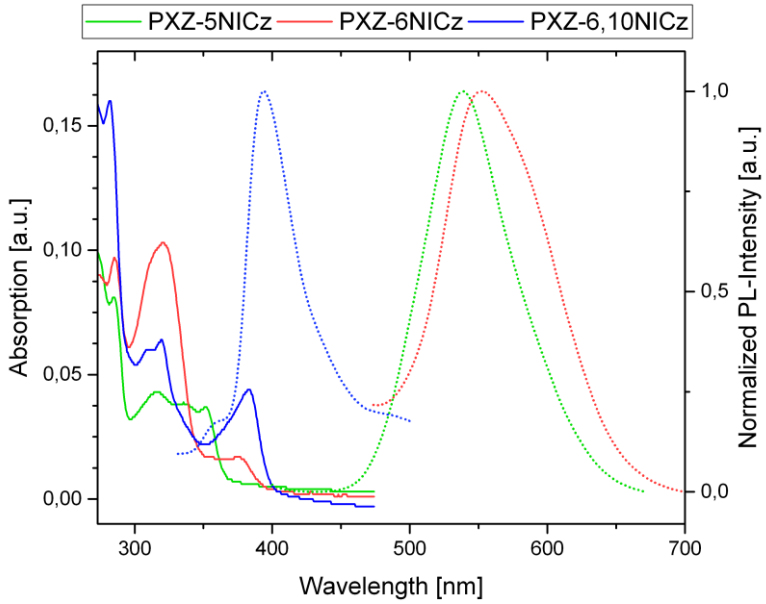

Figure C.2: UV/Vis absorption (full lines) and normalized fluorescence spectra (dotted lines) of the synthesized systems **PXZ-5NICz, PXZ-6-NICz** and **PXZ-6,10NICz**. All spectra recorded as 5 µM solutions in DCM.

Absorption peaks at around 285 nm can be attributed, as expected, to a π-π* transition of the conjugated moieties.[19] Systems, where nitrogen is introduced in *meta*-position in the ICz scaffold (**PXZ-6NICz** and **PXZ6,10NICz**) exhibit almost the same absorption onset of about 400 nm, though the single nitrogen induced **PXZ-6NICz** shows decently a decrease of the corresponding absorption maximum. On the other hand, the absorption onset of the nitrogen *para*-positioned **PXZ-5NICz**, is clearly blue shifted to 365 nm. This trend corresponds with the observation of the influence of the nitrogen position in the isolated NICz units.[28] The **PXZ-6NICz** absorption spectrum also features a strong absorbance at 318 nm, which is lowered in the other two molecules. Furthermore, it can be observed, that **PXZ-6,10NICz** shows a blue shifted shoulder in this area.

Concerning fluorescence, it is visualized, that mono induced nitrogen species show a close maximum at 529 nm in the case of **PXZ-5NICz** and 553 nm for **PXZ-6NICz**. Again, the system including the *para*-positioned nitrogen is slightly blue shifted. **PXZ-6,10NICz** shows a distinct maximum fluorescence peak at shorter wavelengths of 394 nm.

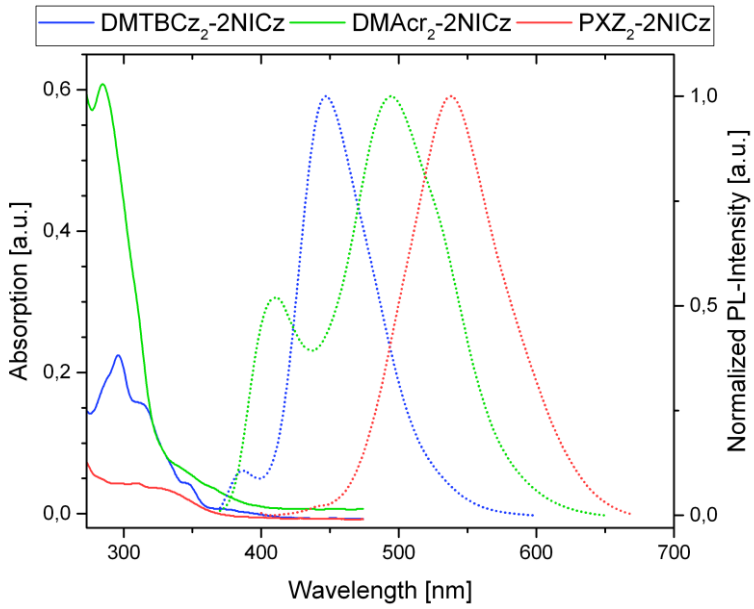

Figure C.3: UV/Vis absorption (full lines) and normalized fluorescence spectra (dotted lines) synthesized systems **DMTBCz$_2$-2NICz, DMACr$_2$-2NICz** and **PXZ$_2$-2NICz**. All spectra recorded as 5 µM solutions in DCM.

In the case of the double substituted donor systems, **DMACr$_2$-2NICz** shows the highest absorption intensity at 284 nm. The quite distinct π-π* transition signal lowers and broadens to higher wavelengths in the case of **DMTBCz$_2$-2NICz**, including a red shifted shoulder peak in this area. In contrast **PXZ$_2$-2NICz** shows no distinct peaks in this area. The highest absorption onset corresponds to the system including phenoxazine as donors (**PXZ$_2$-2NICz**) with 371 nm, followed by **DMTBCz$_2$-2NICz** and further **DMACr$_2$-2NICz** with blue shifted onsets.

Accordingly, the highest fluorescent emission wavelength shows **PXZ_2-2NICz** at 538 nm. Shifted to shorter wavelengths, **$DMACr_2$-2NICz** exhibits a maximum at 494 nm, as well as a blue shifted shoulder at about 400 nm. Also, **$DMTBCz_2$-2NICz** with a fluorescent peak at 447 nm displays this shoulder, though it is lowered. If we have a close look at 439 nm also **PXZ_2-2NICz** exhibits this shoulder, but at very low photoluminescence intensity.

C.9.2 Phosphorescence

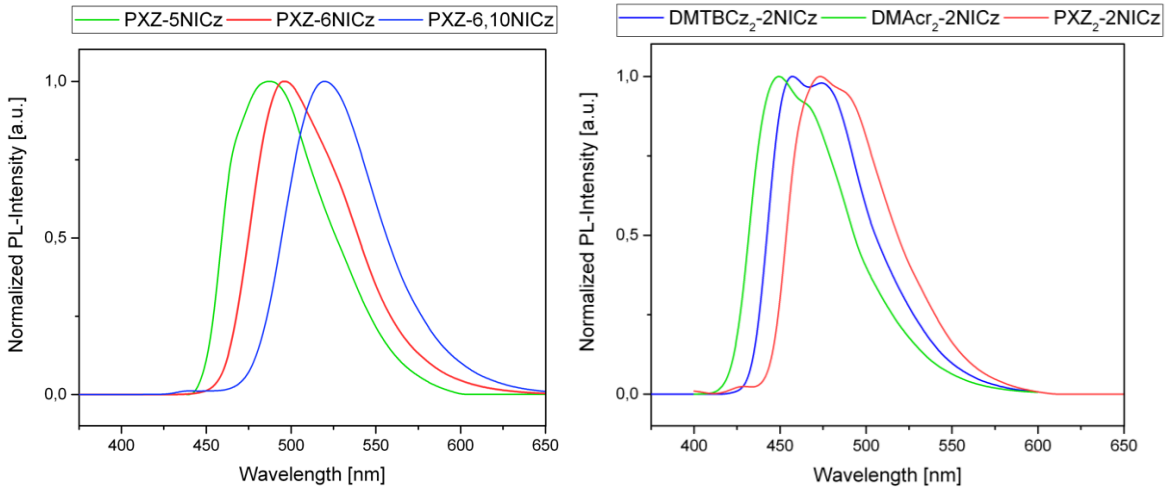

Figure C.4: Normalized low-temperature phosphorescence spectra (77 K) of the synthesized systems.

In order to determine the triplet energies of the materials, low temperature phosphorescence spectra at 77 K were recorded. Surprisingly, the maxima of all spectra with exception of **PXZ-6,10NICz** are blue shifted to the corresponding fluorescence spectra, which contradicts basic physical-chemical principles. A possible explanation is the use of different polar solvents. As the fluorescence is measured in a more polar solvent an excited charge transfer complex is better stabilized and therefore might be redshifted. Another explanation would be the higher temperature which might cause stronger relaxation and therefore a distinct red shift. In contrast to single donor systems the molecules **$DMTBCz_2$-2NICz**, **$DMACr_2$-2NICz** and **PXZ_2-2NICz** show a shoulder at higher wavelengths.

C.9.3 Cyclic voltammetry (CV)

The HOMO energy levels of the novel phenoxazine based bipolar systems were determined by CV. For measurements ferrocene was used as an internal standard and the levels calculated from the onsets of the oxidation peaks. All three compounds show, as expected, reversible oxidation behavior which indicates good electron hole injection and transport.[54]

The measurement of the remaining systems could not be conducted, as the fragile working electrode broke in a cleaning step between.

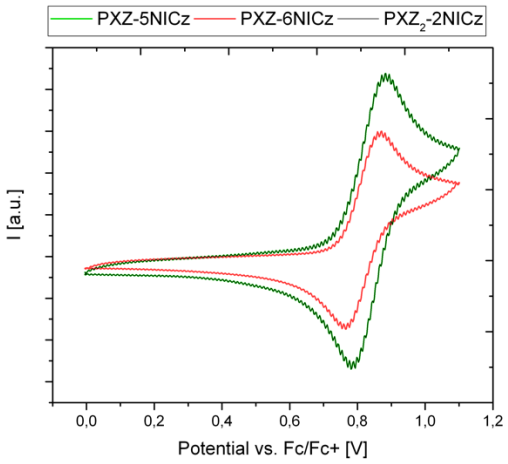

Figure C.5: Cyclic voltammograms of oxidation for **PXZ-5NICz**, **PXZ-6NICz** and **PXZ$_2$-6,10NICz** as 12.5 mM solution in DCM.

C.9.4 Summary

The same trend, regarding the influence of the nitrogen position within the scaffold of isolated NICz, is reflected in the synthesized materials. The photoluminescence distributes over a broad range and therefore possibly enables the use as emitters with a wide spectral color range. Especially the materials with the strongest blueshift are potential candidates for deep blue devices which are, at the moment, one of the biggest challenges in the field of OLEDs. Anyhow, the decreased optical bandgaps for the tested systems could allow high device efficiency, as low driving voltages can be applied. The triplet energy values vary between 2.38 eV and 2.76 eV and could thereby achieve a good device performance. At this point the photoluminescence spectra must be handled with care, as the redshift of the fluorescence compared to the phosphorescence has to be further investigated. Therefore, ΔE_{ST} of the materials could not be determined, at the moment.

Table C.6: Physical data of target materials

Substance	***Opt. BG [eV]^{a,b}***	***$\lambda_{PL,max}$ [nm]^{b}***	***E_T [eV]^{c}***	***ΔE_{ST} [eV]^{d}***	***HOMO/LUMO^{e,f}***
PXZ-5NICz	3.39	539	2.55	0.02	-5.12/-2.88
PXZ-6NICz	3.13	553	2.49	0.02	-5.11/-2.48
PXZ-6,10NICz	3.11	394	2.38	0.17	-5.12/-2.96
DMTBCz$_2$-2NICz	3.46	447	2.71	0.02	-
DMAcr$_2$-2NICz	3.78	494	2.76	0.01	-
PXZ$_2$-2NICz	3.34	538	2.62	0.02	-

[a] *Determined from the absorption onset.*
[b] *Measured in DCM (5 µM) at rt.*
[c] *Determined from phosphorescent maxima measured in toluene/EtOH 9:1 (1mg/mL) at 77 K.*
[d] *Theoretical calculated from density functional theory.*
[e] *HOMO levels calculated from the on sets of the oxidation peaks from cyclic voltammetry measurements as 12.5 mM solution in DCM.*
[f] *LUMO levels were calculated from HOMO levels and the optical bandgap.*

C.10 Results and Discussion

Throughout this thesis novel NICz based donor-acceptor materials, as potential TADF emitters, could successfully be synthesized. Synthetic pathways, including nucleophilic substitution, CHA, diazotization and BHA were utilized to engineer the target molecules, by the use of commercially low-cost starting materials. Research showed effects due various synthetic approaches, caused by the alternating nitrogen amounts and position in the scaffold.

In detail the investigated routes gave pre-functionalized reaction routes in the case of **PXZ-6NICz** and **2NICz**. All other materials were synthesized post-functional, including an alternative route for **2NICz**, as synthesis appeared challenging, especially towards the secondary brominated acceptor. Nevertheless, CHA was used as a main method for intramolecular ring closing of acceptor building blocks including **Br-5NICz**, **Br-6,10NICz**, **Br_2-2NICz** and **Br-2NICz**. In the case of **Br-6NICz**, CHA showed hardly any conversion, as oxidative addition probably occurs first in the sterically less hindered *para*-position and therefore diazotization was chosen as a method of choice to achieve the desired product.

Though several attempts, the synthesis of the **Br-5,11NICz** acceptor could not be accomplished, as establishment of the functional group appeared to fail.

The synthesized target materials exhibit same trends regarding the influence of the nitrogen position within the scaffold of isolated NICz according to earlier research.[28] The phosphorescent maxima of all spectra, with exception of **PXZ-6,10NICz**, are blue shifted to the corresponding fluorescence spectra, which contradicts basic physical-chemical principles, might be caused by the polarity of different solvents. Anyhow, the use as emitters with a wide spectral color range can possibly be given, as the photoluminescence distributes over a broad range. Thereby, materials with a strong blue shift, like **DMTBCz_2-2NICz**, appear to be very promising, as these emitters relate to one of the big challenges in the field of OLEDs.

In future investigation, the establishment of **PDX-5,11NICz**, as well as the use of **Br-2NICz** as a acceptor building block can be further approached. In addition, the turnout of the characterization observations should be investigated, in order to explain the behavior in detail and receive experimental values concerning the singlet-triplet transition energy gap.

D. Experimental Part

D.1 General remarks

Unless explicitly mentioned otherwise, all reagents from commercial suppliers were used without further purification. Absolute, anhydrous solvents like toluene and THF were absolutized by the *PURESOLV*-system from Innovative Technology Inc. Other anhydrous solvents like DMA or DMF were purchased from commercial suppliers. The commercially available lithiation reagent *n*-BuLi was used without additional quantitative analysis, using the declared value.

D.2 Chromatographic methods

D.2.1 Thin layer chromatography

Thin layer chromatography (TLC) was performed using TLC-aluminum foil (Merck, silica 60 F254).

D.2.2 Column Chromatography

Preparative column chromatography was performed using a BÜCHI Sepacore flash system, which was equipped with the following components:

- Pump system:
    - BÜCHI pump modules C-605 (2 units)
    - BÜCHI pump manager C-615
- Detector:
    - BÜCHI UV photometer C-635
- Fraction collector:
    - BÜCHI fraction collector C-660

The appropriate PP-cartridges were packed with silica (Merck, 40-63 µm).

D.3 Sublimation

For purification a self-made, turbomolecular-supported high vacuum sublimation system with following components was used:

- Pump system:
    - Leybold Turbovac 50 turbomolecular pump
    - Rotary vacuum pump
- Oven:
    - BÜCHI Glass Oven B-585
- Cold trap: filled with liquid nitrogen
- Pressure sensor

The flow chart of the used sublimation system is shown below:

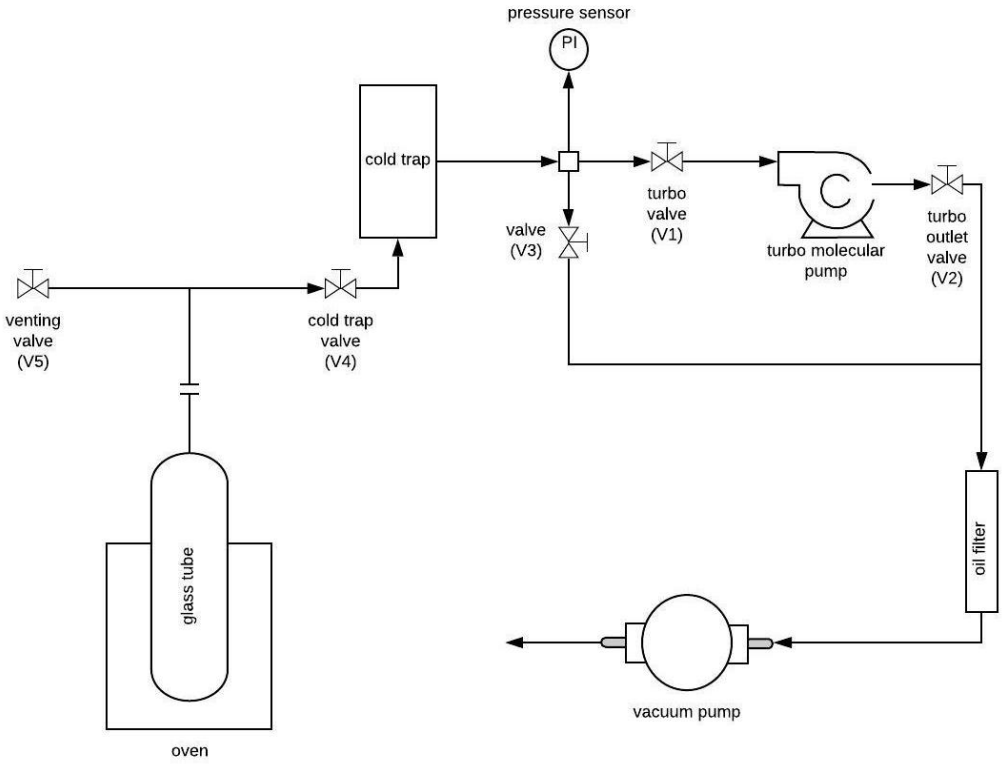

Figure D.1: Sublimation flow chart.

D.4 Microwave assisted reactions

Reaction supported by microwave irradiation was conducted using a *BIOTAGE® Initiator EXP EU 355301*.

D.5 Analytical methods

D.5.1 NMR-Spectroscopy

NMR spectra were recorded using a Bruker Avance DRX400 MHz (400 MHz for ^{1}H; 100 MHz for ^{13}C) or DRX-600 MHz (600 MHz for ^{1}H; 150 MHz for ^{13}C) Fourier transform spectrometer. ^{1}H- and ^{13}C-spectra are given as stated: chemical shift in parts per million (ppm) referenced to the according solvent (^{1}H: $CDCl_3$ δ=7.26 ppm, CD_2Cl_2 δ=5.32 ppm, DMSO-d6 δ=2.50 ppm; ^{13}C $CDCl_3$ δ=77.0 ppm, CD_2Cl_2 δ=54.0 ppm, DMSO-d6 δ=39.5 ppm) with tetramethylsilane (TMS) at δ=0 ppm. Multiplicities of the signals are given as: ^{1}H: s=singlet, d=doublet, t=triplet and m=multiplet.

D.5.2 GC-MS measurements

GC-MS measurements were conducted using a GC-MS interface from *Thermo Scientific*™:

- *TRACE*™ 1300 Gas Chromatograph with a Restek® Rxi®-5Sil MS column (l=30 m, ID=0.25 mm, 0.25 µm film, achiral).
- ISQ™ LT Single Quadrupole Mass Spectrometer (EI - electron ionization).

D.5.3 Absorption spectroscopy

Absorption spectroscopy was conducted on a NanoDrop™ One/OneC Microvolume UV-Vis Spectrophotometer from *Thermo Scientific*™ in DCM as a 5 µM solution.

D.5.4 Fluorescence and phosphorescence spectroscopy

Fluorescence and phosphorescence spectra were recorded on a PerkinElmer LS 55 Fluorescence spectrometer. Thereby, fluorescence was measured in degassed DCM solution (5 µM) and phosphorescence in a 1mg/mL degassed solution of toluene and ethanol (9:1) at 77 K.

D.5.5 Cyclic voltammetry (CV)

CV was conducted using a three-electrode configuration consisting of a Pt working electrode, a Pt counter electrode and an Ag/AgCl reference electrode and a PGSTAT128N potentiostat provided by Metrohm Autolab B.V. The measurements for the reduction scans were carried out in anhydrous DCM as 12.5 mM solutions. As a supporting electrolyte Bu_4NBF_4 (2.5 mM solution in DCM) was used, as well as ferrocene (12.5 mM), as a reference for potential calibration. Each sample was purged with nitrogen for 10 min before measuring.

D.6 Synthesis and characterization of the compounds

D.6.1 Donor synthesis

Methyl 2-(phenylamino)benzoate

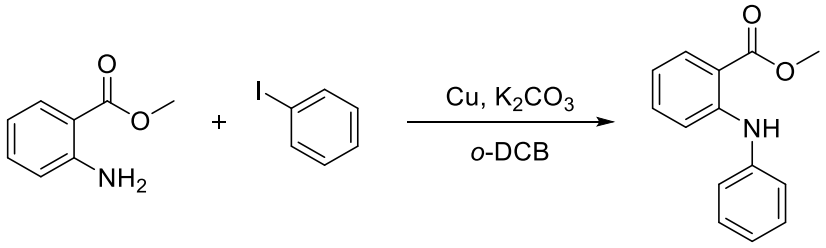

1	**2**	**3**
$C_8H_9NO_2$	C_6H_5I	$C_{14}H_{13}NO_2$
151,17	204,01	227,26

Synthesis of **3** followed the procedure according to Liu *et al.*[35]

Potassium carbonate (41.5 g, 300 mmol, 2 eq.) and copper (0.191 g, 3 mmol, 0.02 eq.) were weighed, under inert conditions, in a three-neck flask, equipped with a condenser and thermometer. A solution of **1** (22.7 g, 150 mmol, 1 eq.) and **2** (30.9 g, 150 mmol, 1 eq.), dissolved in 400 mL degassed *o*-DCB, was added. The reaction mixture was heated to 180 °C and allowed to stir for 28 h until full conversion (according to TLC) was observed. The suspension was cooled to rt, filtered off and the residue washed with DCM. The filtrate was concentrated under vacuum and the crude product purified *via* column chromatography (PE/EA 1:3) yielding **3** (27.3 g, 120 mmol, 80%) as a light yellow solid.

^{1}H NMR (400 MHz, $CDCl_3$, FID NIK010/20) δ = 9.45 (s, 1H), 7.97 (dd, J = 8.0, 1.6 Hz, 1H), 7.39 – 7.22 (m, 6H), 7.09 (ddt, J = 8.5, 7.4, 1.2 Hz, 1H), 6.73 (ddd, J = 8.1, 6.9, 1.3 Hz, 1H), 3.91 (s, 3H) ppm.

2-(2-(Phenylamino)phenyl)propan-2-ol

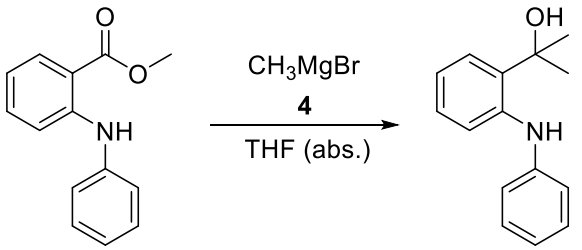

3
$C_{14}H_{13}NO_2$
227,26

5
$C_{15}H_{17}NO$
227,31

The synthesis of **5** was performed according to Reddy *et al.*[33]

Methylmagnesiumbromide **4** (158 mL, 475 mmol, 4 eq.) was placed in a dry three-neck flask, equipped with thermometer and condenser and covered with 300 mL degassed THF (abs.). Compound **3** (27.0 g, 119 mmol, 1 eq.), dissolved in 150 mL degassed THF (abs.), was added dropwise under cooling to 0 °C. After full addition, the reaction was stirred for 1 h at 50 °C followed by 20 h at rt (full conversion according to TLC). Subsequently, the reaction mixture was quenched by pouring on 500 mL ice water, followed by neutralization with saturated NH_4Cl solution and extraction with EA. The combined organic layers were dried over Na_2SO_4 and the solvent evaporated under reduced pressure. After flashing over silica and evaporating the solvent, **5** (27.03 g, 121 mmol, 99%) was obtained as a dark brown oil.

^{1}H NMR (400 MHz, DMSO-d6, FID NIK007/21) δ = 8.48 (s, 1H), 7.24 (dtd, J = 14.8, 7.6, 7.2, 1.5 Hz, 4H), 7.15 (td, J = 8.1, 7.6, 1.5 Hz, 1H), 7.01 – 6.95 (m, 2H), 6.83 (dtd, J = 13.1, 7.4, 1.3 Hz, 2H), 5.77 (s, 1H), 1.51 (s, 6H) ppm.

9,9-Dimethyl-9,10-dihydroacridine

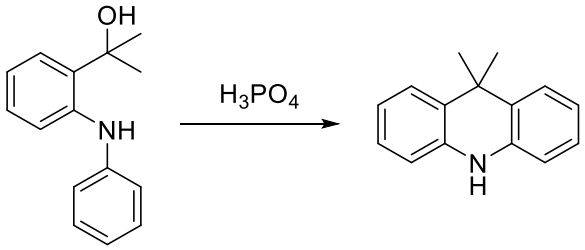

5
$C_{15}H_{17}NO$
227,31

6
$C_{15}H_{15}N$
209,29

Synthesis of **6** was conducted following Reddy *et al.*[33]

A solution of **5** (15.5 g, 68 mmol, 1 eq.) in 335 mL H_3PO_4 was weighed in a flask and stirred at rt overnight. The reaction mixture was diluted with water and neutralized with 4N NaOH. The green solid was filtered off and washed with water. The crude product was purified *via* column chromatography (PE/EA 8:1), yielding **6** (13,12 g, 63 mmol, 92%) as a yellow solid.

^{1}H NMR (400 MHz, $CDCl_3$, FID NIK009/10) δ = 7.39 (d, J = 7.7, 1.4 Hz, 2H), 7.11 (t, J = 7.6, 1.4 Hz, 2H), 6.92 (s, 2H), 6.70 (t, 2H), 6.09 (s, 1H), 1.59 (s, 6H) ppm.

D.6.2 Acceptor synthesis

D.6.3 Synthesis of carbolines

2,3,4,9-Tetrahydro-1*H*-pyrido[3,4-*b*]indole-3-carboxylic acid

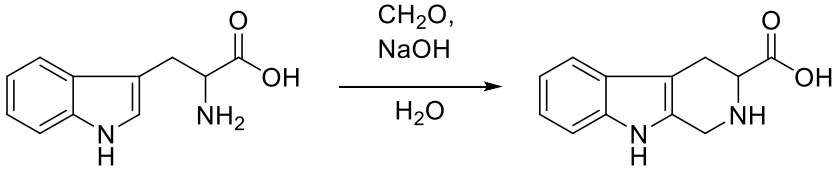

7
$C_{11}H_{12}N_2O_2$
204,23

8
$C_{12}H_{12}N_2O_2$
216,24

Synthesis of **8** followed the procedure according to Lippke *et al.*[40]

To an aqueous solution of L-Tryptophan **7** (15.3 g, 75 mmol, 1 eq.) and NaOH (3.00 g, 75 mmol, 1 eq.) in 50 mL water, formaldehyde (6.06 g, 75 mmol, 1 eq., aqueous solution 37%)

was added and the reaction was stirred for 1 h at rt. The reaction was refluxed for 2 h and after cooling to rt, 6N HCl was added until pH 6 was achieved. Subsequently, the solid was filtered and repeatedly washed with water, MeOH and DCM. The crude product was dried under reduced pressure giving **8** (13.5 g, 62 mmol, 83%) as a white solid.

^{1}H NMR (400 MHz, DMSO-d6, FID AYA013/110) δ = 10.97 (s, 1H), 7.43 (d, J = 7.8 Hz, 1H), 7.33 (d, J = 8.0 Hz, 1H), 7.07 (t, J = 7.6 Hz, 1H), 6.99 (t, J = 7.4 Hz, 1H), 4.34 – 4.07 (m, 2H), 3.61 (dd, J = 10.5, 5.0 Hz, 1H), 3.14 (dd, J = 16.1, 5.1 Hz, 1H), 2.81 (dd, J = 16.1, 10.5 Hz, 1H) ppm.

9*H*-Pyrido[3,4-*b*]indole / β-carboline

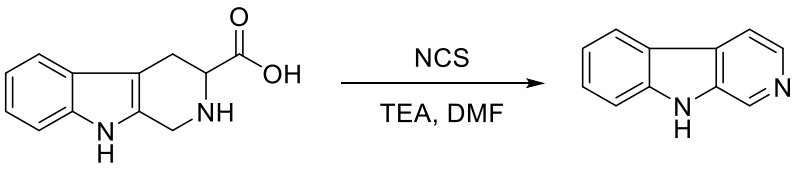

8
$C_{12}H_{12}N_2O_2$
216,24

9
$C_{11}H_8N_2$
168,20

The synthesis of **9** was performed according to Kamal *et al.*[42]

To a suspension of compound **8** (19.1 g, 88 mmol, 1 eq.) in 135 mL DMF, a solution of TEA (26.8 g, 265 mmol, 3 eq.) and NCS (24.8 g, 186 mmol, 2.1 eq.) in 135 mL DMF was added. The orange-brown suspension reaction was stirred 2 h at rt and afterwards quenched with water. The resulting suspension was repeatedly extracted with EA and the organic phase washed with saturated $NaHCO_3$ solution and water until neutral. The combined organic layers were dried over Na_2SO_4 and the solvent evaporated in vacuo leading to product **9** (12.2 g, 72 mmol, 82%) as an orange-beige solid.

^{1}H NMR (400 MHz, DMSO-d6, FID NIK004/10) δ = 11.61 (s, 1H), 8.90 (d, J = 1.2 Hz, 1H), 8.34 (d, J = 5.3 Hz, 1H), 8.24 (d, J = 7.9 Hz, 1H), 8.10 (d, J = 5.2 Hz, 1H), 7.60 (dd, 1H), 7.54 (ddd, J = 8.2, 6.9, 1.2 Hz, 1H), 7.24 (ddd, J = 8.0, 6.8, 1.2 Hz, 1H) ppm.

_N_-(2-Bromophenyl)pyridin-4-amine

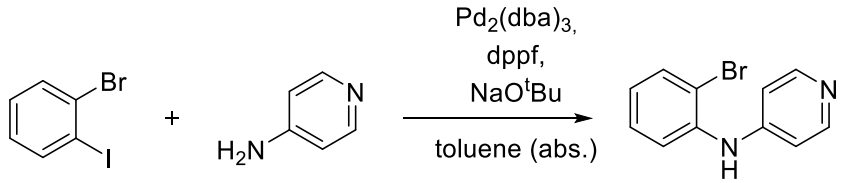

10	**11**	**12**
C_6H_4BrI	$C_5H_6N_2$	$C_{11}H_9BrN_2$
282,91	94,12	249,11

Synthesis of **12** was conducted following Iwaki *et al.*[43]

To a suspension of **11** (2.35 g, 25 mmol, 1 eq.), NaO^{t}Bu (3.36 g, 35 mmol, 1.4 eq.), $Pd_2(dba)_3$ (28.0 mg, 0.25 mmol, 1 mol%) and dppf (0.280 g, 0.5 mmol, 2 mol%) in 100 mL degassed toluene (abs.), **10** (8.49 g, 30 mmol, 1.2 eq.) was added *via* a syringe, under inert conditions and heated to reflux. After 2 days, the reaction was quenched with 40 mL distilled water and repeatedly extracted with EA. The combined organic layers were dried over Na_2SO_4 and the solvent evaporated under reduced pressure. The crude product was purified *via* column chromatography (DCM/MeOH 1% → 4%) yielding **12** (3.50 g, 14 mmol, 56 %) as a dark-brown, viscous liquid.

^{1}H NMR (400 MHz, $CDCl_3$, FID NIK001/20): δ = 7.85 (dd, J= 4.7 Hz, 1.6 Hz, 1H), 7.43 (dd, J = 8.0 Hz, 1.8 Hz, 1H), 7.39-7.34 (m, 2H), 7.18-7.07 (m, 4H), 6.16 (bs, 1H) ppm.

5*H*-Pyrido[4,3-*b*]indole / γ-carboline

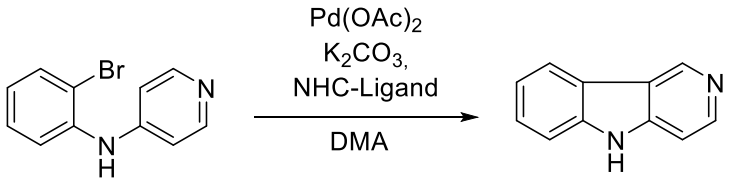

12	**13**
$C_{11}H_9BrN_2$	$C_{11}H_8N_2$
249,11	168,20

Synthesis of **13** followed the procedure according to Iwaki *et al.*[43]

$Pd(OAc)_2$ (65.0 mg, 0.29 mmol, 2 mol%), the NHC-ligand **65** (124 mg, 0.29 mmol, 2 mol%) and potassium carbonate (3.88 g, 30 mmol, 2 eq.), were weighed in a three-neck flask equipped with thermometer and condenser under inert atmosphere. Compound **12** (3.50 g, 15 mmol, 1 eq.), in 70 mL degassed DMA, was added dropwise and the reaction heated to

130 °C. After 71 h, more $Pd(OAc)_2$ (65.0 mg, 0.29 mmol, 2 mol%) and NHC-ligand 65 (124 mg, 0.29 mmol, 2 mol%) were added and the reaction finally quenched after further 2 days. The suspension was diluted with EA, filtered, and the filtrate repeatedly washed with brine and distilled water. The combined organic layers were dried over Na_2SO_4 and the solvent evaporated under reduced pressure. The crude product was recrystallized from toluene yielding **13** (1.53 g, 9 mmol, 38%) as a light brown solid.

^{1}H NMR (400 MHz, DMSO-d6, FID NIK003) δ = 11.70 (s, 1H), 9.33 (s, 1H), 8.42 (d, J = 5.6 Hz, 1H), 8.23 (d, J = 7.8 Hz, 1H), 7.56 (d, J = 8.1 Hz, 1H), 7.53 – 7.39 (m, 2H), 7.33 – 7.22 (m, 1H) ppm.

N-Acetyl-3-bromo-4-piperidone, hydrobromide

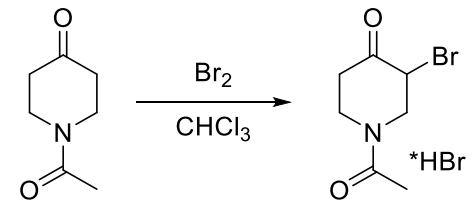

14
$C_7H_{11}NO_2$
141,17

15
$C_7H_{11}Br_2NO_2$
300,98

The synthesis of **15** was performed according to F. Dennone.[44]

14 (6.15 g, 44 mmol, 1 eq.) was dissolved in 116 mL $CHCl_3$ and cooled to 0 °C. Br_2 (7.66 g, 48 mmol, 1.1 eq.), diluted with 2 mL $CHCl_3$, was added at 0 °C and the reaction mixture was stirred under further cooling for 5 min. The reaction was allowed to heat up to rt and stirred for another 2 h. Thereby, the color of the dispersion changed from an intense orange to white. Subsequently, the solid was filtered, washed with $CHCl_3$ and dried under vacuum, yielding **15** (11.3 g, 37 mmol, 86%) as a white solid.

5*H*-Pyrido[4,3-*b*]indole / γ-carboline

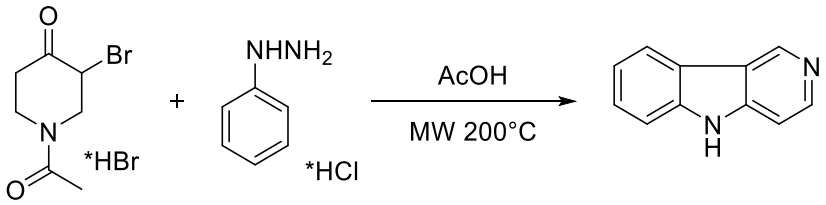

15
$C_7H_{11}Br_2NO_2$
300,98

16
$C_6H_9ClN_2$
144,60

13
$C_{11}H_8N_2$
168,20

Synthesis **13** of was conducted following Chen *et al*.[45]

A microwave vial was charged with **15** (2.40 g, 8 mmol, 1 eq.), **16** (1.74 g, 12 mmol, 1.5 eq.) and 20 mL acetic acid (98%-100%). The reaction was stirred in the microwave for 10 min at 200 °C, the residue was taken up with 1N HCl, followed by neutralization with 2N NaOH. The aqueous solution was repeatedly extracted with EA and the combined organic layers were dried over Na_2SO_4. The solvent was evaporated under reduced pressure and the crude product was purified *via* column chromatography (DCM/MeOH 5% → 30%), yielding **13** (302 mg, 1.8 mmol, 23%) as a grey-brown solid.

^{1}H NMR (400 MHz, DMSO-d6, FID NIK026/20) δ 12.33 (s, 1H), 9.93 (d, J = 1.0 Hz, 1H), 9.01 (d, J = 5.7 Hz, 1H), 8.81 (dt, J = 7.9, 1.0 Hz, 1H), 8.15 (dt, J = 8.2, 1.0 Hz, 1H), 8.10 – 7.99 (m, 2H), 7.85 (ddd, J = 8.0, 7.1, 1.1 Hz, 1H).

3-Chloro-*N*-(pyridin-4-yl)pyridin-4-amine

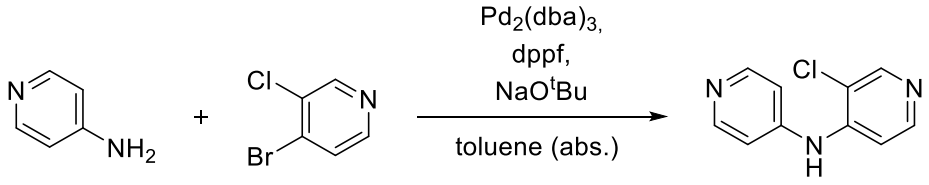

11
$C_5H_6N_2$
94,12

17
C_5H_3BrClN
192,44

18
$C_{10}H_8ClN_3$
205,65

Synthesis of **18** followed a modified procedure according to Iwaki *et al.*[43]

Compound **11** (1.88 g, 20 mmol, 1 eq.), **17** (4.23 g, 22 mmol, 1.1 eq.), $Pd_2(dba)_3$ (366 mg, 0.4 mmol, 2 mol%), dppf (444 mg, 0.8 mmol, 4 mol%) and NaO^tBu (2.69 g, 28 mmol, 1.4 eq.)

were suspended in 80 mL degassed toluene (abs.) and refluxed under inert atmosphere overnight. The reaction was quenched with distilled water and extracted repeatedly with EA. The combined organic layers were dried over Na_2SO_4 and the solvent evaporated under reduced pressure. The crude product was purified *via* column chromatography (DCM/MeOH 1% → 5%), yielding **18** (3.51 g, 17 mmol, 85%) as an off-white solid.

^{1}H NMR (400 MHz, $CDCl_3$, FID NIK034/20) δ = 8.52 (d, J = 8.7 Hz, 3H), 8.32 (d, J = 5.6 Hz, 1H), 7.31 (d, J = 5.5 Hz, 1H), 7.11 (d, J = 5.4 Hz, 2H), 6.87 (s, 1H) ppm.

5*H*-Pyrrolo[3,2-*c*:4,5-*c'*]dipyridine

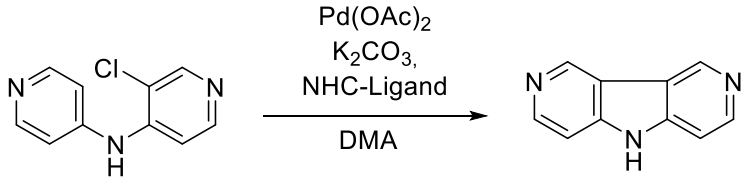

18
$C_{10}H_8ClN_3$
205,65

19
$C_{10}H_7N_3$
169,19

The synthesis of **19** was performed according to a modified procedure from Iwaki *et al.*[43]

Compound **18** (823 mg, 4.0 mmol, 1 eq.) $Pd(OAc)_2$ (78.0 mg, 0.32 mmol, 8 mol%), the NHC-ligand **65** (126 mg, 0.32 mmol, 8 mol%) and potassium carbonate (1.11 g, 8 mmol, 2 eq.) were charged under argon in a vial in 18 mL degassed DMA. The reaction was heated to 130 °C for 6 days and after cooling to rt, the black suspension was diluted with EA. Subsequently, the solid was filtered off and the filtrate repeatedly washed with saturated $NaHCO_3$ solution, 2N NaOH and distilled water. The combined organic layers were dried over Na_2SO_4 and the solvent evaporated under reduced pressure. The crude product was purified *via* column chromatography (DCM/MeOH 10%), giving **19** (388 mg, 2.2 mmol, 57%) as a light-beige solid.

^{1}H NMR (400 MHz, DMSO-d6, FID NIK043/20) δ = 12.12 (s, 1H), 9.44 (d, J = 1.1 Hz, 2H), 8.51 (d, J = 5.7 Hz, 2H), 7.55 (dd, J = 5.7, 1.1 Hz, 2H) ppm.

D.6.4 Synthesis of pre-functionalization carboline derivatives

6-Bromo-9*H*-pyrido[3,4-*b*]indole

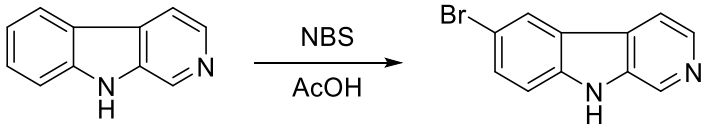

9
$C_{11}H_8N_2$
168,20

20
$C_{11}H_7BrN_2$
247,10

Synthesis of **20** was conducted following Kamal *et al.*[42]

β-Carboline **9** (392 mg, 2.3 mmol, 1 eq.) was dissolved in 12 mL AcOH (98%-100%) and NBS (456 mg, 2.6 mmol, 1.1 eq.) added as a solid. After 2 h and full conversion (according to TLC), the solution was concentrated under vacuum and the residue neutralized with saturated $NaHCO_3$ solution. The aqueous solution was extracted with EA and repeatedly washed with distilled water. The combined organic layers were dried over Na_2SO_4 and the solvent evaporated under reduced pressure. The crude product was recrystallized from ACN and further purified *via* column chromatography (PE/EA 1:4), yielding **20** (505 mg, 2.0 mmol, 86%) as a beige solid.

^{1}H NMR (400 MHz, DMSO-d6, FID NIK005/20) δ = 11.78 (s, 1H), 8.94 (d, J = 1.1 Hz, 1H), 8.52 (d, J = 2.0 Hz, 1H), 8.36 (d, J = 5.2 Hz, 1H), 8.16 (dd, J = 5.3, 1.1 Hz, 1H), 7.66 (dd, J = 8.7, 2.0 Hz, 1H), 7.58 (d, J = 8.7 Hz, 1H) ppm.

8-Bromo-5*H*-pyrido[4,3-*b*]indole

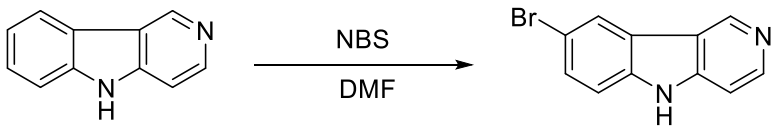

13
$C_{11}H_8N_2$
168,20

21
$C_{11}H_7BrN_2$
247,10

γ-Carboline **13** (673 mg, 4.0 mmol, 1 eq.) was dissolved in 20 mL DMF and cooled to 0 °C. NBS (783 mg, 4.4 mmol, 1.1 eq.) was added as a solid and the reaction mixture allowed stirring for 1 h at 0 °C. After further stirring for 24 h at rt, the reaction was quenched with distilled water

and extracted repeatedly with EA. The combined organic layers were dried over Na_2SO_4 and the solvent evaporated under reduced pressure. The crude product was purified *via* column chromatography (PE/EA 1:4), yielding **21** (520 mg, 2.1 mmol, 53%) as a beige solid.

^{1}H NMR (400 MHz, DMSO-d6, FID NIK036/20) δ = 11.86 (s, 1H), 9.38 (s, 1H), 8.49 (d, J = 1.9 Hz, 1H), 8.44 (d, J = 5.7 Hz, 1H), 7.65 – 7.40 (m, 3H) ppm.

D.6.5 Synthesis of functionalized carboline derivatives

9-(3-Chloropyridin-4-yl)-9*H*-carbazole

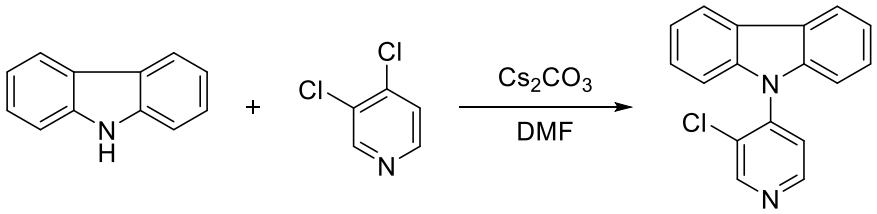

22
$C_{12}H_9N$
167,21

23
$C_5H_3Cl_2N$
147,99

24
$C_{17}H_{11}ClN_2$
278,74

The synthesis of **24** was performed modified according to Kader *et al.*[28]

Carbazole **22** (5.02 g, 30 mmol, 1 eq.) and Cs_2CO_3 (10.8 g, 33 mmol, 1.1 eq.) were suspended in 55 mL DMF and **23** (4.44 g, 30 mmol, 1 eq.) in 5 mL DMF was added. The reaction was heated to 130 °C for 64 h, afterwards quenched with distilled water and extracted repeatedly with DCM. The combined organic layers were dried over Na_2SO_4 and the solvent evaporated under vacuum. The crude product was purified *via* column chromatography (DCM/PE 50% → 80%), yielding **24** (6.94 g, 25 mmol, 83%) as a yellow solid.

^{1}H NMR (400 MHz, DMSO-d6, FID NIK014/20) δ = 9.03 (s, 1H), 8.81 (d, J = 5.1 Hz, 1H), 8.26 (dt, J = 7.7, 1.0 Hz, 2H), 7.81 (d, J = 5.1 Hz, 1H), 7.44 (ddd, J = 8.3, 7.2, 1.3 Hz, 2H), 7.33 (td, J = 7.5, 1.0 Hz, 2H), 7.17 (dt, J = 8.2, 0.9 Hz, 2H) ppm.

6-Bromo-9-(2-nitrophenyl)-9*H*-pyrido[3,4-*b*]indole

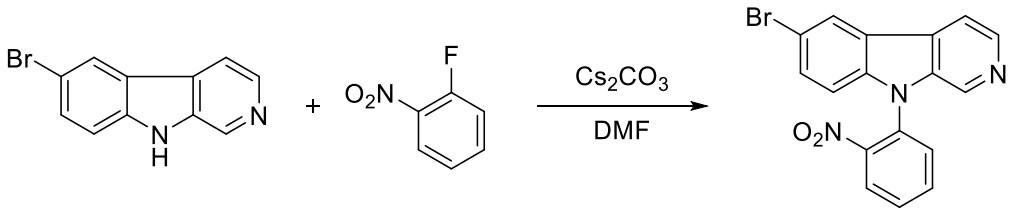

20	**25**	**XXVI**
$C_{11}H_7BrN_2$	$C_6H_4FNO_2$	$C_{17}H_{10}BrN_3O_2$
247,10	141,10	368,19

Synthesis of **XXVI** was conducted following a modified procedure from Wharton *et al.*[48]

Compound **20** (1.98 g, 8 mmol, 1 eq.) and Cs_2CO_3 (2.87 g, 8.8 mmol, 1.1 eq.) were suspended in 12 mL DMF and **25** (1.13 g, 8 mmol, 1 eq.) in 4 mL DMF was added. The reaction was heated to 130 °C for 64 h and then quenched with distilled water and extracted repeatedly with DCM. The combined organic layers were dried over Na_2SO_4 and the solvent evaporated under vacuum. The crude product was purified *via* column chromatography (DCM/MeOH 10%), yielding **XXVI** (2.22 g, 6 mmol, 75%) as a brown solid.

^{1}H NMR (400 MHz, $CDCl_3$, FID NIK019/1) δ = 8.59 (s, 1H), 8.56 (d, J = 5.3 Hz, 1H), 8.32 (d, J = 1.9 Hz, 1H), 8.24 (dd, J = 8.2, 1.5 Hz, 1H), 7.98 (dd, J = 5.3, 1.1 Hz, 1H), 7.91 (td, J = 7.7, 1.5 Hz, 1H), 7.78 (td, J = 7.9, 1.4 Hz, 1H), 7.68 (dd, J = 7.9, 1.4 Hz, 1H), 7.61 (dd, J = 8.7, 1.9 Hz, 1H), 7.02 (d, J = 8.8 Hz, 1H) ppm.

2-(6-Bromo-9*H*-pyrido[3,4-*b*]indol-9-yl)aniline

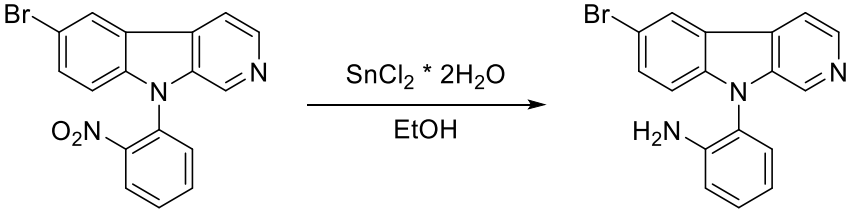

XXVI	**XXVII**
$C_{17}H_{10}BrN_3O_2$	$C_{17}H_{12}BrN_3$
368,19	338,21

Synthesis of **XXVII** followed the procedure according to Dunlop and Tucker.[38]

To a suspension of **XXVI** (786 mg, 2.1 mmol, 1 eq.) in 10 mL EtOH, $SnCl_2*2H_2O$ (1.69 g, 7.5 mmol, 3.5 eq.) was added as a solid and the mixture was refluxed for 18 h. After cooling to rt, the reaction mixture was neutralized with 2N NaOH and repeatedly extracted with DCM. The combined organic layers were washed with distilled water, dried over Na_2SO_4 and the solvent evaporated under reduced pressure, yielding **XXVII** (620 mg, 1.8 mmol, 86%) as a beige solid.

^{1}H NMR (400 MHz, $CDCl_3$, FID NIK038/30) δ = 8.55 (d, J = 1.1 Hz, 1H), 8.45 (d, J = 5.3 Hz, 1H), 8.24 (d, J = 1.9 Hz, 1H), 7.88 (dd, J = 5.3, 1.1 Hz, 1H), 7.54 (dd, J = 8.8, 1.9 Hz, 1H), 7.28 (ddd, J = 8.6, 7.4, 1.5 Hz, 1H), 7.16 (dd, J = 7.8, 1.5 Hz, 1H), 7.07 (d, J = 8.7 Hz, 1H), 6.91 (dd, J = 8.1, 1.3 Hz, 1H), 6.85 (td, J = 7.6, 1.3 Hz, 1H), 3.50 (s, 2H) ppm.

6-Bromo-9-(2-bromophenyl)-9*H*-pyrido[3,4-*b*]indole

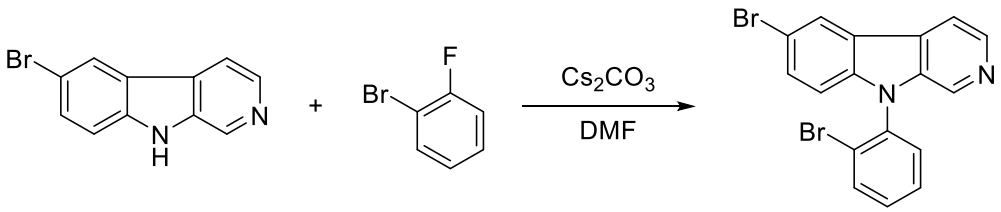

20	**28**	**XXIX**
$C_{11}H_7BrN_2$	C_6H_4BrF	$C_{17}H_{10}Br_2N_2$
247,10	175,00	402,09

The synthesis of **XXIX** was performed modified according to Kader *et al.*[28]

The carboline **20** (1.24 g, 5.0 mmol, 1 eq.) and Cs_2CO_3 (3.26 g, 10 mmol, 2 eq.) were suspended in 8 mL DMF and heated to 130 °C. After 15 min, **28** (1.75 g, 10 mmol, 2 eq.) in 5 mL DMF was added, while keeping the temperature. After 17 h and full conversion (according to TLC), the reaction was cooled to rt, quenched with distilled water and extracted repeatedly with DCM. The combined organic layers were dried over Na_2SO_4 and the solvent evaporated under vacuum. The crude product was purified *via* column chromatography (DCM/EA 1:2), yielding **XXIX** (1.68 g, 4.2 mmol, 84%) as an orange solid.

^{1}H NMR (400 MHz, $CDCl_3$, FID NIK006/30) δ = 8.55 (d, J = 6.4 Hz, 2H), 8.34 (d, J = 1.9 Hz, 1H), 8.02 (dd, J = 5.3, 1.1 Hz, 1H), 7.89 (dd, J = 8.4, 1.4 Hz, 1H), 7.64 (dd, J = 8.8, 1.9 Hz, 1H), 7.62 – 7.55 (m, 1H), 7.49 (ddd, J = 8.6, 7.3, 1.3 Hz, 2H), 7.04 (d, J = 8.8 Hz, 1H) ppm.

9-(4-Chloropyridin-3-yl)-9*H*-pyrido[3,4-*b*]indole

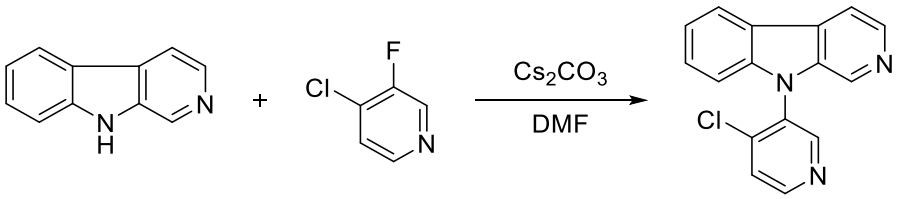

9
$C_{11}H_8N_2$
168,20

29
C_5H_3ClFN
131,53

30
$C_{16}H_{10}ClN_3$
279,73

Synthesis of **30** was conducted under modification of Kader *et al.*[28]

β-Carboline **9** (1.02 g, 6.1 mmol, 1 eq.) and Cs_2CO_3 (2.18 g, 6.7 mmol, 1.1 eq.) were suspended in 8 mL DMF and **29** (799 mg, 6.1 mmol, 1 eq.), in 8 mL DMF, was added. The reaction was heated to 130 °C for 42 h, quenched afterwards with distilled water and extracted repeatedly with DCM. The combined organic layers were dried over Na_2SO_4 and the solvent evaporated under vacuum. The crude product was purified *via* column chromatography (PE/EA 75% → 80%), yielding **30** (523 mg, 1.9 mmol, 31%) as a brown solid.

^{1}H NMR (400 MHz, $CDCl_3$, FID NIK056/20) δ = 8.80 (s, 1H), 8.74 (d, J = 5.3 Hz, 1H), 8.62 – 8.50 (m, 2H), 8.22 (dt, J = 7.9, 1.0 Hz, 1H), 8.04 (dd, J = 5.2, 1.1 Hz, 1H), 7.69 (d, J = 5.3 Hz, 1H), 7.57 (ddd, J = 8.3, 7.2, 1.2 Hz, 1H), 7.40 (ddd, J = 8.0, 7.2, 1.0 Hz, 1H), 7.15 (dt, J = 8.3, 0.9 Hz, 1H) ppm.

5-(2-Bromophenyl)-5*H*-pyrido[4,3-*b*]indole

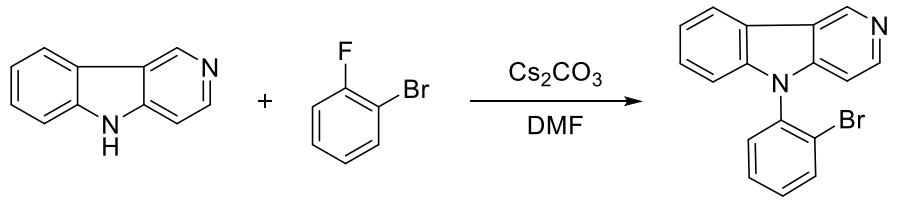

13
$C_{11}H_8N_2$
168,20

28
C_6H_4BrF
175,00

31
$C_{17}H_{11}BrN_2$
323,19

Synthesis of **31** followed a modified procedure according to Kader *et al.*[28]

γ-Carboline **13** (672 mg, 4.0 mmol, 1 eq.) and Cs_2CO_3 (2.61 g, 8.0 mmol, 2 eq.) were suspended in 4 mL DMF and **28** (1.40 g, 8.0 mmol, 2 eq.), in 4 mL DMF, was added. The

reaction was heated to 130 °C for 15 h, afterwards quenched with distilled water and extracted repeatedly with DCM. The combined organic layers were dried over Na_2SO_4 and the solvent evaporated under vacuum. The crude product was purified *via* column chromatography (PE/EA 1:3) yielding **31** (718 mg, 2.2 mmol, 55%) as a brown solid.

^{1}H NMR (400 MHz, $CDCl_3$, FID NIK040/20) δ = 9.40 (s, 1H), 8.52 (d, J = 5.7 Hz, 1H), 8.22 (dt, J = 7.7, 1.0 Hz, 1H), 7.93 – 7.83 (m, 1H), 7.57 (ddd, J = 8.3, 7.2, 1.4 Hz, 1H), 7.53 – 7.42 (m, 3H), 7.39 (td, J = 7.5, 1.1 Hz, 1H), 7.11 (dt, J = 8.1, 0.9 Hz, 1H), 7.00 (dd, J = 5.7, 1.0 Hz, 1H) ppm.

3,5-Dichloro-*N*,*N*-diphenylpyridin-4-amine

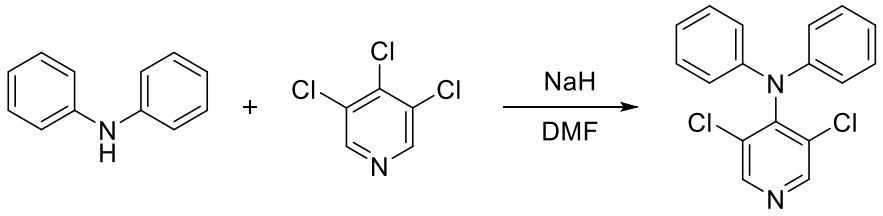

32
$C_{12}H_{11}N$
169,23

33
$C_5H_2Cl_3N$
182,43

34
$C_{17}H_{12}Cl_2N_2$
315,20

Synthesis of **34** was performed according to Kautny *et al.*[27]

Diphenylamine **32** (338 mg, 1.9 mmol, 1 eq.) and NaH (96 mg, 4.0 mmol, 4 eq., from 60% oil dispersion, washed with PE) were dissolved in 7 mL DMF and stirred for 30 min at rt. **33** (438 mg, 2.4 mmol, 1.2 eq.) was added and the reaction mixture heated to 50 °C. After 20 h, more NaH (48 mg, 2 mmol, 1 eq., 60% oil solution dispersion, washed with PE) was added and stirred for another 6 h. Subsequently, the reaction was quenched with distilled water and extracted repeatedly with DCM. The combined organic layers were dried over Na_2SO_4 and the solvent evaporated under vacuum, leaving a black solid. The crude product was purified *via* column chromatography, (DCM/PE 10%→60%), yielding **34** (0.329 g, 0.8 mmol, 52%) as white crystals.

^{1}H NMR (400 MHz, $CDCl_3$, FID NIK074/20) δ = 8.83 (s, 2H), 7.57 (td, J = 7.3, 1.7 Hz, 4H), 7.36 (td, J = 7.3, 1.2 Hz, 2H), 7.25 (dd, J = 8.6, 1.2 Hz, 3H) ppm.

4-Nitro-*N*-phenylaniline

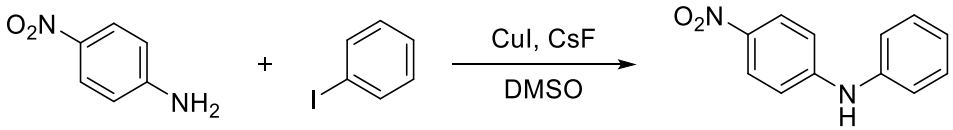

35	**2**	**36**
$C_6H_6N_2O_2$	C_6H_5I	$C_{12}H_{10}N_2O_2$
138,13	204,01	214,22

Synthesis of **36** was conducted following Güell and Ribas.[50]

4-Nitroaniline **35** (138 mg, 1.0 mmol, 2 eq.) and CsF (152 mg, 1.0 mmol, 2 eq.) were weighed in a vial and a mixture of iodobenzene **2** (102 mg, 0.5 mmol, 1 eq.) and CuI (9.00 mg, 0.05 mmol, 10 mol%), in 1 mL DMSO, was added. The reaction was heated to 130 °C for 18 h and after full conversion (according to TLC) diluted with EA and filtered. The filtrate was concentrated under reduced pressure and the crude product was purified *via* column chromatography (DCM/PE 20% → 60%), yielding **36** (35.0 mg, 0.2 mmol, 33%) as a yellow solid.

^{1}H NMR (400 MHz, $CDCl_3$, FID NIK097/40) δ = 8.16 – 8.08 (m, 2H), 7.47 – 7.31 (m, 2H), 7.25 – 7.17 (m, 2H), 7.17 (tt, J = 7.4, 1.1 Hz, 1H), 6.99 – 6.89 (m, 2H), 6.27 (s, 1H) ppm.

3,5-Dichloro-*N*-(4-nitrophenyl)-*N*-phenylpyridin-4-amine

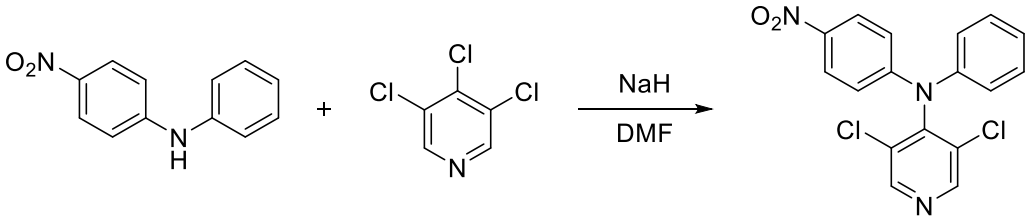

36	**33**	**XXXVII**
$C_{12}H_{10}N_2O_2$	$C_5H_2Cl_3N$	$C_{17}H_{11}Cl_2N_3O_2$
214,22	182,43	360,19

Synthesis of **XXXVII** followed a modified procedure according to Kautny *et al.*[27]

Compound **36** (574 mg, 2.7 mmol, 1 eq.) and NaH (193 mg, 8.0 mmol, 3 eq., from 60% oil dispersion, washed with PE) were dissolved in 13 mL DMF and stirred for 15 min at rt. Trichloropyridine **33** (587 mg, 3.2 mmol, 1.2 eq.) was added and the reaction mixture heated to 130 °C. After 18 h the reaction was quenched with distilled water and extracted repeatedly

with DCM. The combined organic layers were dried over Na_2SO_4 and the solvent evaporated under vacuum. The crude product was purified *via* column chromatography (DCM/PE 10% → 60%), yielding **XXXVII** (276 mg, 0.8 mmol, 29%) as a dark brown solid.

^{1}H NMR (400 MHz, $CDCl_3$, FID NIK093/20) δ = 8.72 (s, 2H), 8.27 – 8.14 (m, 2H), 7.47 (tt, J = 7.7, 1.8 Hz, 2H), 7.39 – 7.30 (m, 1H), 7.25 (dq, J = 6.8, 1.2 Hz, 2H), 6.97 – 6.82 (m, 2H) ppm.

5-(2-Bromo-4-nitrophenyl)-5*H*-pyrido[4,3-*b*]indole

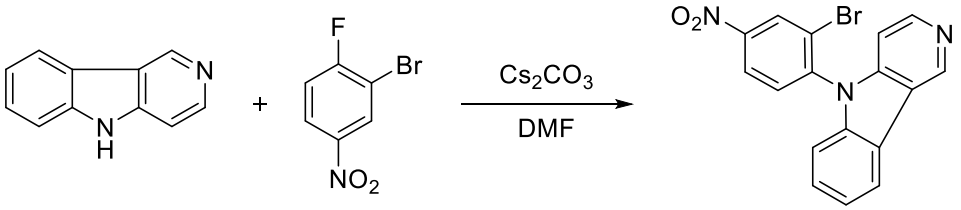

13
$C_{11}H_8N_2$
168,20

38
$C_6H_3BrFNO_2$
220,00

XXXIX
$C_{17}H_{10}BrN_3O_2$
368,19

Synthesis of **XXXIX** was performed modified according to Wharton *et al.*[48]

γ-Carboline **13** (336 mg, 2.0 mmol, 1 eq.) and Cs_2CO_3 (717 mg, 2.2 mmol, 1.1 eq.) were suspended in 3 mL DMF and **38** (440 mg, 2.0 mmol, 1 eq.), in 1 mL DMF, was added. The reaction was heated to 130 °C for 22 h, quenched with distilled water and extracted repeatedly with DCM. The combined organic layers were dried over Na_2SO_4 and the solvent evaporated under vacuum. The crude product was purified *via* column chromatography (PE/EA 1:3), leading to product **XXXIX** (301 mg, 0.8 mmol, 41%) as a yellow solid.

^{1}H NMR (400 MHz, $CDCl_3$, FID NIK016/20) δ = 9.45 – 9.38 (m, 1H), 8.77 (d, J = 2.5 Hz, 1H), 8.56 (d, J = 5.8 Hz, 1H), 8.45 (dd, J = 8.6, 2.5 Hz, 1H), 8.24 (dt, J = 7.7, 1.0 Hz, 1H), 7.72 (d, J = 8.6 Hz, 1H), 7.52 (ddd, J = 8.3, 7.3, 1.3 Hz, 1H), 7.45 (td, J = 7.5, 1.1 Hz, 1H), 7.12 (dt, J = 8.2, 0.9 Hz, 1H), 7.02 (dd, J = 5.8, 1.0 Hz, 1H) ppm.

8-Bromo-5-(2-nitrophenyl)-5*H*-pyrido[4,3-*b*]indole

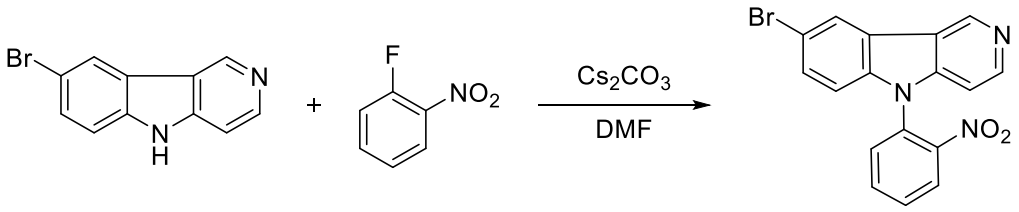

21	**25**	**XL**
$C_{11}H_7BrN_2$	$C_6H_4FNO_2$	$C_{17}H_{10}BrN_3O_2$
247,10	141,10	368,19

Synthesis of **XL** was conducted modified following Wharton *et al.*[48]

The carboline **21** (417 mg, 1.7 mmol, 1 eq.) and Cs_2CO_3 (605 mg, 1.9 mmol, 1.1 eq.) were suspended in 2 mL DMF and **25** (238 mg, 1.7 mmol, 1 eq.), in 2 mL DMF, was added. The reaction was heated to 130 °C for 19 h, quenched with distilled water and extracted repeatedly with DCM. The combined organic layers were dried over Na_2SO_4 and the solvent evaporated under vacuum. The crude product was purified *via* column chromatography (DCM/MeOH 1% → 5%), yielding **XL** (369 mg, 1 mmol, 59%) as a brown oil.

^{1}H NMR (400 MHz, $CDCl_3$, FID NIK042/20) δ = 9.35 (s, 1H), 8.54 (d, J = 6.0 Hz, 1H), 8.33 (d, J = 1.9 Hz, 1H), 8.24 (dd, J = 8.2, 1.5 Hz, 1H), 7.96 – 7.86 (m, 1H), 7.79 (td, J = 7.8, 1.3 Hz, 1H), 7.65 (dd, J = 7.9, 1.4 Hz, 1H), 7.55 (dt, J = 8.7, 1.4 Hz, 1H), 7.06 – 6.96 (m, 2H) ppm.

2-(8-Bromo-5*H*-pyrido[4,3-*b*]indol-5-yl)aniline

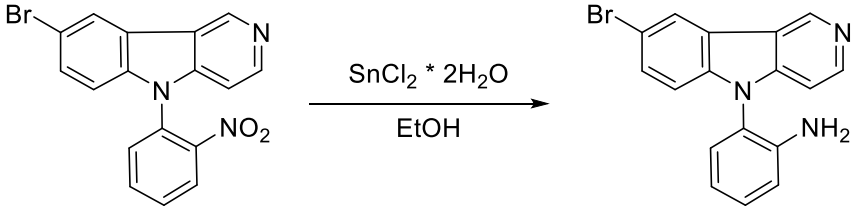

XL	**XLI**
$C_{17}H_{10}BrN_3O_2$	$C_{17}H_{12}BrN_3$
368,19	338,21

Synthesis of **XLI** followed the procedure according to Dunlop and Tucker.[38]

To a suspension of **XL** (330 mg, 0.9 mmol, 1 eq.) in 4 mL EtOH, $SnCl_2$*$2H_2O$ (708 mg, 3.14 mmol, 3.5 eq.) was added as a solid and refluxed for 18 h. After cooling to rt the reaction mixture was neutralized with 2N NaOH and repeatedly extracted with DCM. The combined

organic layers were washed with distilled water, dried over Na_2SO_4 and the solvent evaporated under reduced pressure, yielding **XLI** (0.302 g, 0.9 mmol, 99%) as a brown solid.

^{1}H NMR (400 MHz, $CDCl_3$, FID NIK044/10) δ = 9.33 (s, 1H), 8.52 (d, J = 5.7 Hz, 1H), 8.33 (d, J = 1.9 Hz, 1H), 7.56 (dd, J = 8.7, 1.9 Hz, 1H), 7.42 – 7.29 (m, 1H), 7.21 (dd, J = 7.8, 1.5 Hz, 1H), 7.15 – 7.06 (m, 2H), 6.98 (dd, J = 8.2, 1.3 Hz, 1H), 6.93 (td, J = 7.6, 1.4 Hz, 1H), 3.55 (s, 2H) ppm.

5-(2-Bromophenyl)-5*H*-pyrrolo[3,2-*c*:4,5-*c'*]dipyridine

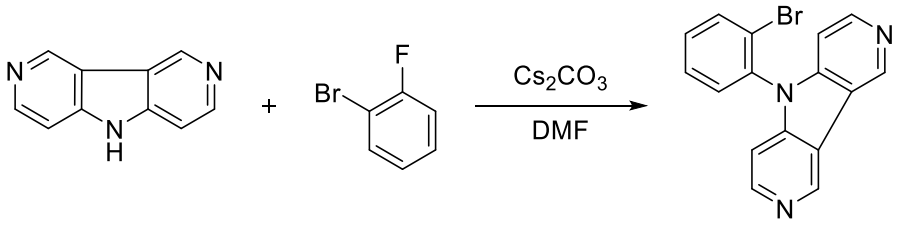

19	**28**	**XLII**
$C_{10}H_7N_3$	C_6H_4BrF	$C_{16}H_{10}BrN_3$
169,19	175,00	324,18

The synthesis of **XLII** was performed as a modification according to Kader *et al.*[28]

19 (379 mg, 2.2 mmol, 1 eq.) and Cs_2CO_3 (1.46 g, 4.5 mmol, 2 eq.) were suspended in 3 mL DMF and **28** (784 mg, 4.5 mmol, 2 eq.), in 3 mL DMF, was added. The reaction was heated to 130 °C for 22 h and then quenched with distilled water and extracted repeatedly with DCM. The combined organic layers were dried over Na_2SO_4 and the solvent evaporated in vacuo. The crude product was purified *via* column chromatography (DCM/MeOH 1% → 3%), yielding **XLII** (402 mg, 1.2 mmol, 55%) as a yellow solid.

^{1}H NMR (400 MHz, $CDCl_3$, FID NIK073/10) δ = 9.47 (s, 2H), 8.60 (d, J = 5.7 Hz, 2H), 7.90 (dd, J = 8.0, 1.5 Hz, 1H), 7.60 (td, J = 7.6, 1.5 Hz, 1H), 7.56 – 7.43 (m, 2H), 7.06 (dd, J = 5.8, 1.0 Hz, 2H) ppm.

5-(2-Bromo-4-nitrophenyl)-5*H*-pyrrolo[3,2-*c*:4,5-*c'*]dipyridine

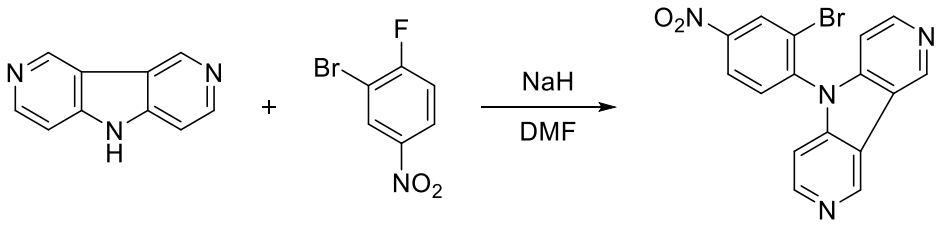

19	**38**	**XLIII**
$C_{10}H_7N_3$	$C_6H_3BrFNO_2$	$C_{16}H_9BrN_4O_2$
169,19	220,00	369,18

Synthesis of **XLIII** was conducted modified following Wharton *et al.*[48]

Compound **19** (614 mg, 3.6 mmol, 1 eq.) and NaH (0.218 g, 9.1 mmol, 2.5 eq., from 60% oil dispersion, washed with PE) were dissolved in 6 mL DMF and stirred for 15 min at rt. **38** (959 mg, 4.4 mmol, 1.2 eq.) was added and the reaction mixture heated to 50 °C. After 17 h the reaction was quenched with distilled water and extracted repeatedly with DCM. The combined organic layers were dried over Na_2SO_4 and the solvent evaporated under vacuum. The crude product was purified *via* column chromatography (DCM/MeOH 3% → 15%), yielding **XLIII** (463 mg, 1.2 mmol, 35%) as an off-white solid.

^{1}H NMR (400 MHz, $CDCl_3$, FID NIK086/20) δ = 9.50 (d, J = 1.0 Hz, 2H), 8.79 (d, J = 2.5 Hz, 1H), 8.65 (d, J = 5.7 Hz, 2H), 8.47 (dd, J = 8.6, 2.5 Hz, 1H), 7.72 (d, J = 8.6 Hz, 1H), 7.05 (dd, J = 5.7, 1.0 Hz, 2H) ppm.

D.6.6 Ring closure towards acceptors

General procedure 1 (GP1): CHA

GP1 followed the protocol according to the procedure from Kader *et al.*[28] All compounds, including the corresponding precursor, the base and either the precatalysts Pd-NHC **67** or $Pd(OAc)_2$ and the NHC-ligand **65** were weighed. The flask, equipped with condenser or glass vials was flushed with argon and closed with a septum, including an argon balloon, to keep inert conditions straight. Degassed DMA was added, and the reaction heated to 130 °C until full conversion of the product. The reaction mixture was then cooled to rt, quenched with water and extracted repeatedly with DCM or EA. The combined organic layers were dried over Na_2SO_4 and the solvent evaporated under reduced pressure.

Pyrido[3',4':4,5]pyrrolo[3,2,1-*jk*]carbazole

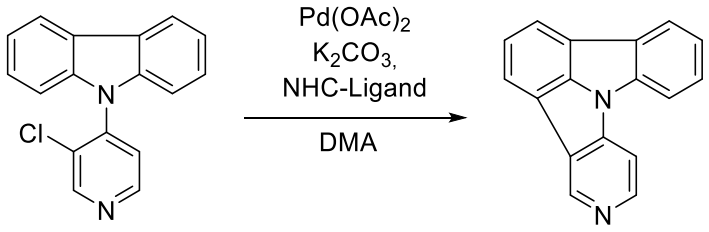

24
$C_{17}H_{11}ClN_2$
278,74

44
$C_{17}H_{10}N_2$
242,28

Synthesis of **44** followed GP1.

$Pd(OAc)_2$ (106 mg, 0.24 mmol, 2 mol%), NHC-ligand **65** (202 mg, 0.47 mmol, 2 mol%), potassium carbonate (6.55 g, 47 mmol, 2 eq.), **24** (6.61 g, 24 mmol, 1 eq.), 48 mL DMA were used and heated for 26 h. After the work up with EA, the crude product was flashed over silica (PE/EA 1:3), yielding **44** (5.63 g, 23 mmol, 98%) as a light brown solid.

^{1}H NMR (400 MHz, $CDCl_3$, FID NIK017/30) δ = 9.34 (d, J = 1.0 Hz, 1H), 8.71 (d, J = 5.6 Hz, 1H), 8.12 (dt, J = 7.8, 0.9 Hz, 1H), 8.06 (t, J = 7.4 Hz, 2H), 7.88 (dt, J = 8.0, 0.9 Hz, 1H), 7.79 (dd, J = 5.7, 1.1 Hz, 1H), 7.64 (td, J = 7.4, 1.0 Hz, 1H), 7.58 (td, J = 7.8, 1.2 Hz, 1H), 7.43 (td, J = 7.6, 1.0 Hz, 1H) ppm.

Pyrido[3,4-*b*]pyrido[4',3':4,5]pyrrolo[3,2,1-*hi*]indole

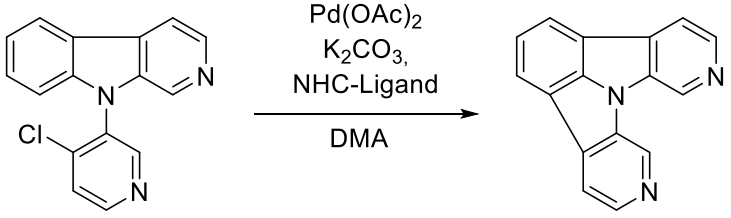

30
$C_{16}H_{10}ClN_3$
279,73

XLV
$C_{16}H_9N_3$
243,08

Synthesis of **XLV** followed GP1.

30 (503 mg, 1.8 mmol, 1 eq.), $Pd(OAc)_2$ (8.00 mg, 0.036 mmol, 2 mol%), NHC-ligand **65** (15.0 mg, 0.036 mmol, 2 mol%) and potassium carbonate (497 mg, 3.6 mmol, 2 eq.) were heated in 4 mL DMA for 2 days. After the work up with DCM, the crude product was purified *via* column chromatography (PE/EA 1:3), yielding **XLV** (157 mg, 0.6 mmol, 35%) as a light brown solid.

^{1}H NMR (400 MHz, $CDCl_3$, FID NIK060/20) δ = 9.20 (s, 2H), 8.63 (d, J = 5.2 Hz, 2H), 8.14 (d, J = 7.5 Hz, 2H), 7.95 (dd, J = 5.2, 1.1 Hz, 2H), 7.64 (t, J = 7.5 Hz, 1H) ppm.

Dibenzo[*b,e*]pyrido[3,4,5-*gh*]pyrrolizine

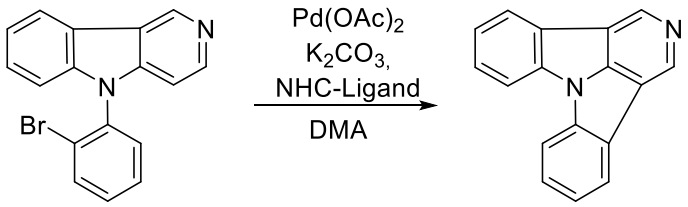

31
$C_{17}H_{11}BrN_2$
323,19

46
$C_{17}H_{10}N_2$
242,28

Synthesis of **46** followed GP1.

A suspension of $Pd(OAc)_2$ (27.0 mg, 0.11 mmol, 5 mol%), NHC-ligand **65** (47.0 mg, 0.11 mmol, 5 mol%), potassium carbonate (609 mg, 4.4mmol, 2 eq.) and **31** (713 mg, 2.21 mmol, 1 eq.) were weighed and 1.8 mL DMA added. The reaction mixture was heated for 19 h. After the work up with DCM, the crude product was purified *via* column chromatography (DCM/MeOH 10%), yielding **46** (358 mg, 1.5 mmol, 67%) as a light brown solid.

^{1}H NMR (400 MHz, $CDCl_3$, FID NIK041/30) δ = 9.22 (s, 1H), 8.15 (dt, J = 7.8, 1.0 Hz, 1H), 7.86 (dt, J = 8.1, 0.9 Hz, 1H), 7.59 (td, J = 7.8, 1.2 Hz, 1H), 7.41 (td, J = 7.6, 1.0 Hz, 1H) ppm.

Dibenzo[*b,e*]pyrido[3,4,5-*gh*]pyrrolizine

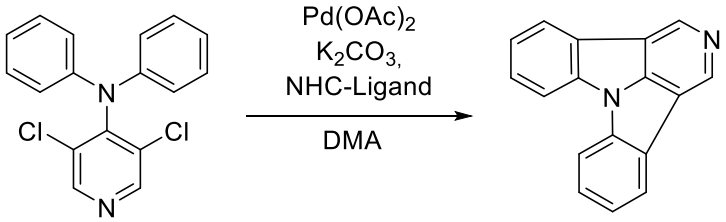

34
$C_{17}H_{12}Cl_2N_2$
315,20

46
$C_{17}H_{10}N_2$
242,28

Synthesis of **46** followed GP1.

34 (900 mg, 2.86 mmol, 1 eq.), $Pd(OAc)_2$ (35.0 mg, 0.14 mmol, 5 mol%), NHC-ligand **65** (61.0 mg, 0.14 mmol, 5 mol%) and potassium carbonate (789 mg, 5.71 mmol, 2 eq.) were placed in a glass vial and 6 mL DMA was added. The suspension was heated for 20 h. After the work up with DCM, the crude product was flashed over silica (DCM/MeOH 10%), yielding **46** (685 mg, 2.83 mmol, 99%) as a grey-brown solid.

^{1}H NMR (400 MHz, $CDCl_3$, FID NIK083/20) δ = 9.18 (s, 2H), 8.11 (dt, J = 7.8, 1.0 Hz, 2H), 7.81 (dt, J = 8.1, 0.9 Hz, 2H), 7.56 (td, J = 7.8, 1.2 Hz, 2H), 7.38 (td, J = 7.6, 1.0 Hz, 2H) ppm.

5-Nitrodibenzo[*b,e*]pyrido[3,4,5-*gh*]pyrrolizine

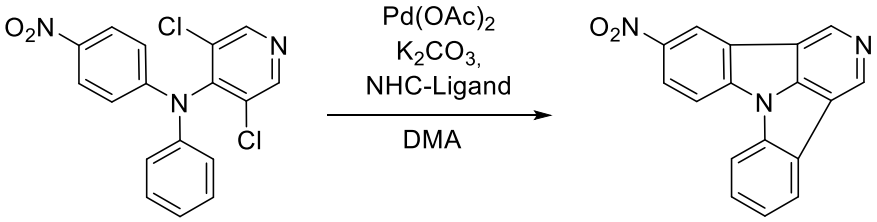

XXXVII
$C_{17}H_{11}Cl_2N_3O_2$
360,19

XLVII
$C_{17}H_9N_3O_2$
287,28

Synthesis of **XLVII** followed GP1.

XXXVII (200 mg, 0.6 mmol, 1 eq.), $Pd(OAc)_2$ (7.00 mg, 0.03 mmol, 5 mol%), NHC-ligand **65** (12.0 mg, 0.03 mmol, 5 mol%) and potassium carbonate (153 mg, 1.1 mmol, 2 eq.) were weighed and 1 mL DMA was added. The reaction mixture was heated for 20 h and after the work up with DCM, the crude product was flashed over silica (DCM/MeOH 10%), yielding **XLVII** (86.0 mg, 0.3 mmol, 54%) as a yellow solid.

^{1}H NMR (400 MHz, $CDCl_3$, FID NIK094/10) δ = 9.34 (d, J = 14.7 Hz, 2H), 9.10 (d, J = 2.2 Hz, 1H), 8.57 (dd, J = 8.9, 2.2 Hz, 1H), 8.22 (d, J = 7.8 Hz, 1H), 7.98 (dd, J = 8.4, 2.7 Hz, 2H), 7.73 – 7.65 (m, 1H), 7.53 (t, J = 7.7 Hz, 1H) ppm.

5-Nitrodibenzo[*b,e*]pyrido[3,4,5-*gh*]pyrrolizine

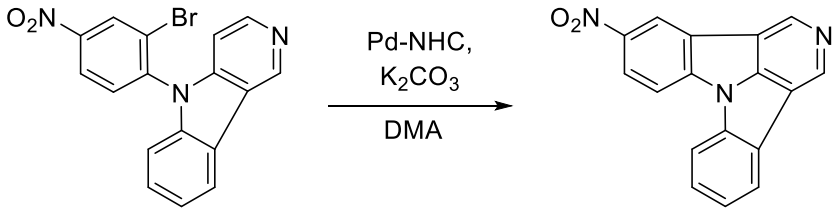

XXXIX
$C_{17}H_{10}BrN_3O_2$
368,19

XLVII
$C_{17}H_9N_3O_2$
287,28

Synthesis of **XLVII** followed GP1.

A suspension of Pd-NHC **67** (22.0 mg, 0.039 mmol, 5 mol%), potassium carbonate (213 mg, 1.5 mmol, 2 eq.) and **XXXIX** (284 mg, 0.8 mmol, 1 eq.) in 7 mL degassed DMA was heated for 6 h. After the work up with DCM, the crude product was purified *via* column chromatography (PE/EE 1:6), yielding **XLVII** (48.0 mg, 0.2 mmol, 22%) as a yellow solid.

^{1}H NMR (400 MHz, $CDCl_3$, FID NIK018/30) δ = 9.44 (d, J = 1.0 Hz, 1H), 9.07 (d, J = 2.2 Hz, 1H), 8.82 (d, J = 5.7 Hz, 1H), 8.55 (dd, J = 8.9, 2.3 Hz, 1H), 8.20 (t, J = 7.1 Hz, 2H), 8.01 (d, J = 8.9 Hz, 1H), 7.93 (dd, J = 5.7, 1.0 Hz, 1H), 7.81 – 7.75 (m, 1H) ppm.

Benzo[*b*]dipyrido[4,3-*e*:3',4',5'-*gh*]pyrrolizine

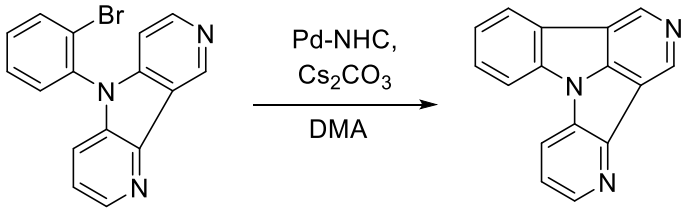

XLII
$C_{16}H_{10}BrN_3$
324,18

48
$C_{16}H_9N_3$
243,27

Synthesis of **48** followed GP1.

XLII (362 mg, 1.12 mmol, 1 eq.), Pd-NHC **67** (32.0 mg, 0.06 mmol, 5 mol%) and potassium carbonate (309 mg, 2.23 mmol, 2 eq.) were weighed and 1.5 mL DMA added. The reaction mixture was heated for 15 h. After the work up with DCM, the crude product was flashed over silica (PE/EA 1:3) yielding **48** (208 mg, 0.86 mmol, 76%) as a brown solid.

^{1}H NMR (400 MHz, $CDCl_3$, FID NIK075/10) δ = 9.36 (s, 1H), 9.23 (d, J = 13.4 Hz, 2H), 8.76 (d, J = 5.6 Hz, 1H), 8.23 – 8.09 (m, 1H), 7.85 (d, J = 8.1 Hz, 1H), 7.76 (dd, J = 5.6, 1.0 Hz, 1H), 7.63 (td, J = 7.8, 1.2 Hz, 1H), 7.47 (td, J = 7.7, 1.0 Hz, 1H) ppm.

5-Nitrobenzo[*b*]dipyrido[3,2-e:3',4',5'-*gh*]pyrrolizine

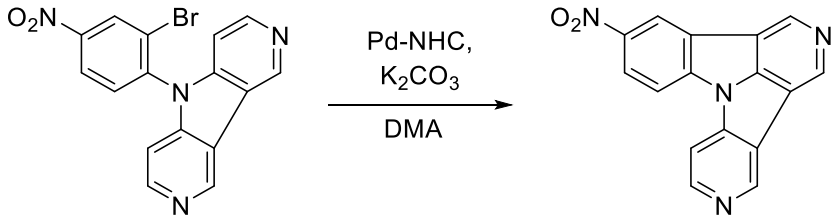

XLIII
$C_{16}H_9BrN_4O_2$
369,18

XLIX
$C_{16}H_8N_4O_2$
288,27

Synthesis of **XLIX** followed GP1.

A suspension of Pd-NHC **67** (33.0 mg, 0.06 mmol, 5 mol%), potassium carbonate (321 mg, 2.32 mmol, 2 eq.) and **XLIII** (430 mg, 1.16 mmol, 1 eq.) was heated in 1.4 mL DMA for 18 h. After the work up with DCM, the crude product was flushed over silica and **XLIX** (93.0 mg, 0.32 mmol, 28%) received as a dark-orange solid.

^{1}H NMR (400 MHz, $CDCl_3$, FID NIK089/20) δ = 9.48 (s, 1H), 9.41 (d, J = 1.5 Hz, 2H), 9.14 (d, J = 2.2 Hz, 1H), 8.87 (d, J = 5.5 Hz, 1H), 8.61 (dd, J = 8.9, 2.2 Hz, 1H), 8.05 (d, J = 8.7 Hz, 1H), 7.97 – 7.89 (d, 1H) ppm.

Diazotization

2-Bromopyrido[4',3':4,5]pyrrolo[3,2,1-*jk*]carbazole

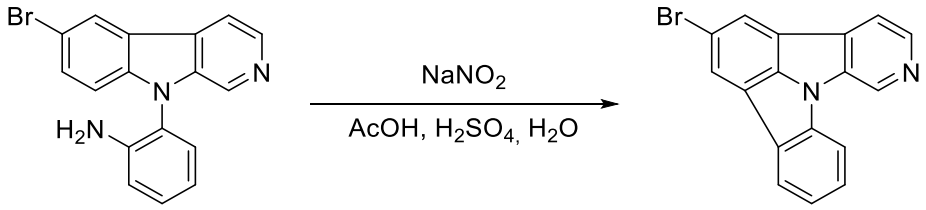

XXVII
$C_{17}H_{12}BrN_3$
338,21

L
$C_{17}H_9BrN_2$
321,18

Synthesis **L** of was conducted following Dunlop and Tucker.[38]

XXVII (338 mg, 1.0 mmol, 1 eq.) was dissolved in a mixture of 2.6 mL AcOH (98% - 100%) and 0.6 mL H_2SO_4 (98%) and cooled to 0 °C. $NaNO_2$ (76.0 mg, 1.1 mmol, 1.1 eq.) was dissolved in 1.6 mL distilled water and added slowly, without crossing a temperature limit of 4 °C. The reaction mixture was stirred for 5 min, followed by refluxing for 2 h. After cooling to rt the reaction was quenched with distilled water, neutralized with 2N NaOH and extracted repeatedly with DCM. The crude product was purified *via* column chromatography (PE/EA 1:2 → 1:3), yielding **L** (70.0 mg, 0.2 mmol, 22%) as a beige solid.

^{1}H NMR (600 MHz, $CDCl_3$, FID NIK100/60) δ = 9.21 (s, 1H), 8.61 (d, J = 5.2 Hz, 1H), 8.17 – 8.12 (m, 2H), 8.02 (dd, J = 7.7, 0.9 Hz, 1H), 7.92 (dd, J = 5.2, 1.1 Hz, 1H), 7.82 (d, J = 8.0 Hz, 1H), 7.61 (td, J = 7.7, 1.2 Hz, 1H), 7.43 – 7.37 (td, 1H) ppm.

^{13}C NMR (151 MHz, $CDCl_3$, FID NIK0100/61) δ = 142.41, 142.32, 138.66, 135.06, 134.86, 134.28, 128.97, 128.17, 124.85, 123.65, 122.89, 120.54, 117.74, 117.31, 116.38, 112.78 ppm.

D.6.7 Synthesis of post-functionalization carboline derivatives

2-Bromopyrido[3',4':4,5]pyrrolo[3,2,1-*jk*]carbazole

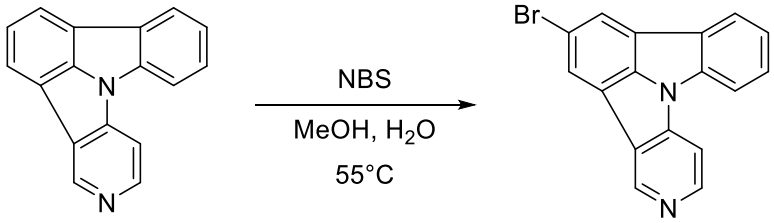

44
$C_{17}H_{10}N_2$
242,28

LI
$C_{17}H_9BrN_2$
321,18

γ -NICz **44** (1.28 g, 5.3 mmol, 1 eq.) was suspended in 75 mL MeOH and 32 mL distilled water (7:3 mixture) and heated to 55 °C. NBS (797 mg, 4.5 mmol, 0.8 eq.) was added in portions as a solid and the reaction mixture allowed to stir. After 2 days, more NBS (234 mg, 1.3 mmol, 0.25 eq.) was added and further stirred for 24 h. Subsequently, the reaction mixture was poured on 2N NaOH and stirred for 30 min at rt, followed by repeated extraction with DCM. The combined organic layers were dried over Na_2SO_4 and the solvent evaporated under reduced pressure. The crude product was refluxed in ACN, cooled to rt and filtered. The filtrate was dried and further purified *via* recrystallization from toluene, yielding **LI** (779 mg, 2.4 mmol, 46%) as a beige solid.

^{1}H NMR (400 MHz, $CDCl_3$, FID NIK095/30) δ = 9.21 (s, 1H), 8.70 (d, J = 5.6 Hz, 1H), 8.05 (dd, J = 8.9, 1.4 Hz, 2H), 7.99 (d, J = 7.8 Hz, 1H), 7.77 (d, J = 8.2 Hz, 1H), 7.67 (d, J = 5.5 Hz, 1H), 7.61 – 7.50 (m, 1H), 7.40 (t, J = 7.6 Hz, 1H) ppm.

^{13}C NMR (151 MHz, $CDCl_3$, FID NIK095/81) δ = 147.18, 144.69, 142.39, 141.45, 138.16, 129.59, 127.82, 125.08, 123.49, 123.31, 123.08, 122.68, 119.63, 116.97, 116.90, 112.82, 107.47 ppm.

2-Bromopyrido[3,4-*b*]pyrido[4',3':4,5]pyrrolo[3,2,1-*hi*]indole

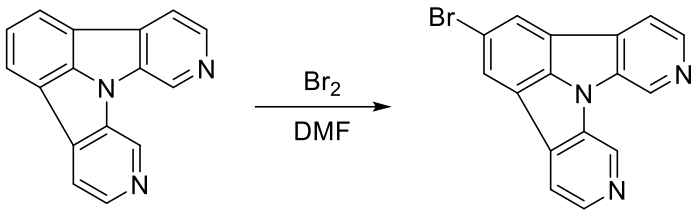

XLV
$C_{16}H_9N_3$
243,08

LII
$C_{16}H_8BrN_3$
322,17

Compound **XLV** (338 mg, 1.4 mmol, 1 eq.) was suspended in 35 mL DMF and Br_2 (444 mg, 2.8 mmol, 2 eq.) added dropwise. The reaction mixture was stirred for 7 h at rt and more Br_2 (444 mg, 2.8 mmol, 2 eq.) added. After 24 h the reaction was poured on 2N NaOH and stirred for 30 min at rt. The solid was filtered off, washed with distilled water and the filtrate extracted repeatedly with DCM. The combined organic layers were dried over Na_2SO_4 and the solvent evaporated under reduced pressure. The crude product was purified *via* recrystallization from toluene, yielding **LII** (304 mg, 0.9 mmol, 67%) as a yellow solid.

^{1}H NMR (400 MHz, $CDCl_3$, FID NIK067/70) δ = 9.36 (d, J = 1.0 Hz, 2H), 8.71 (d, J = 5.2 Hz, 2H), 8.39 (s, 2H), 8.02 (dd, J = 5.2, 1.1 Hz, 2H) ppm.

5,11-Dibromodibenzo[*b,e*]pyrido[3,4,5-*gh*]pyrrolizine

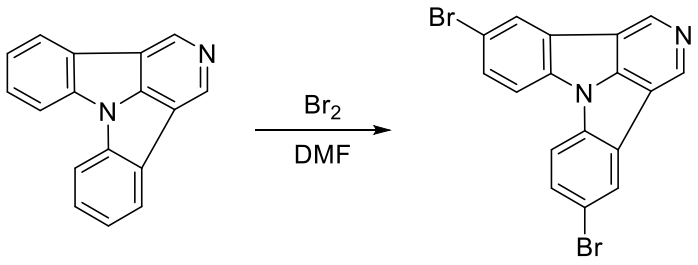

46
$C_{17}H_{10}N_2$
242,28

LIII
$C_{17}H_8Br_2N_2$
400,07

Compound **46** (848 mg, 3.5 mmol, 1 eq.) was suspended in 85 mL DMF and Br_2 (1.68 g, 10.5 mmol, 3 eq.) added quickly. The reaction mixture was stirred overnight at rt and more Br_2 (2.01 g, 13 mmol, 3.6 eq.) added in portions over 6 days. Subsequently, the reaction was

poured on 2N NaOH stirred for 2 h at rt. The solid was filtered off, washed with distilled water and the filtrate extracted repeatedly with DCM. The combined organic layers were dried over Na_2SO_4 and the residue refluxed in nitrobenzene, cooled to rt. The solid was filtered and washed with toluene. The product was dried in vacuo, yielding **LIII** (682 mg, 1.7 mmol, 49%) as a beige solid.

^{1}H NMR (600 MHz, DMSO-d6, FID NIK084/80) δ = 9.40 (s, 2H), 8.66 (d, J = 2.0 Hz, 2H), 8.36 (d, J = 8.6 Hz, 2H), 7.86 (dd, J = 8.6, 2.0 Hz, 2H) ppm.

5-Bromodibenzo[*b,e*]pyrido[3,4,5-*gh*]pyrrolizine

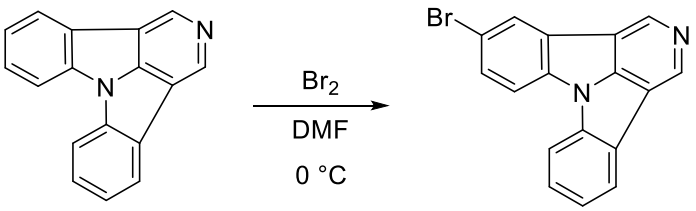

46
$C_{17}H_{10}N_2$
242,28

LIV
$C_{17}H_9BrN_2$
321,18

Compound **46** (700 mg, 2.9 mmol, 1 eq.) was suspended in 70 mL DMF and Br_2 (888 mg, 5.6 mmol, 6 eq.) added slowly, dropwise at 0 °C. The reaction mixture was stirred overnight at rt and more Br_2 (888 mg, 5.6 mmol, 6 eq.) added in portions and heated to 55 °C. After 6 days the reaction was poured on 2N NaOH stirred for 2 h at rt. The solid was filtered off, washed with distilled water and the filtrate extracted repeatedly with DCM. The combined organic layers were dried over Na_2SO_4 and the residue refluxed in nitrobenzene, cooled to rt. The solid was filtered and washed with toluene. The product was dried in vacuo, yielding **LIV** (355 mg, 1.1 mmol, 38%) as a beige solid.

^{1}H NMR (400 MHz, $CDCl_3$, FID NIK111/20) δ = 9.22 (d, J = 14.1 Hz, 2H), 8.28 (td, J = 2.0, 0.7 Hz, 1H), 8.18 (ddd, J = 7.8, 1.2, 0.7 Hz, 1H), 7.85 (dt, J = 8.0, 0.9 Hz, 1H), 7.78 – 7.68 (m, 2H), 7.63 (ddd, J = 8.1, 7.5, 1.2 Hz, 1H), 7.45 (td, J = 7.6, 1.0 Hz, 1H) ppm.

Dibenzo[*b,e*]pyrido[3,4,5-*gh*]pyrrolizin-5-amine

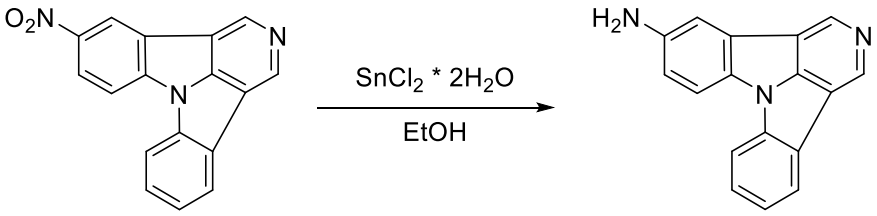

XLVII
$C_{17}H_9N_3O_2$
287,28

LV
$C_{17}H_{11}N_3$
257,30

Synthesis of **LV** was performed according to Dunlop and Tucker.[38]

To a suspension of **XLVII** (69.0 mg, 0.24 mmol, 1 eq.) in 1 mL EtOH, $SnCl_2$*$2H_2O$ (189 mg, 3.5 mmol, 3.5 eq.) was added as a solid and refluxed for 3 days. After cooling to rt the reaction mixture was neutralized with 2N NaOH and repeatedly extracted with EA. The combined organic layers were washed with distilled water, dried over Na_2SO_4 and the solvent evaporated under reduced pressure. The crude product was purified *via* column chromatography (DCM/Et_2O 3:1), yielding **LV** (44.0 mg, 0.2 mmol, 76%) as an off-white solid.

^{1}H NMR (400 MHz, $CDCl_3$, FID NIK097/30) δ = 9.15 (dd, J = 24.5, 1.4 Hz, 2H), 8.20 – 8.07 (m, 1H), 7.77 (dt, J = 7.8, 1.0 Hz, 1H), 7.66 – 7.51 (m, 2H), 7.48 – 7.30 (m, 2H), 6.92 (dt, J = 8.5, 1.8 Hz, 1H), 3.46 (s, 2H) ppm.

5-Bromodibenzo[*b,e*]pyrido[3,4,5-*gh*]pyrrolizine

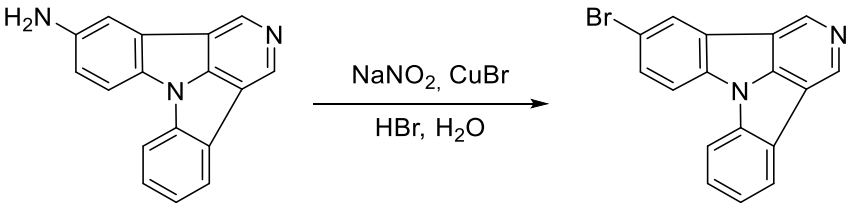

LV
$C_{17}H_{11}N_3$
257,30

LIV
$C_{17}H_9BrN_2$
321,18

Synthesis of **LIV** was conducted following Fries and Imbert.[49]

Compound **LV** (44.0 mg, 0.17 mmol, 1 eq.) was dissolved in 1.5 mL HBr (aq. solution) and cooled to 0 °C. A solution of $NaNO_2$ (13.0 mg, 0.19 mmol, 1.05 eq.) in 1.5 mL distilled H_2O was slowly added, while the temperature didn't cross 5 °C. After stirring 30 min at rt, CuBr (13.0 mg,

0.09 mmol, 0.5 eq.) was added as a solid. The reaction was quenched after 4 days with 2N NaOH, followed by repeated extraction with EA. The combined organic layers were dried over Na_2SO_4 and the solvent evaporated under reduced pressure yielding **LIV** (11.0 mg, 0.03 mmol, 19%) as a brown solid.

^{1}H NMR (400 MHz, $CDCl_3$, FID NIK111/20) δ = 9.22 (d, J = 14.1 Hz, 2H), 8.28 (td, J = 2.0, 0.7 Hz, 1H), 8.18 (ddd, J = 7.8, 1.2, 0.7 Hz, 1H), 7.85 (dt, J = 8.0, 0.9 Hz, 1H), 7.78 – 7.68 (m, 2H), 7.63 (ddd, J = 8.1, 7.5, 1.2 Hz, 1H), 7.45 (td, J = 7.6, 1.0 Hz, 1H) ppm.

D.6.8 Synthesis of donor-acceptor systems

General procedure 2 (GP2): Buchwald-Hartwig Amination

GP2 followed the procedure modified according to Iwaki *et al.*[43] All compounds, including the corresponding acceptors and donors, NaO^tBu, $Pd_2(dba)_3$ and $P(^tBu)_3$*HBF_4 were weighed solid in a glass vial. The vial was flushed with argon and sealed with a septum, equipped with an argon balloon to keep inert conditions straight. Degassed toluene (abs.) was added, and the reaction heated to 110 °C until full conversion of the product. The reaction mixture was then cooled to rt, quenched with water and extracted repeatedly with DCM. The combined organic layers were dried over Na_2SO_4 and the solvent evaporated under reduced pressure.

10-(Pyrido[3',4':4,5]pyrrolo[3,2,1-*jk*]carbazol-2-yl)-4a,5a,9a,10a-tetrahydro-10*H*-phenoxazine

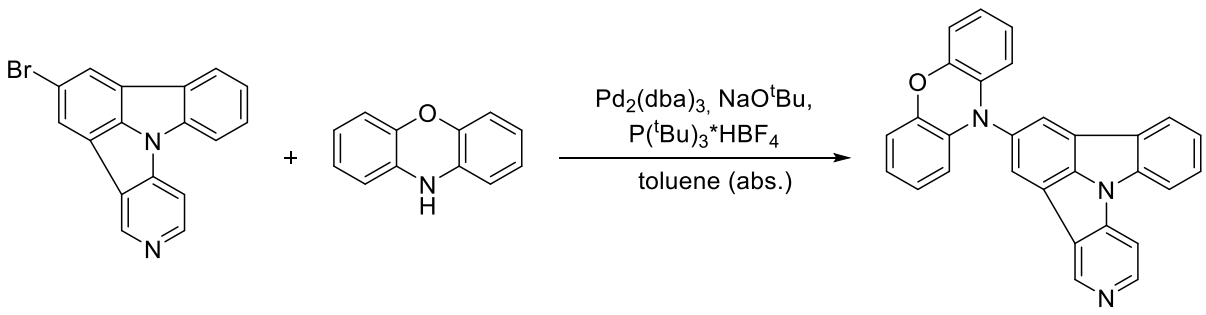

LI
$C_{17}H_9BrN_2$
321,18

56
$C_{12}H_9NO$
183,21

LVII
$C_{29}H_{17}N_3O$
423,48

Synthesis of **LVII** followed GP2.

Compound **LI** (523 mg, 1.6 mmol, 1 eq.), **56** (328 mg, 1.8 mmol, 1.1 eq.), $Pd_2(dba)_3$ (149 mg, 0.2 mmol, 0.1 eq.), $P(^tBu)_3$*HBF_4 (189 mg, 0.7 mmol, 0.4 eq.) and NaO^tBu (469 mg, 4.9 mmol, 3.0 eq.) were weighed, 13 mL toluene added and the reaction mixture heated for 24 h. After work up, the crude product was purified *via* column chromatography (PE/EE 1:3), yielding **LVII** (663 mg, 1.6 mmol, 96%) as a dark-yellow solid.

^{1}H NMR (600 MHz, $CDCl_3$, FID NIK102/40) δ = 9.36 (d, J = 0.9 Hz, 1H), 8.79 (d, J = 5.6 Hz, 1H), 8.13 (dt, J = 7.7, 0.9 Hz, 1H), 8.11 (d, J = 1.2 Hz, 1H), 8.08 (d, J = 1.3 Hz, 1H), 7.98 (dt, J = 8.1, 0.9 Hz, 1H), 7.89 (dd, J = 5.6, 1.0 Hz, 1H), 7.66 (ddd, J = 8.2, 7.4, 1.2 Hz, 1H), 7.47 (td, J = 7.6, 1.0 Hz, 1H), 6.74 (dd, J = 8.0, 1.5 Hz, 2H), 6.66 (td, J = 7.7, 1.5 Hz, 2H), 6.61 – 6.49 (m, 2H), 5.91 (dd, J = 8.0, 1.5 Hz, 2H) ppm.

^{13}C NMR (151 MHz, $CDCl_3$, FID NIK102/41) δ = 147.37, 145.12, 143.96, 143.10, 142.81, 138.74, 135.38 (d, J = 14.6 Hz), 130.31, 128.02, 125.82, 123.85 (d, J = 4.5 Hz), 123.57 (d, J = 2.5 Hz), 123.25, 121.41, 120.98, 118.24, 115.46, 113.57, 113.13, 107.76 ppm.

10-(Pyrido[4',3':4,5]pyrrolo[3,2,1-*jk*]carbazol-2-yl)-4a,5a,9a,10a-tetrahydro-10*H*-phenoxazine

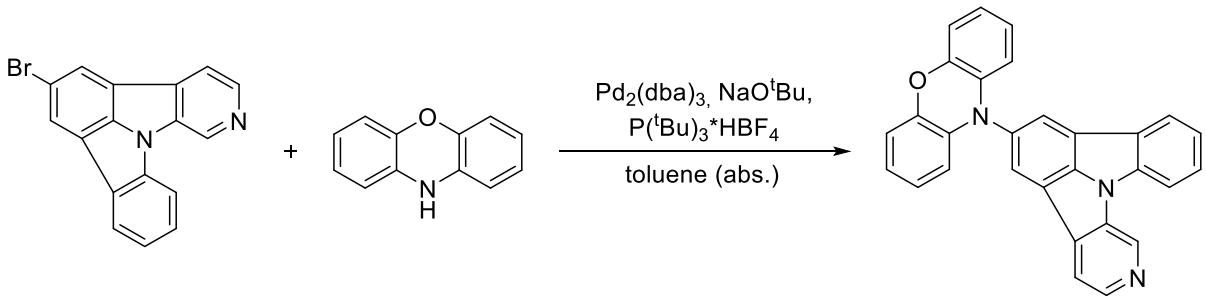

L
$C_{17}H_9BrN_2$
321,18

56
$C_{12}H_9NO$
183,21

LVIII
$C_{29}H_{17}N_3O$
423,48

Synthesis of **LVIII** followed GP2.

L (80.0 mg, 0.25 mmol, 1 eq.), **56** (50.0 mg, 0.28 mmol, 1.1 eq.), $Pd_2(dba)_3$ (23.0 mg, 0.03 mmol, 0.1 eq.), $P(^tBu)_3$*HBF_4 (29.0 mg, 0.1 mmol, 0.4 eq.) and NaO^tBu (72.0 mg, 0.75 mmol, 3.0 eq.) were weighed, 2 mL toluene added and the reaction mixture heated for 24 h. After work up, the crude product was purified *via* column chromatography (PE/EE 45% → 60%) and **LVIII** (80. mg, 0.19 mmol, 75%) obtained as a yellow solid.

^{1}H NMR (600 MHz, $CDCl_3$, FID NIK105/20) δ = 9.40 (s, 1H), 8.67 (d, J = 5.2 Hz, 1H), 8.16 (d, J = 1.3 Hz, 1H), 8.15 – 8.11 (m, 2H), 8.03 (dd, J = 5.1, 1.1 Hz, 1H), 8.00 (d, J = 8.0 Hz, 1H), 7.68 (td, J = 7.8, 1.2 Hz, 1H), 7.45 (td, J = 7.6, 1.0 Hz, 1H), 6.75 (d, J = 1.5 Hz, 1H), 6.74 (d, J = 1.5 Hz, 1H), 6.66 (td, J = 7.7, 1.5 Hz, 2H), 6.55 (td, J = 7.7, 1.5 Hz, 2H), 5.90 (dd, J = 8.0, 1.5 Hz, 2H) ppm.

^{13}C NMR (151 MHz, CDCl3, FID NIK105/21) δ = 143.96, 143.37, 142.70, 139.00, 135.59, 135.31 (d, *J* = 7.5 Hz), 134.82, 134.57, 129.55, 128.24, 125.42, 124.43, 123.25, 123.04, 121.65, 121.45, 118.24, 117.96, 115.49, 113.57, 112.96 ppm.

10-(Pyrido[3,4-*b*]pyrido[4',3':4,5]pyrrolo[3,2,1-*hi*]indol-2-yl)-10*H*-phenoxazine

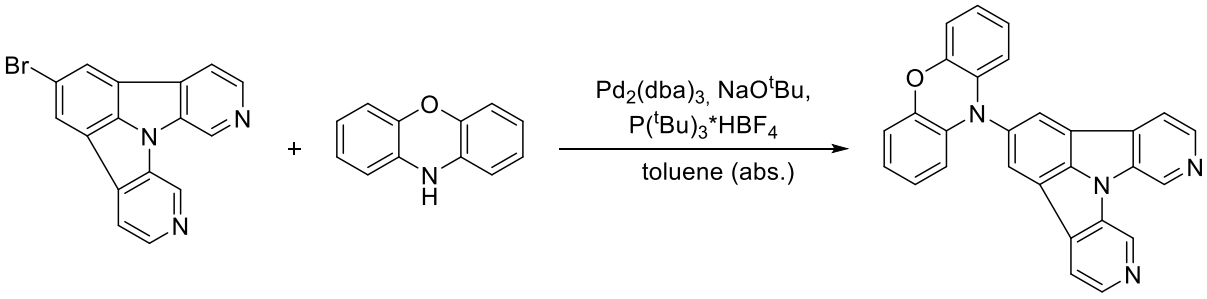

LII
$C_{16}H_8BrN_3$
322,17

56
$C_{12}H_9NO$
183,21

LIX
$C_{28}H_{16}N_4O$
424,46

Synthesis of **LIX** followed GP2.

Compound **LII** (80.0 mg, 0.25 mmol, 1 eq.), **56** (50.0 mg, 0.25 mmol, 1.1 eq.), $Pd_2(dba)_3$ (23.0 mg, 0.02 mmol, 0.1 eq.), $P(^tBu)_3$*HBF_4 (29.0 mg, 0.09 mmol, 0.4 eq.) and NaO^tBu (72.0 mg, 0.75 mmol, 3.0 eq.) were weighed, 2 mL toluene added and the reaction mixture heated for 24 h. After work up, the crude product was purified *via* column chromatography (DCM/MeOH 10%), yielding **LIX** (62.0 mg, 0.15 mmol, 59%) as an orange solid.

^{1}H NMR (600 MHz, $CDCl_3$, FID NIK081/70) δ = 9.52 – 9.42 (m, 2H), 8.75 (d, J = 5.1 Hz, 2H), 8.32 (s, 2H), 8.10 (dd, J = 5.1, 1.1 Hz, 2H), 6.77 (dd, J = 7.9, 1.4 Hz, 2H), 6.69 (td, J = 7.6, 1.5 Hz, 2H), 6.56 (ddd, J = 8.0, 7.4, 1.5 Hz, 2H), 5.86 (dd, J = 8.1, 1.4 Hz, 2H) ppm.

^{13}C NMR (151 MHz, CDCl3, FID NIK081/71) δ = 142.89 (d, J = 4.3 Hz), 142.21, 134.78, 134.72, 134.01, 133.63, 126.58, 122.23, 120.72, 118.44, 117.21, 114.63, 112.43 ppm.

5,11-Bis(9,9-dimethylacridin-10(9*H*)-yl)dibenzo[*b,e*]pyrido[3,4,5-*gh*]pyrrolizine

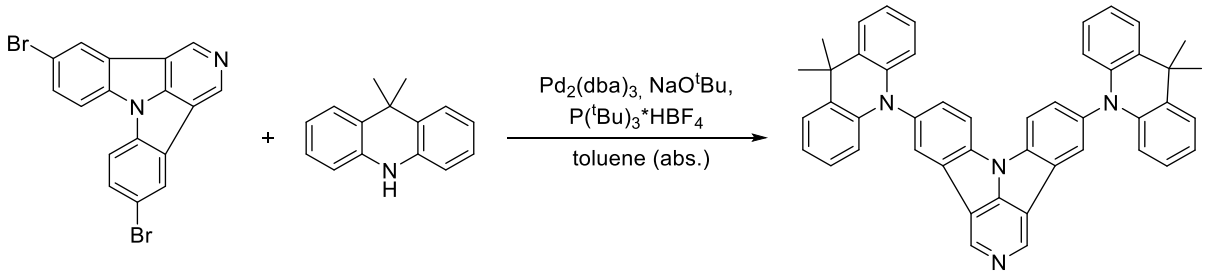

LIII
$C_{17}H_8Br_2N_2$
400,07

60
$C_{15}H_{15}N$
209,29

LXI
$C_{47}H_{36}N_4$
656,83

Synthesis of **LXI** followed GP2.

LIII (81.0 mg, 0.20 mmol, 1 eq.), **60** (127 mg, 0.61 mmol, 3 eq.), $Pd_2(dba)_3$ (37.0 mg, 0.04 mmol, 0.2 eq.), $P(^tBu)_3$*HBF_4 (47.0 g, 0.09 mmol, 0.8 eq.) and NaO^tBu (117.0 g, 1.21 mmol, 6 eq.) were weighed, 2 mL degassed toluene added and the reaction mixture heated for 24 h. After work up the crude product was purified *via* column chromatography (PE/EE 20%) and **LXI** (86.0 mg, 0.13 mmol, 65%) isolated as a dark brown solid.

^{1}H NMR (400 MHz, $CDCl_3$, FID NIK108/40) δ = 9.30 (s, 2H), 8.32 – 8.19 (m, 4H), 7.67 (dd, J = 8.5, 1.9 Hz, 2H), 7.59 – 7.48 (m, 4H), 7.06 – 6.92 (m, 8H), 6.42 – 6.33 (m, 4H), 1.78 (s, 12H) ppm.

5,11-Di(10*H*-phenoxazin-10-yl)dibenzo[*b,e*]pyrido[3,4,5-*gh*]pyrrolizine

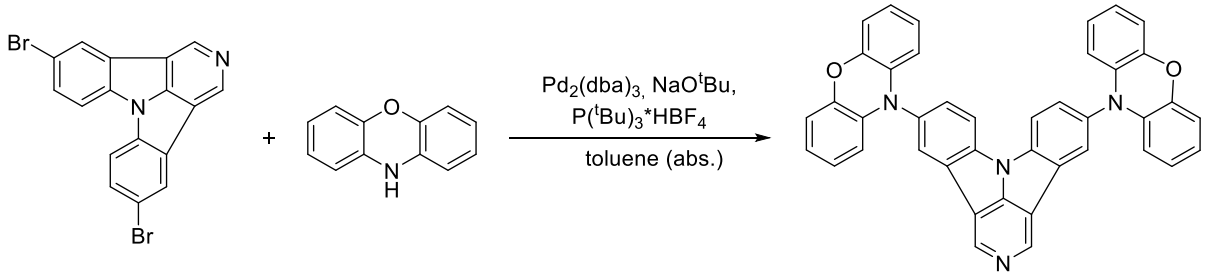

LIII
$C_{17}H_8Br_2N_2$
400,07

56
$C_{12}H_9NO$
183,21

LXII
$C_{41}H_{24}N_4O_2$
604,67

Synthesis of **LXII** followed GP2.

LIII (84.0 mg, 0.21 mmol, 1 eq.), **56** (115 mg, 0.63 mmol, 3 eq.), $Pd(dba)_3$ (38.0 mg, 0.04 mmol, 0.2 eq.), $P(^tBu)_3$*HBF_4 (0.049 g, 0.17 mmol, 0.8 eq.) and NaO^tBu (0.121 g, 1.26 mmol, 6 eq.) were weighed, 3 mL toluene added and the reaction mixture heated 24 h. After work up the

crude product was purified *via* column chromatography (PE/EE 2:1) and **LXII** (80 mg, 0.13 mmol, 63%) isolated as a brown solid.

^{1}H NMR (400 MHz, $CDCl_3$, FID NIK110/50) δ = 9.31 (s, 2H), 8.25 (d, J = 2.0 Hz, 2H), 8.20 (d, J = 8.5 Hz, 2H), 7.68 (d, J = 2.0 Hz, 1H), 7.66 (d, J = 2.0 Hz, 1H), 6.76 (dd, J = 7.8, 1.6 Hz, 4H), 6.69 (td, J = 7.6, 1.5 Hz, 4H), 6.61 (td, J = 7.6, 1.6 Hz, 4H), 6.00 (dd, J = 7.9, 1.5 Hz, 4H) ppm.

Solid Phase Reaction

5,11-Bis(3,6-di-tert-butyl-9*H*-carbazol-9-yl)dibenzo[*b,e*]pyrido[3,4,5-*gh*]pyrrolizine

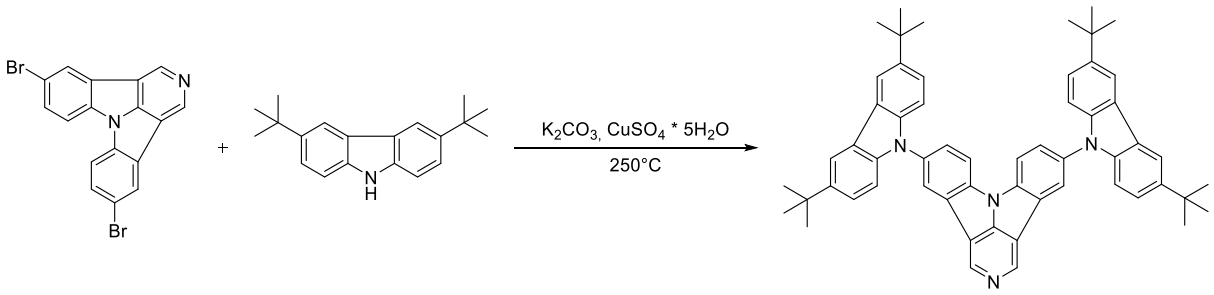

LIII
$C_{17}H_8Br_2N_2$
400,07

63
$C_{20}H_{25}N$
279,43

LXIV
$C_{57}H_{56}N_4$
797,10

Synthesis of **LXIV** followed the procedure according to Kautny *et al.*[19]

A glass vial was charged with compound **LIII** (81.0 mg, 0.20 mmol, 1 eq.), **63** (169 mg, 0.61 mmol, 3 eq.), potassium carbonate (112 mg, 0.81 mmol, 4 eq.) and $CuSO_4$*$5H_2O$ (10.0 mg, 0.04 mmol, 0.2 eq.) and heated to 230 °C. After 20 h the reaction was quenched with distilled water and extracted repeatedly with DCM. The crude product was purified *via* column chromatography (PE/EA 3:1), yielding **LXIV** (68.0 mg, 0.09 mmol, 45%) as an off-white solid.

^{1}H NMR (600 MHz, $CDCl_3$, FID NIK106/60) δ = 9.33 (s, 2H), 8.42 (d, J = 2.1 Hz, 2H), 8.21 (d, J = 2.1 Hz, 4H), 8.20 (d, J = 8.4 Hz, 2H), 7.87 (dd, J = 8.4, 2.1 Hz, 2H), 7.53 (dd, J = 8.7, 1.9 Hz, 4H), 7.43 (d, J = 8.6 Hz, 4H), 1.50 (s, 36H) ppm.

^{13}C NMR (151 MHz, $CDCl_3$, FID NIK106/61) δ = 149.51, 143.15, 139.72, 137.46, 133.75, 129.59, 127.16, 124.62 – 122.28 (m), 116.46, 113.48, 109.00 ppm.

D.6.9 Synthesis of the Pd-NHC catalyst

[1,3-Bis[2,6-bis(1-methylethyl)phenyl]-1,3-dihydro-2H-imidazol-2-yliden]chloro(η3-2propen-1-yl)palladium

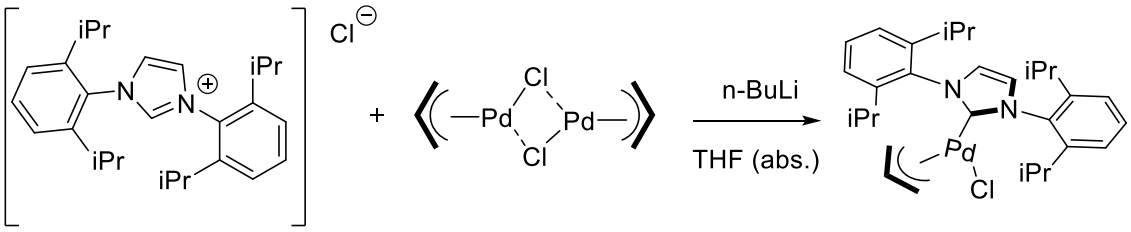

65	**66**	**67**
$C_{27}H_{37}ClN_2$	$C_6H_{10}Cl_2Pd$	$C_{30}H_{41}N_2ClPd$
425,06	377,86	571,52

Synthesis of **67** followed the procedure according to Navarro and Nolan.[51]

The NHC-ligand **65** (3.72 g, 8.75 mmol, 5 eq.) was dissolved in 53 mL THF (abs.) and *n*-butyllithium (3.57 mL, 8.93 mmol, 5.1 eq., 2.5 M in hexane) was added slowly at rt. After 30 min, **66** (670 mg, 1.75 mmol, 1 eq.) was added and the reaction mixture stirred for another 2 h. The suspension was filtered over celite and the filtrate concentrated under vacuum. The crude product was purified *via* column chromatography (DCM/$Et_2$0 0% → 3%), yielding **67** (1.81 g, 3.17 mmol, 89%) as a beige solid.

^{1}H NMR (400 MHz, $CDCl_3$, FID NIK090) δ = 7.42 (t, J = 7.7 Hz, 2H), 7.31 – 7.23 (m, 4H), 7.15 (s, 2H), 4.81 (tt, J = 13.2, 7.2 Hz, 1H), 3.90 (dd, J = 7.5, 2.2 Hz, 1H), 3.18 – 3.01 (m, 3H), 2.91 – 2.73 (m, 3H), 1.57 (d, J = 11.8 Hz, 1H), 1.39 (d, J = 6.7 Hz, 6H), 1.33 (d, J = 6.8 Hz, 6H), 1.17 (d, J = 6.8 Hz, 6H), 1.08 (d, J = 6.9 Hz, 6H) ppm-

E. Bibliography

[1] S. R. Forrest, “The path to ubiquitous and low-cost organic electronic appliances on plastic,” *Nature*, vol. 428, no. 6986, p. 911, Apr. 2004.

[2] L. Lan, J. Zou, C. Jiang, B. Liu, L. Wang, and J. Peng, “Inkjet printing for electroluminescent devices: emissive materials, film formation, and display prototypes,” *Front. Optoelectron.*, vol. 10, no. 4, pp. 329–352, Dec. 2017.

[3] A. Bernanose, M. Comte, and P. Vouaux, “Sur un nouveau mode d’émission lumineuse chez certains composés organiques,” *J. Chim. Phys.*, vol. 50, pp. 64–68, 1953.

[4] M. Pope, H. P. Kallmann, and P. Magnante, “Electroluminescence in Organic Crystals,” *J. Chem. Phys.*, vol. 38, no. 8, pp. 2042–2043, Apr. 1963.

[5] C. W. Tang and S. A. VanSlyke, “Organic electroluminescent diodes,” *Appl. Phys. Lett.*, vol. 51, no. 12, pp. 913–915, Sep. 1987.

[6] Y. Shirota and H. Kageyama, “Charge Carrier Transporting Molecular Materials and Their Applications in Devices,” *Chem. Rev.*, vol. 107, no. 4, pp. 953–1010, Apr. 2007.

[7] “OLED Mobile Phones Market Research and Analysis Report – DolceraWiki.” [Online]. Available: https://dolcera.com/wiki/index.php/OLED_Mobile_Phones_Market_Research_and_Analysis_Report. [Accessed: 30-Mar-2019].

[8] T. Tsuboi, “Recent advances in white organic light emitting diodes with a single emissive dopant,” *J. Non-Cryst. Solids*, vol. 356, no. 37–40, pp. 1919–1927, Aug. 2010.

[9] N. J. Miller and F. A. Leon, “OLED Lighting Products: Capabilities, Challenges, Potential,” PNNL-SA--25479, 1374109, May 2016.

[10] R. Gómez-Bombarelli *et al.*, “Design of efficient molecular organic light-emitting diodes by a high-throughput virtual screening and experimental approach,” *Nat. Mater.*, vol. 15, no. 10, pp. 1120–1127, Oct. 2016.

[11] T. Tsuboi, “Recent advances in white organic light emitting diodes with a single emissive dopant,” *J. Non-Cryst. Solids*, vol. 356, no. 37–40, pp. 1919–1927, Aug. 2010.

[12] S.-F. Wu *et al.*, “White Organic LED with a Luminous Efficacy Exceeding 100 lm W−1 without Light Out-Coupling Enhancement Techniques,” *Adv. Funct. Mater.*, vol. 27, no. 31, Aug. 2017.

[13] C. J. Cleveland and C. Morris, Eds., “Section 25 - Lighting/HVAC/Refrigeration,” in *Handbook of Energy*, Amsterdam: Elsevier, 2013, pp. 827–838.

[14] X. Ding, J. Liu, and T. A. L. Harris, “A review of the operating limits in slot die coating processes,” *AIChE J.*, vol. 62, no. 7, pp. 2508–2524, 2016.

[15] J. P. Spindler, J. Hamer, and M. E. Kondakova, “OLED Manufacturing Equipment and Methods,” in *Handbook of Advanced Lighting Technology*, 2017.

[16] N.-T. Nguyen, “Chapter 4 - Fabrication technologies,” in *Micromixers (Second Edition)*, N.-T. Nguyen, Ed. Oxford: William Andrew Publishing, 2012, pp. 113–161.

[17] Y. Karzazi, “Organic Light Emitting Diodes: Devices and applications,” *J. Mater. Env. Sci*, p. 12, 2014.

[18] Y. Tao, C. Yang, and J. Qin, “Organic host materials for phosphorescent organic light-emitting diodes,” *Chem. Soc. Rev.*, vol. 40, no. 5, p. 2943, 2011.

[19] P. Kautny *et al.*, “Indolo[3,2,1-jk]carbazole based planarized CBP derivatives as host materials for PhOLEDs with low efficiency roll-off,” *Org. Electron.*, vol. 34, pp. 237–245, Jul. 2016.

[20] Y. Kawamura, K. Goushi, J. Brooks, J. J. Brown, H. Sasabe, and C. Adachi, “100% phosphorescence quantum efficiency of Ir(III) complexes in organic semiconductor films,” *Appl. Phys. Lett.*, vol. 86, no. 7, p. 071104, 2005.

[21] Y. Tao *et al.*, “Thermally Activated Delayed Fluorescence Materials Towards the Breakthrough of Organoelectronics,” *Adv. Mater.*, vol. 26, no. 47, pp. 7931–7958, Dec. 2014.

[22] H. Xu *et al.*, “Recent progress in metal–organic complexes for optoelectronic applications,” *Chem. Soc. Rev.*, vol. 43, no. 10, pp. 3259–3302, 2014.

[23] H. Fukagawa *et al.*, “Highly efficient and stable organic light-emitting diodes with a greatly reduced amount of phosphorescent emitter,” *Sci. Rep.*, vol. 5, no. 1, Sep. 2015.

[24] Q. Zhang, B. Li, S. Huang, H. Nomura, H. Tanaka, and C. Adachi, “Efficient blue organic light-emitting diodes employing thermally activated delayed fluorescence,” *Nat. Photonics*, vol. 8, no. 4, pp. 326–332, Apr. 2014.

[25] H. Sasabe and J. Kido, “Multifunctional Materials in High-Performance OLEDs: Challenges for Solid-State Lighting †,” *Chem. Mater.*, vol. 23, no. 3, pp. 621–630, Feb. 2011.

[26] H. Puntscher *et al.*, “Structure–property studies of P-triarylamine-substituted dithieno[3,2-b:2′,3′-d]phospholes,” *RSC Adv.*, vol. 5, no. 114, pp. 93797–93807, Nov. 2015.

[27] P. Kautny *et al.*, “Oxadiazole based bipolar host materials employing planarized triarylamine donors for RGB PHOLEDs with low efficiency roll-off,” *J Mater Chem C*, vol. 2, no. 11, pp. 2069–2081, 2014.

[28] T. Kader, B. Stöger, J. Fröhlich, and P. Kautny, “Azaindolo[3,2,1-jk]carbazoles: New Building Blocks for Functional Organic Materials,” *Chem. – Eur. J.*, vol. 25, pp. 4412–4425, Jan. 2019.

[29] Y. Im, S. H. Han, and J. Y. Lee, “Deep blue thermally activated delayed fluorescent emitters using CN-modified indolocarbazole as an acceptor and carbazole-derived donors,” *J. Mater. Chem. C*, vol. 6, no. 18, pp. 5012–5017, 2018.

[30] A. R. Muci and S. L. Buchwald, “Practical Palladium Catalysts for C-N and C-O Bond Formation,” in *Cheminform*, vol. 34, 2002, pp. 131–209.

[31] F. Paul, J. Patt, and J. F. Hartwig, “Palladium-catalyzed formation of carbon-nitrogen bonds. Reaction intermediates and catalyst improvements in the hetero cross-coupling of aryl halides and tin amides,” *J. Am. Chem. Soc.*, vol. 116, no. 13, pp. 5969–5970, Jun. 1994.

[32] A. R. Kapdi *et al.*, “The Elusive Structure of Pd2(dba)3. Examination by Isotopic Labeling, NMR Spectroscopy, and X-ray Diffraction Analysis: Synthesis and Characterization of Pd2(dba-Z)3 Complexes,” *J. Am. Chem. Soc.*, vol. 135, no. 22, pp. 8388–8399, 2013.

[33] S. S. Reddy *et al.*, “Highly Efficient Bipolar Deep-Blue Fluorescent Emitters for Solution-Processed Non-Doped Organic Light-Emitting Diodes Based on 9,9-Dimethyl-9,10-dihydroacridine/Phenanthroimadazole Derivatives,” *Adv. Opt. Mater.*, vol. 4, no. 8, pp. 1236–1246, Aug. 2016.

[34] X.-L. Chen, J.-H. Jia, R. Yu, J.-Z. Liao, M.-X. Yang, and C.-Z. Lu, “Combining Charge-Transfer Pathways to Achieve Unique Thermally Activated Delayed Fluorescence Emitters for High-Performance Solution-Processed, Non-doped Blue OLEDs,” *Angew. Chem. Int. Ed.*, vol. 56, no. 47, pp. 15006–15009, 2017.

[35] X.-Y. Liu, F. Liang, Y. Yuan, L.-S. Cui, Z.-Q. Jiang, and L.-S. Liao, “An effective host material with thermally activated delayed fluorescence formed by confined conjugation for red phosphorescent organic light-emitting diodes,” *Chem. Commun.*, vol. 52, no. 52, pp. 8149–8151, 2016.

[36] J. B. Henry, S. I. Wharton, E. R. Wood, H. McNab, and A. R. Mount, “Specific Indolo[3,2,1-*jk*]carbazole Conducting Thin-Film Materials Production by Selective Substitution,” *J. Phys. Chem. A*, vol. 115, no. 21, pp. 5435–5442, Jun. 2011.

[37] L. Crawford, H. McNab, A. Mount, J. Verhille, and S. Wharton, “Synthesis of Azapyrrolo[3,2,1-jk]carbazoles, Azaindolo[3,2,1-jk]carbazoles, and Carbazole-1-carbonitriles by Gas-Phase Cyclization of Aryl Radicals,” *Synthesis*, vol. 2010, no. 06, pp. 923–928, Mar. 2010.

[38] H. G. Dunlop and S. H. Tucker, “Attempts to prepare Optically Active Tervalent Nitrogen Compounds. Part I. Syntheses of 1:9-Phenylenecarbazole and Derivatives,” *J. Chem. Soc.*, pp. 1945–1956, 1939.

[39] J. Lv, Q. Liu, J. Tang, F. Perdih, and K. Kranjc, “A facile synthesis of indolo[3,2,1-jk]carbazoles via palladium-catalyzed intramolecular cyclization,” *Tetrahedron Lett.*, vol. 53, no. 39, pp. 5248–5252, Sep. 2012.

[40] K. P. Lippke, W. G. Schunack, W. Wenning, and W. E. Mueller, .“beta.-Carbolines as benzodiazepine receptor ligands. 1. Synthesis and benzodiazepine receptor interaction of esters of .beta.-carboline-3-carboxylic acid,” *J. Med. Chem.*, vol. 26, no. 4, pp. 499–503, Apr. 1983.

[41] L. Zeng and J. Zhang, “Design, synthesis, and evaluation of a novel class of 2,3-disubstituted-tetrahydro-β-carboline derivatives,” *Bioorg. Med. Chem. Lett.*, vol. 22, no. 11, pp. 3718–3722, Jun. 2012.

[42] A. Kamal *et al.*, “An efficient one-pot decarboxylative aromatization of tetrahydro-β-carbolines by using N-chlorosuccinimide: total synthesis of norharmane, harmane and eudistomins,” *RSC Adv.*, vol. 5, no. 109, pp. 90121–90126, Oct. 2015.

[43] T. Iwaki, A. Yasuhara, and T. Sakamoto, “Novel synthetic strategy of carbolines via palladium-catalyzed amination and arylation reaction,” *J. Chem. Soc. Perkin 1*, no. 11, pp. 1505–1510, 1999.

[44] F. Dennone, S. Celanire, A. Valade, S. Defays, and V. Durieux, “Cyclobutoxydihydrothiazolopyridines and related compounds as histamine H3 ligands and their preparation and use in the treatment of diseases,” Jul. 2009, WO2009092764A1.

[45] J. Chen, W. Chen, and Y. Hu, “Microwave-Enhanced Fischer Reaction: An Efficient One-Pot Synthesis of γ-Carbolines,” *Synlett*, vol. 2008, no. 01, pp. 77–82, Dec. 2007.

[46] M. A. Ponce and R. Erra-Balsells, “Synthesis and isolation of nitro-bT-carbolines obtained by nitration of commercial β-carboline alkaloids,” *J. Heterocycl. Chem.*, vol. 38, no. 5, pp. 1071–1082, Sep. 2001.

[47] M. Kneeteman, A. Baena, C. Rosa, and P. Mancini, “Polar Diels-Alder Reactions Using Heterocycles as Electrophiles. Influence of Microwave Irradiation,” *Int. Res. J. Pure Appl. Chem.*, vol. 8, no. 4, pp. 229–235, Jan. 2015.

[48] S. I. Wharton, J. B. Henry, H. McNab, and A. R. Mount, “The Production and Characterisation of Novel Conducting Redox-Active Oligomeric Thin Films From Electrooxidised Indolo[3,2,1-jk]carbazole,” *Chem. – Eur. J.*, vol. 15, no. 22, pp. 5482–5490, May 2009.

[49] P. H. Fries and D. Imbert, “Parallel NMR Based on Solution Magnetic-Susceptibility Differences. Application to Isotopic Effects on Self-Diffusion †,” *J. Chem. Eng. Data*, vol. 55, no. 5, pp. 2048–2054, May 2010.

[50] I. Güell and X. Ribas, “Ligand-Free Ullmann-Type C–Heteroatom Couplings Under Practical Conditions,” *Eur. J. Org. Chem.*, vol. 2014, no. 15, pp. 3188–3195, May 2014.

[51] O. Navarro and S. P. Nolan, “Large-Scale One-Pot Synthesis of N-Heterocyclic Carbene-Pd(allyl)Cl Complexes,” *Synthesis*, vol. 2006, no. 02, pp. 366–367, Jan. 2006.

[52] A. J. Arduengo, R. L. Harlow, and M. Kline, “A stable crystalline carbene,” *J. Am. Chem. Soc.*, vol. 113, no. 1, pp. 361–363, Jan. 1991.

[53] N. Marion, O. Navarro, J. Mei, E. D. Stevens, N. M. Scott, and S. P. Nolan, “Modified (NHC)Pd(allyl)Cl (NHC = *N* -Heterocyclic Carbene) Complexes for Room-Temperature Suzuki−Miyaura and Buchwald−Hartwig Reactions,” *J. Am. Chem. Soc.*, vol. 128, no. 12, pp. 4101–4111, Mar. 2006.

[54] A. Nowakowska-Oleksy, J. Sołoducho, and J. Cabaj, “Phenoxazine based units--synthesis, photophysics and electrochemistry,” *J. Fluoresc.*, vol. 21, no. 1, pp. 169–178, Jan. 2011.